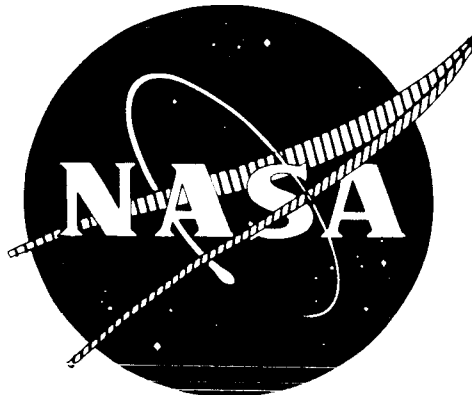


SINGLE STAGE EXPERIMENTAL EVALUATION
OF
SLOTTED ROTOR AND STATOR BLADING

PART IV - DATA AND PERFORMANCE
FOR SLOTTED ROTOR 2

10	(THRU)
1	(CODE)
1	(CATEGORY)
12	(ACCESSION NUMBER)
12	(PAGE(S))
12	(NASA CR OR TMX OR AD NUMBER)



200 PRICE \$ _____

UFSTI PRICE(S) \$ _____

Hard copy (HC) _____

Microfiche (MF) _____

M 653 Rev 65

PREPARED FOR

NATIONAL AERONAUTICS AND SPACE ADMINISTRATION

CONTRACT NAS3-7603

Pratt & Whitney Aircraft
FLORIDA RESEARCH AND DEVELOPMENT CENTER

DIVISION OF UNITED AIRCRAFT CORPORATION



SINGLE STAGE EXPERIMENTAL EVALUATION
OF
SLOTTED ROTOR AND STATOR BLADING

PART IV - DATA AND PERFORMANCE
FOR SLOTTED ROTOR 2

PREPARED FOR
NATIONAL AERONAUTICS AND SPACE ADMINISTRATION
CONTRACT NAS3-7603
24 FEBRUARY 1967

CONTRACTOR PROGRAM MANAGER: Charles G. Linder
CONTRACTOR PROGRAM ADVISOR: Burton A. Jones

TECHNICAL MANAGEMENT
NASA LEWIS RESEARCH CENTER
CLEVELAND, OHIO

NASA PROGRAM MANAGER: John E. McAulay
Air Breathing Engines Division

NASA RESEARCH ADVISOR: L. Joseph Herrig
Fluid Systems Components Division

Pratt & Whitney Aircraft
FLORIDA RESEARCH AND DEVELOPMENT CENTER



ABSTRACT

A single-stage investigation of a slotted rotor was conducted as part of an overall program to evaluate the effect of slots on the performance of highly loaded compressor rotor and stator blade rows. The test rotor blades were 65-series airfoils having a calculated unslotted D-factor loading of 0.51 and an inlet relative Mach number of 0.833 at a radial station 10% of the span from the blade tip. For design equivalent rotor speed, the slotted rotor achieved a maximum adiabatic efficiency of 88.5% and a corresponding pressure ratio of 1.29.

CONTENTS

SECTION	PAGE
I SUMMARY	I-1
II INTRODUCTION	II-1
III TEST EQUIPMENT	III-1
A. Facility	III-1
B. Compressor Test Rig.	III-1
C. Stage Blading Design	III-2
D. Instrumentation.	III-5
IV PROCEDURES	IV-1
A. Test Procedure	IV-1
B. Data Reduction Procedures.	IV-2
V RESULTS AND DISCUSSION	V-1
A. Overall Performance.	V-1
B. Blade Element Performance.	V-2
VI CONCLUDING DISCUSSION.	VI-1
VII ILLUSTRATIONS.	VII-1
APPENDIX A - Definition of Symbols	A-1
APPENDIX B - Tabulated Performance	B-1
APPENDIX C - References.	C-1

ILLUSTRATIONS

FIGURE	PAGE
III-1 Compressor Research Facility	VII-2
III-2 Rotating Axial Flow Cascade Test Rig	VII-3
III-3 Flow Path.	VII-4
III-4 Rotating Cascade Rig Bleed System.	VII-5
III-5 Slot Geometry and Location	VII-6
III-6 Typical Slotted Rotor 2 Blade.	VII-7
III-7 Instrumentation, Station 1 (View Looking Downstream).	VII-8

ILLUSTRATIONS (Continued)

FIGURE		PAGE
III-8	Instrumentation, Station 2 (View Looking Downstream).	VII-9
III-9	Instrumentation, Station 2A (View Looking Downstream).	VII-10
III-10	Instrumentation, Station 3 (View Looking Downstream).	VII-11
III-11	Probe Configurations	VII-12
III-12	Anemometer Probe	VII-13
III-13	Strain Gage Locations.	VII-14
V-1	Overall Performance; Slotted Rotor 2 Only.	VII-15
V-2	Overall Performance; Inlet Guide Vane, Slotted Rotor 2.	VII-16
V-3	Overall Performance; Inlet Guide Vane, Slotted Rotor 2, Unslotted Stator 1.	VII-17
V-4	Airflow Continuity Comparison.	VII-18
V-5	Guide Vane Exit Air Angle Distribution - 100% Design Equivalent Rotor Speed	VII-19
V-6	Relative Air Angle and Mach Number Distribution Into Slotted Rotor 2 - 100% Design Equivalent Rotor Speed.	VII-20
V-7	Rotor Blade Element Performance - 100% Design Equivalent Rotor Speed, 90% Span From Tip.	VII-21
V-8	Rotor Blade Element Performance - 100% Design Equivalent Rotor Speed, 70% Span From Tip.	VII-22
V-9	Rotor Blade Element Performance - 100% Design Equivalent Rotor Speed, 50% Span From Tip.	VII-23
V-10	Rotor Blade Element Performance - 100% Design Equivalent Rotor Speed, 30% Span From Tip.	VII-24
V-11	Rotor Blade Element Performance - 100% Design Equivalent Rotor Speed, 10% Span From Tip.	VII-25
V-12	Variation of Rotor Blade Element Parameters With Incidence, Slotted Rotor 2, 90% Span From Tip	VII-26
V-13	Variation of Rotor Blade Element Parameters With Incidence, Slotted Rotor 2, 70% Span From Tip	VII-27
V-14	Variation of Rotor Blade Element Parameters With Incidence, Slotted Rotor 2, 50% Span From Tip	VII-28

ILLUSTRATIONS (Continued)

FIGURE	PAGE
V-15 Variation of Rotor Blade Element Parameters With Incidence, Slotted Rotor 2, 30% Span From Tip	VII-29
V-16 Variation of Rotor Blade Element Parameters With Incidence, Slotted Rotor 2, 10% Span From Tip	VII-30
V-17a Loss Parameter Versus Diffusion Factor at 70 and 50% Span (From Tip) - 90, 100, and 110% Design Equivalent Rotor Speed.	VII-31
V-17b Loss Parameter Versus Diffusion Factor at 90 and 30% Span (From Tip) - 90, 100, and 110% Design Equivalent Rotor Speed.	VII-32
V-17c Loss Parameter Diffusion Factor at 10% Span (From Tip) 90, 100, and 110% Design Equivalent Rotor Speed	VII-33
V-18 Stress Survey Map.	VII-34
V-19 Typical Rotating Stall Recording; Rotor Speed 6200 RPM	VII-35
V-20 Rotor Wake Surveys - 50% Design Equivalent Rotor Speed	VII-36
V-21 Rotor Wake Surveys - 70% Design Equivalent Rotor Speed	VII-37
V-22 Rotor Wake Surveys - 100% Design Equivalent Rotor Speed	VII-38
V-23 Stator Inlet Air Angle and Mach Number Distribution, Slotted Rotor 2 Configuration, Design Rotor Speed	VII-39

SECTION I
SUMMARY

A single-stage investigation of a slotted rotor was conducted as part of an overall program to evaluate the effect of slots on the performance of highly loaded compressor rotor and stator blade rows. The test rotor blades were 65-series airfoils and had a calculated unslotted blade D-factor loading of 0.512 and an inlet relative Mach number of 0.833 at a radial station 10% of the span from the blade tip. The rotor blades were slotted at approximately 50% chord; the slots extended from 5% to 45% span from the tip and from 50 to 90% span in each blade. The single-stage rig had a hub/tip ratio of 0.8, and the rotor tip diameter was about 40 in. The rotor blades had a constant chord length of 2.21 in., an aspect ratio of 1.71 and solidity of 1.15 at the mean radius. Design rotor tip velocity was 935 fps.

For design equivalent rotor speed the slotted rotor achieved a maximum adiabatic efficiency of 88.5% and a corresponding pressure ratio of 1.29. The measured D-factor values corresponding to maximum efficiency flow conditions were approximately 0.48 at the root and tip and 0.40 at midspan. Measured deviation angles were essentially the same as the predicted unslotted blade deviation angles in the midspan and tip regions, and approximately 6 degrees greater than the predicted deviation angle at the hub. Measured loss coefficient was comparable to the predicted unslotted blade loss coefficient at 30, 50, and 70% span locations, and was greater than the predicted loss at 10 and 90% span.

Comparison of the slotted rotor loss and D-factor loading characteristics for high incidence conditions with correlated NASA rotating cascade minimum loss incidence data indicates that the slot configuration for this investigation was effective in the achievement of loss levels equal to or less than those indicated by the NASA design curves for D-factor loading from 0.50 to 0.70.

SECTION II
INTRODUCTION

Pratt & Whitney Aircraft is engaged in a program under NASA Contract NAS3-7603 to investigate the application of slots to rotors and stators. A systematic investigation is being conducted to establish the feasibility and extent to which slotted blade concepts can be used to increase allowable blade loadings and the stable operating range of compressor stages. To accomplish this objective, three stator blade rows and three rotor blade rows have been built for test. Tests with stators use a representative state-of-the-art rotor to generate the stator inlet flow.

An aerodynamic analysis and design of the test blading and associated hardware were accomplished under the design phase of the program (Reference 1).* All rotors and stators were designed with the same rotor exit and stator inlet absolute velocities and air angle distributions to permit testing of any combination of rotor and stator. It was assumed, for design purposes, that the flow deviation angles for slotted rotors and stators would be approximately one-half the values normally used for unslotted blades. As part of the design effort, a series of annular cascade tests with slotted stators was conducted to establish preliminary criteria for the design of slotted rotors and stators for the rotating stage test program (Reference 2). Data and performance results obtained with the first slotted rotor configuration of the series are presented in Reference 3.

This report presents the data and performance results obtained with the second slotted rotor configuration (Rotor 2) which has a higher loading level than Rotor 1. Rotor 2 blading was designed with 65-series airfoil sections and had calculated design tip values of D-factor loading and inlet relative Mach number (without slots) of 0.512 and 0.833, respectively. The rotor blades were slotted at approximately 50% chord; the slots extended from 5 to 45% span, and from 50 to 90% span (from the tip) in each blade. A set of inlet guide vanes was used to establish the whirl

*References are given in Appendix C.

distribution into the test rotor. One of the test stator configurations, prior to slotting, was employed to remove some of the exit swirl. A set of exit guide vanes was used to remove the remaining exit swirl.

Overall performance and blade element data were obtained at 50, 70, and 100% of the design equivalent rotor speed. Blade element data were obtained at five radial locations behind each of the three blade rows, and rotating stall measurements were obtained at each of the three rotor speed conditions. Rotor wake surveys at five spanwise locations, using a hot-film anemometer, were obtained at choke, near-stall, and approximately maximum efficiency flow conditions at each rotor speed.

Details of the test equipment, procedures, and test results for the slotted Rotor 2 test configuration are presented in this report. Some design details are also included herein for convenience. Reference 1 gives further aerodynamic and mechanical design information.

SECTION III TEST EQUIPMENT

A. FACILITY

The compressor test facility is shown schematically in figure III-1*. The compressor rotor is powered by a single-stage drive turbine using exhaust gases from a J75 slave engine. The drive turbine speed is regulated by a hydraulically actuated inlet flow control valve. The slave engine exhaust is also used to drive a two-stage exhaust-ejector system.

Air entered the compressor test rig through a 103-ft combined inlet duct, plenum, and bellmouth inlet, and exhausted through an exit diffuser to the atmosphere. A 7-degree diffuser in front of the inlet plenum ensured uniform flow conditions across the plenum, and an area contraction ratio from plenum to compressor inlet of approximately 10:1 provided essentially stagnation conditions in the plenum. The inlet duct and plenum were mounted on a track and could be rolled away from the compressor rig inlet to facilitate configuration changes. The plenum was sealed to the compressor rig inlet section with an inflatable rubber tube seal.

B. COMPRESSOR TEST RIG

The compressor rig, shown in figure III-2, comprises bellmouth inlet, test section, and exhaust section. The test section has a hub/tip ratio of 0.8 and a rotor tip diameter of approximately 40 in. The rotor assembly and shaft are supported on two bearings that transmit loads to the outer case through struts located in the inlet and exhaust case assemblies. The test section has a split outer case that permits guide vane, rotor, and stator assembly changes without removing the rig from the test stand. A set of motor-driven throttle vanes is located in the exhaust case to vary flow rate.

A section view of the flow path is shown in figure III-3. Flow is accelerated through the inlet strut station and guide vanes in a convergent passage to the rotor inlet. Thereafter, the inner wall diameter remains constant at 32.85 in. while the outer wall converges further through the rotor blade and stator vane rows to a diameter of

*All illustrations will be found in Section VII.

40 in. In general, the flow path is designed to simulate the middle-stage environment of a state-of-the-art multistage compressor.

Provisions were made for end wall bleed at the rotor tip and stator root and tip, as shown in figure III-4. Bleed air flowed through perforated plate shrouds, shroud manifolds, and 24 approximately equally spaced tubes to individual main collector manifolds for the rotor and stator. The collector manifolds exhausted through the facilities ejector system. Rotor and stator bleed flow rates were controlled and measured separately.

C. STAGE BLADING DESIGN

To expedite this research program, the aerodynamic and mechanical design of the blading was completed and fabrication initiated prior to the completion of the annular cascade program. Final slot configurations were based on the results of the cascade tests.

1. Inlet Guide Vane

The inlet guide vanes were designed to provide a rotor prewhirl distribution of 16.6 deg at the root (90% span) to 18.2 deg at the tip (10% span). NACA series-400 blade sections were chosen for this purpose. Details of the guide vane design are presented in table III-1.

2. Rotor 2

a. Blade Design

Slotted Rotor 2 blading was designed with a camber distribution of 36.0 deg at the root (90% span) to 18.1 deg at the tip (10% span). NACA series-65 blade sections were selected for the rotor blades because this series of airfoil has adequate thickness for slots, suitable loading distribution, and is capable of operating in the required Mach number range ($M_{tip} = 0.8$). It was assumed, for design purposes, that slots would reduce the flow deviation angle approximately one-half the normal values. Slotted rotor blade trailing edge metal angles were established in accordance with this assumption. Design D-factor loading at the rotor tip was 0.590 for the slotted blading and 0.512 for the same blading without slots (i.e., with full deviation).

Table III-1. Geometry Design Data

INLET GUIDE VANE 2

Percent Span (From Tip)	κ_1	κ_2	ϕ	γ°	c	σ	t/c	δ°
90	0.00	24.04	-24.04	14.36	2.204	1.044	0.060	7.46
50	0.00	24.84	-24.84	14.92	2.204	0.956	0.060	8.30
10	0.00	28.88	-28.88	17.21	2.204	0.880	0.060	10.73

ROTOR 2

Percent Span (From Tip)	κ_1	κ_2	ϕ	γ°	i _m	0/0*	c	σ	t/c	δ°	$\bar{\omega}$
90	52.16	16.15	36.01	34.21	0.42	1.247	2.210	0.075	11.43	0.062	
50	55.03	29.24	25.79	42.10	0.70	1.253	2.210	1.149	0.059	8.05	0.053
10	56.79	38.65	18.14	47.75	1.26	1.250	2.210	1.071	0.044	5.97	0.047

STATOR 1

Percent Span (From Tip)	κ_1	κ_2	ϕ	* γ°	i _m	0/0*	c	σ	t/c	δ°	$\bar{\omega}$
90	52.15	22.14	30.01	37.20	-1.68	1.187	2.182	1.192	0.090	10.14	0.040
50	52.15	22.14	30.01	37.20	-0.22	1.273	2.182	1.099	0.090	9.46	0.036
10	52.15	22.14	30.01	37.20	0.61	1.355	2.182	1.026	0.090	9.93	0.034

*Stators were actually installed at a blade-chord angle of 32.0 deg.

Solidity, thickness ratios, and aspect ratios for the selected series airfoils were representative of the middle stage of a state-of-the-art compressor. Details of the rotor design are presented in table III-1.

b. Slot Design

Rotor 2 slot geometry and location were based on the results of preliminary annular cascade tests of slotted stator vanes and an analysis of Rotor 2 suction surface boundary layer separation (References 1 and 2).

The selected slot geometry was similar to a preferred slot geometry determined in the annular cascade program. Blade thickness at the intersection of slot centerline and blade meanline was selected as an approximate scaling parameter to scale the slot size from the oversize (6.5-in. chord) annular cascade vanes to the 2.21 in. chord Rotor 2 blading. The angle between slot centerline and blade meanline was held constant over the Rotor 2 blade span; that is, the slot followed the twist of the blade. The slot spanwise position and geometry variables with corresponding dimensions at root, mean, and tip sections are presented in figure III-5.

The slot centerline intersected the blade suction surface at 50% chord, approximately halfway between the minimum pressure point and the calculated separation point. This slot location was determined under the annular cascade tests to be superior to an alternative location near the separation point.

The resulting slotted blade configuration is shown in figure III-6.

3. Stator

Three stators having unslotted root D-factor loading levels of 0.52, 0.60, and 0.70 were designed for evaluation of slotted stators under the contract program (Reference 1). The stators are 65-series airfoil sections. The stator having the lowest of the three loading levels (Stator 1, $D = 0.52$) was selected for use behind the slotted rotors. Even though this stator was unslotted for these tests, it was considered to have an incidence range that would not limit slotted rotor evaluation. The selected stator had a constant equivalent circular arc camber of 30 deg and was untwisted. Because the annular cascade test results (Reference 2) indicated that slots did not produce the assumed decrease in deviation angle, the stator was installed behind slotted Rotor 2 with a blade chord

angle of 32 deg instead of the original design blade chord angle of 37.2 deg. This stagger angle was so selected to ensure that stator minimum loss incidence would occur within the expected range of rotor exit angle. Additional details of the stator design are presented in table III-1.

D. INSTRUMENTATION

Instrumentation was provided for overall and blade element performance measurements for each blade row. Axial locations of instrumentation stations are indicated in figure III-3, and schematics showing the detailed instrumentation at each axial location are presented in figures III-7 through III-10.

1. Rig Inlet Conditions

Weight flow was measured with an ASME standard thin plate orifice located in the inlet duct.

Six static pressure taps and six temperature probes were located in the plenum chamber for measurement of inlet total pressure and temperature.

Six equally spaced static pressure taps were located on both the inner and outer walls upstream of the inlet guide vanes (Station 0). From a rig calibration over a wide range of weight flows, a calibration between these static pressures was derived and used to check subsequent weight flow measurements.

2. Guide Vane Exit/Rotor Inlet - Station 1

A sectional view of the flow path at Station 1 showing the circumferential and radial location of instrumentation is presented in figure III-7. Rotor inlet air angle measurements were obtained at two circumferential locations with 20-deg wedge traverse probes. A 20-tube wake traverse probe, approximately aligned with the average guide vane exit air angle, was installed to measure guide vane wake total pressure distribution. Four static pressure taps were located on both the inner and outer wall. An 8-deg wedge traverse probe was used for measurement of radial static pressure distribution. The wedge probes and static

pressure taps were located approximately along extensions of guide vane midchannel lines. The guide vane trailing edge was oriented to keep the instrumentation locations used for Rotor 1 testing along midchannel streamlines. Redundant static and mid-passage total pressure data were available from the 20-deg wedge probe.

3. Rotor Exit/Stator Inlet - Station 2

A sectional view of the flow path showing the circumferential and radial location of instrumentation at Station 2 is presented in figure III-8. Two 20-deg wedge traverse probes were used for air angle, total pressure, and total temperature measurements. Three sets of Kiel head total pressure probes were located at radial positions corresponding to 30 and 50%. Two sets of Kiel probes were located at 10, 70, and 90% span. The probes were circumferentially located so that each set approximately averaged the pressures across a guide vane wake. A set of Kiel head temperature probes were located at 10, 30, 50, 70, and 90% span positions to provide a check against the 20-deg wedge probe temperature measurement. Four static pressure taps were located on both the inner and outer wall. An 8-deg wedge traverse probe was used for radial static pressure measurement.

4. Stator Exit - Station 2A

A sectional view of the flow path showing circumferential and radial location of instrumentation at Station 2A is presented in figure III-9. Stator exit air angle was measured with a 20-deg wedge traverse probe. A 20-tube rake traverse probe was used for measurement of stator vane wake total pressure distribution. Four static pressure taps were located on both the inner and outer wall, and an 8-deg wedge traverse probe was provided for radial static pressure measurement.

5. Station 3

Station 3 is one chord-length farther from the stator exit plane than Station 2A. Instrumentation at this station (figure III-10) included two 20-deg wedge traverse probes, one 8-deg wedge traverse probe, four sets of Kiel head total pressure probes at 10, 30, 50, 70, and 90% span location, three sets of Kiel head temperature probes at the same five span locations, and four static pressure taps on both the inner and outer wall.

Stage exit total temperature was based on the Kiel head probe temperature measurements at Station 3. Data obtained from the other instrumentation at this station were generally used for comparison with the Station 2A data.

6. Description of Probes

Details of the 20-deg and 8-deg probes, wake probe, and Kiel pressure and temperature probes are shown in figure III-11. The wedge probe contained side pressure pickups for air angle measurement, a total pressure pickup and a total temperature pickup.

The wake probe contained 20 total pressure pickups formed by 0.042 inch OD hypo tubing and spaced as shown in the figure.

7. Instrumentation Readout

Traverse probe data (total pressure, static pressure, air angle, total temperature, and radial travel) were recorded on magnetic tape at the rate of 60 samples (2.5-in. probe travel) per minute. Steady-state pressure measurements were obtained using a scannivalve multichannel pressure transducer system that includes automatic data recording on IBM cards. Kiel probe temperatures were indicated on a precision potentiometer, and manually recorded.

Plenum pressures, three OD static pressures at Station 0, primary and bleed system flow-measuring-orifice pressures, and three Station 3 midspan Kiel probe pressures were recorded on manometer tubes in the test stand control room to permit setting the desired flow conditions.

8. Special Instrumentation

a. Rotating Stall Instrumentation

Three Kistler (601A) pressure transducers were installed at Station 2 for rotating stall measurement (figure III-8). Transducer output was recorded on a CEC VR-2800 tape recorder.

b. Rotor Wake Instrumentation

Rotor wake surveys were obtained with DISA 55479 hot-film anemometer probe, located as shown in figure III-8. Anemometer output voltage was recorded on a VR-2800 tape recorder. The hot-film probe is shown in figure III-12.

c. Rotor Exit Boundary Layer Instrumentation

Rotor exit end wall boundary layer total pressure profiles were measured to set bleed flow rates using a three-hole cylindrical yaw probe having a 3/4-in. tip (dimension between sensing ports and probe tip) and a diameter of 3/8 in. Total pressure and radial travel were recorded on an x-y plotter.

d. Rotor Speed

Rotor rpm was measured with an electromagnetic pickup mounted adjacent to a 60-tooth gear on the rotor shaft. Gear tooth passing frequency was displayed as rpm on an Anadex digital readout system. A closed loop control system maintained rotor speed within approximately $\pm 1\%$.

e. Stress Measurements

Five rotor blades and five stator vanes were instrumented with strain gages to monitor and record torsional and bending stresses. Strain gage locations on a typical instrumented rotor blade are shown in figure III-13.

f. Vibration

Displacement pickups were mounted on forward and rear sections of the compressor rig outer case to monitor rig vibration.

g. Bleed Flow Rate

End wall bleed flow from the rotor and stator blade rows was measured by means of standard ASME thin plate orifices located in the respective bleed manifold exhaust ducts.

SECTION IV
PROCEDURES

A. TEST PROCEDURE

1. End Wall Bleed Flow Rate Selection

a. Rotor Bleed

With the compressor operating at design speed and flow conditions, the three-hole yaw probe was traversed between 0 and 20% span at Station 2 behind the rotor for each of three bleed flow settings. The three settings corresponded to near-zero, half of maximum, and maximum bleed flow rates. The bleed flow rate selected was that which produced the most significant improvement in total pressure profile as indicated on the x-y plotter. The valve setting for this bleed flow rate was not changed at other rotor speed and flow conditions.

b. Stator Bleed

With the rotor end wall bleed set at the selected rate, the procedure described above was repeated for the stator. The 20-tube wake probe was positioned at 10 and 90% span locations, and the effect of boundary layer bleed on the stator wake pressures was monitored on manometers. The valve setting corresponding to the bleed flow rate that produced the most significant improvement at either span location at design speed and flow conditions was selected for the test program.

2. Stress Survey and Rotating Stall Tests

A stress survey program was conducted to define the stress and vibration characteristics of the slotted rotor over the operating range and in the stall regions. Blade stresses were monitored and recorded along the choke line, along an assumed operating line, and into the stall region at five rotor speed conditions. Fixed instrumentation was recorded at a sufficient number of speed and flow conditions to define the overall operating range between choke and stall and between 50 and 110% design speed.

Kistler transducer data were recorded during the excursions into stall along each speed line to define rotating stall patterns.

3. Overall and Blade Element Performance Tests

Overall and blade element performance data were obtained at three rotor speed conditions (50, 70, and 100% of design speed) and a sufficient number of points per speed line to define rotor and stage performance between choke and stall. The near-stall test point was determined on the basis of strain gage output and stage exit total pressures indicated on manometers. At each speed and flow set point, the fixed pressure and temperature instrumentation data were recorded five times, corresponding to five discrete radial locations of the inlet guide vane and stator vane wake probes. Traverse data were usually recorded during the last recording of fixed instrumentation. In this manner, representative average values of flow and pressures could be determined for the time period (approximately 45 min) of data recording at each point.

4. Rotor Wake Surveys

Rotor wake surveys were obtained following the recording of blade element and overall performance data at choke, approximately maximum efficiency, and near-stall conditions on each of the three speed lines. Hot-film anemometer output was recorded as the probe was traversed from the inner to the outer wall behind the rotor.

B. DATA REDUCTION PROCEDURES

1. Preliminary Data Reduction

Data reduction was accomplished in three steps using three computer programs. The first step involved conversion of raw data to engineering units. Traverse data (total pressure, static pressure, total temperature, and air angle), obtained at approximately 0.04-in. increments across the span, were automatically plotted (as well as tabulated). The plotted and tabulated data were reviewed to identify and eliminate any obviously questionable data prior to the subsequent data reduction step.

The second data reduction step accomplished the following:

1. Mach number corrections to temperature data
2. Mass average of wake probe data
3. Circumferential arithmetic average of fixed and traverse instrumentation data

4. Correction of all pressure and temperature data to NASA standard day ambient conditions
5. Selection by interpolation of total and static pressure, total temperature, and air angle values at specified radial locations for input for the final data reduction step.

All corrected data were available for further inspection in the printed results from this computer program, which included individual data values as well as averaged quantities. The third step in the data reduction procedure involved calculation of overall and blade element performance parameters, which are defined in the following paragraphs.

2. Parameter Calculation

The following overall and blade element performance parameters were calculated for the analysis of test data and the evaluation of slotted Rotor 2 performance. Symbols are defined in Appendix A.

a. Overall Performance

(1) Weight Flow

Weight flow is presented in terms of corrected weight flow, defined as

$$\frac{w\sqrt{\theta}}{\delta}$$

where:

w = actual (orifice) weight flow

θ = ratio of total temperature (plenum) to NASA standard sea level temperature

δ = ratio of total pressure (plenum) to NASA standard sea level pressure.

Values of corrected weight flow presented in the figures and tables include rotor and stator bleed flow rates. Percentage bleed flow rates for the respective blade rows are tabulated separately (table B-1).

(2) Pressure Ratio

Pressure ratios were calculated for the rotor, guide vane-rotor, and guide vane-rotor-stator blade row combinations. Behind the rotor, fixed Kiel head and traverse probe total pressure data were arithmetically averaged at each span location and the profile thus defined was mass-flow averaged across the span.

Behind the guide vane and stator, the wake probe pressures were first mass-flow integrated at each span location, and the resulting average pressures were than mass-flow averaged in the radial direction.

(3) Adiabatic Efficiency

Adiabatic efficiency across the rotor is defined as

$$\eta_{ad} = \frac{\frac{\gamma - 1}{\gamma}}{\frac{\bar{P}_2}{\bar{P}_1} - 1} - \frac{\frac{\gamma - 1}{\gamma}}{\frac{\bar{T}_3}{T_1} - 1}$$

where:

\bar{P}_1 = mass averaged pressure behind the guide vane

T_1 = 518.7°R

\bar{P}_2 = mass averaged pressure behind the rotor

\bar{T}_3 = mass averaged temperature behind the stator.

To obtain adiabatic efficiencies for the guide vane-rotor combination or for the entire stage, appropriate average pressures were used.

b. Blade Element Performance

(1) Diffusion Factor

Diffusion factor for the rotor is defined as

$$D = 1 - \frac{V'_2}{V'_1} + \frac{\Delta V'_\theta (1 - 2)}{2\sigma V'_1}$$

Diffusion factor for the stator is defined as

$$D = 1 - \frac{V'_{2A}}{V'_2} + \frac{\Delta V'_\theta (2 - 2A)}{2\sigma V'_2}$$

(2) Deviation

Rotor blade deviation is defined as

$$\delta_2^\circ = \beta_2' - \kappa_2'$$

Stator deviation is defined as

$$\delta_{2A}^\circ = \beta_{2A} - \kappa_{2A}$$

where κ_2' and κ_{2A} are the rotor blade and stator vane trailing edge metal angles based on equivalent circular arc camber lines for the 65-series airfoil.

(3) Incidence Angle

Rotor incidence angle is defined as

$$i_{m1} = \beta_1' - \kappa_1'$$

Stator incidence angle is defined as

$$i_{m2} = \beta_2 - \kappa_2$$

where κ_1' and κ_2 are the rotor blade and stator vane leading edge metal angles based on the equivalent circular arc camber lines for the 65-series airfoil.

(4) Total Pressure Loss Coefficient

Total pressure loss coefficient for the rotor is defined as

$$\bar{\omega}_{(1 - 2)} = \frac{\bar{P}_1' - \bar{P}_2'}{\bar{P}_1' - P_1}$$

where $(-)$ refers to mass-averaged wake total pressure.

For the inlet guide vanes, total pressure loss coefficient is defined as

$$\bar{\omega}_{(0 - 1)} = \frac{14.69 - \bar{P}_1}{q_o}$$

where q_o is obtained from isentropic flow relationships using orifice weight flow and the annular area at the guide vane inlet.

Total pressure loss coefficient for the stator is defined as

$$\bar{\omega}_{(2 - 2A)} = \frac{p_2 - \bar{p}_{2A}}{p_2 - p_2}$$

(5) Loss Parameter

Rotor total pressure loss is also presented in terms of the loss parameter,

$$\frac{\bar{\omega}'_{(1 - 2)}}{2\sigma} \cos \beta'_2$$

SECTION V
RESULTS AND DISCUSSION

Slotted Rotor 2 performance was evaluated on the basis of pressure rise and efficiency characteristics as functions of rotative speed and weight flow, as well as blade element diffusion factor, deviation, and loss coefficient as functions of incidence angle. Slotted rotor performance results are compared with (1) predicted unslotted rotor performance and (2) available NASA rotating cascade performance results. Guide vane exit and stator inlet air angles are compared with the respective calculated design radial distributions. Overall and blade element experimental performance parameters and bleed flows as well as blade element vector diagram data for the guide vane, rotor, and stator are tabulated in Appendix B. The results of stress surveys, rotating stall measurements, and rotor wake surveys are included under the discussion of rotor performance.

A. OVERALL PERFORMANCE

Overall performance is presented in terms of efficiency and pressure ratio versus corrected main orifice weight flow, $w\sqrt{\theta}/\delta$, and corrected specific weight flow, $w\sqrt{\theta}/\delta A_A$, in figure V-1, V-2, and V-3, for rotor, guide vane-rotor, and guide vane-rotor-stator combinations. Each figure contains the performance results obtained at the three test rotor speed conditions. Values of corrected airflow obtained from integration of flow profiles downstream of the rotor and stator are compared with the main orifice measured values minus bleed flow in figure V-4. The figure shows that agreement within 0 to -7% was obtained for the majority of data points.

As reported in Reference 1, the design efficiency and pressure ratio for Rotor 2 are 90% and 1.35, respectively, without slots (normal deviation angles) and 91% and 1.42, respectively, with slots (reduced deviation angles) at a design flow of 99 lb/sec. Because it was learned from the annular cascade test results (Reference 2) and the test results obtained with slotted Rotor 1 (Reference 3) that the selected slot design does not produce the assumed reduction in deviation angle, the test results reported herein are compared with the calculated design performance without slots.

For the design equivalent rotor speed, a maximum efficiency of 88.5% was obtained with a corresponding pressure ratio of 1.29, at a flow rate slightly higher than the design flow rate of 99 lb/sec. At design flow conditions the efficiency and pressure ratio were 86% and 1.30, respectively, compared with the predicted values of 90% and 1.35.

The guide vane-rotor performance characteristics in figure V-2 indicate that guide vane total pressure loss had a negligible effect when compared with rotor performance in figure V-1. The stage performance (guide vane-rotor-stator) in figure V-3 shows the effect of stator loss on stage efficiency and pressure ratio when compared with the guide vane-rotor performance in figure V-2. The design rotor speed maximum efficiency was decreased from 88.5% to 83.5% and the pressure ratio corresponding to maximum efficiency decreased from 1.29 to 1.27.

B. BLADE ELEMENT PERFORMANCE

1. Inlet Guide Vane

Inlet guide vane exit air angle distributions are presented in figure V-5 for representative design speed line test data. Air angle data obtained with each of the two 20-deg wedge probes are identified by symbol, and the design air angle distribution is shown for comparison. The average measured air angle is within about 1.0 degree of the predicted value over the entire span.

Inlet guide vane vector diagram and blade element data are presented in table B-2.

2. Rotor

a. Rotor Inlet Conditions

Rotor inlet relative Mach number and air angle radial distributions for the design speed data points are presented in figure V-6. Calculated design point distributions are shown for comparison. The design Mach number distribution is within the range of measured values from choke to stall.

At the weight flow corresponding to maximum efficiency ($w\sqrt{\theta}/\delta = 101.31$ lb/sec), the inlet relative air angle distribution is within 1 or 2 degrees of the design distribution. Design incidence would be attained at a flow of about 98 lb/sec.

b. Loss Coefficient; Deviation; D-factor

Blade element performance data obtained at rotor design equivalent speed are presented in terms of loss coefficient, deviation, and D-factor versus incidence in figures V-7 through V-11. Each figure corresponds to one spanwise location. Calculated design values of loss coefficient, deviation, and D-factor (without slots) are shown in the figures for comparison with the slotted rotor data. The measured D-factor loading levels are generally lower than the corresponding predicted values in the middle of the blade (30, 50, and 70% span positions). The measured D-factor is slightly higher than the predicted value at 90% span from the tip, and equal to the predicted value 10% span from the tip. Slotted Rotor 2 deviation values are approximately the same as the predicted values at 10, 30, 50, and 70% span locations and six degrees greater than the predicted values at 90% span. Measured loss coefficients are approximately the same as the predicted values in the middle of the blade, and significantly higher than the predicted values at the hub and tip. The corresponding hub and tip efficiencies are low compared to the midspan value, as seen in table B-2.

Blade element parameters for the three speed lines are combined in figures V-12 through V-16 to show the general consistencey of the data. Rotor tip inlet relative Mach number varied between about 0.37 and 0.84 over the rotor speed and flow range. An apparent Mach number effect on loss coefficient can be seen at all five span locations. The 50 and 70% speed values are consistently lower than the 100% speed values. Furthermore, the 100% design rotor speed loss coefficient data exhibit a narrower incidence angle range than that formed by the data corresponding to 50 or 70% speed data.

Deviation angle does not appear to be affected by Mach number with the possible exception of the 90% span data in figure V-12. The data in this figure indicate a systematic trend of increasing deviation/incidence angle rate with increasing rotor speed (Mach number). The D-factor values corresponding to design rotor speed are consistently higher than those corresponding to 50 and 70% design speed.

c. Loss Parameter

Loss parameter, $\bar{\omega}_1' - 2 \cos \beta_2'/2\sigma$, is presented as a function of D-factor in figures V-17a, b, and c. NASA correlation curves (reproduced from Reference 3) for NASA 65-series and circular arc series rotating cascade minimum loss (reference incidence) data are shown for comparison. The data are separated in figures V-17a, b, and c according to 70 and 50% span, 90 and 30% span, and 10% span, respectively.

In general, the minimum loss data appear to be consistent with the respective NASA correlation curves for minimum-loss data. The 70 and 50% span data that correspond to incidence angles greater than minimum loss incidence indicate D-factor loading level values up to 0.51 at loss parameter levels that are equivalent to the NASA minimum-loss correlation curve. D-factor values as high as 0.64 at loss levels below the NASA curve are indicated for the blade tip (10% span) data. Although the 90 and 30% span data are slightly above the NASA correlation curve that includes data for these span locations, they extend the loading level range to approximately D = 0.70 without a sharp rise in loss. The results of these comparisons are very similar to the results obtained with slotted Rotor 1, reported in Reference 3. The present results tend to support the indication reported therein that the present slot design and location may be more effective at high incidence angles than at design incidence.

d. Stress Survey Results

A brief stress survey program was performed with slotted Rotor 2 to define the bending and torsion stress characteristics over the planned operating range. Transient recordings of strain gage data as shown in figure III-13 were obtained at each rotor speed condition as the throttle vanes were actuated to reduce flow rate, and along the choke and an approximate operating line as shown in figure V-18.

Bending stress levels were less than 5000 psi along the choke and assumed operating lines as well as the major portions of the constant speed lines. Stall stresses ranged from 13,100 psi at 50% design speed to 45,000 psi at 100% design speed.

First bending and torsion vibration frequencies at design rotor speed were 465 to 490 cps and 1160 to 1250 cps, respectively, which are in good agreement with the calculated values given in Reference 1.

e. Rotating Stall Results

Rotating stall measurements were obtained with three Kistler pressure transducers during the stress survey program as the stall region was approached along each speed line. A typical recording of rotating stall is presented in figure V-19. Rotating stall at each speed condition was characterized by a single stall zone that covered half the annulus and rotated at approximately 20% of the rotor speed. The stall characteristic for this rotor was abrupt at design rotor speed and relatively abrupt at 70% of design speed. Steady-state data in the stall region were not obtained at 70 and 100% of design speed due to prohibitive blade stresses. Stall was relatively gradual at 50% design speed, and two steady-state data points were recorded, as shown on the overall performance map in figure V-3.

f. Rotor Wake Survey Results

Rotor wake surveys were obtained at three flow conditions along each speed line: choke, approximately maximum efficiency, and near stall. A hot-film anemometer probe (figure III-12) was traversed behind the rotor from the inner to the outer wall to obtain blade wake definition at several span locations. A sample of the anemometer output on either side of each desired radial location was displayed on an oscilloscope so that from 10 to 15 consecutive wake traces for an isolated blade were superimposed. The oscilloscope display thus established is presented in figures V-20 through V-22. Major scale division of these figures represent 1/2 in. in the horizontal direction and 60 ft/sec in the vertical direction.

The large blade wakes in the root region (90% span) at all rotor speed conditions reflect the relatively high loss coefficients for this span location. The wake shapes at the other span locations indicate the velocity deterioration on the suction surface side of the wake (left side of the wakes in the figures) as stall conditions are approached.

3. Stator

Stator inlet Mach number and air angle distribution for design rotor speed data are presented in figure V-23. Calculated design values of these two parameters are shown for comparison. The design Mach number distribution is closest to the measured distribution at stall flow conditions. The inlet air angle comparison shows that the stator was not very well matched to the rotor. The midspan region operated with 2 to 14 deg less than design incidence over the flow range. At near design flow conditions the stator was operating 1 deg above design incidence at the tip (10% span), 4 deg less than design incidence at midspan, and about 2 deg above design incidence at the root (90% span). This incidence distribution is not considered to have adversely affected the rotor evaluation near design flow operating conditions. Vector diagrams and blade element data as obtained with unslotted Stator 1 behind slotted Rotor 2 are included in table B-2 for general information. An analysis of unslotted Stator 1 data will be presented in a subsequent report under this program as appropriate for comparison with slotted stator test results.

SECTION VI
CONCLUDING DISCUSSION

Blade element data at five radial locations and overall performance data were obtained for a slotted rotor configuration at several flow conditions, including choke and near-stall, along three rotor speed lines, 50, 70, and 100% of the design speed. Measured slotted rotor pressure ratio and efficiency were lower than the design values predicted for the same rotor without slots. Maximum efficiency for the slotted rotor at design equivalent speed was 88.5% compared with a calculated design efficiency of 0.90, and the corresponding measured pressure ratio was 1.29 compared with a design value of 1.35. At design flow conditions, the measured efficiency was 86%, and the pressure ratio was 1.30. These results reflect the relatively high deviation angle and loss coefficient in the blade root region and the high loss coefficient in the tip region. An apparent flow shift toward the midspan region (particularly from the root region) is suggested by the relatively low values of efficiency at the 10 and 90% span positions in table B-2. Stator losses resulted in a stage maximum efficiency of 83.5% and a stage pressure ratio of 1.27.

The loading levels achieved, as indicated by D-factor, were approximately equal to the predicted values based on normal deviation angles in the root and tip regions, and slightly lower than similarly predicted values at the 30, 50, and 70% span locations. Measured deviation angles for the slotted rotor were within 1 deg of the predicted values at all span locations except at 90% span from the tip. At 90% span the measured deviation angle was about 6 deg more than the predicted value. Measured loss coefficients for the slotted rotor were comparable to the predicted values in the middle of the blade, and considerably higher than predicted values at the root and the tip.

It is difficult to assess the absolute effectiveness of slots on the basis of comparison of measured performance with the calculated performance derived from conventional loss and deviation correlations. On the basis of these comparisons, at design incidence, it might be concluded that the slot had little, if any, favorable effect on rotor performance. On the basis of the comparison of measured D-factor and loss parameter with NASA

design curves from Reference 3, it is concluded that the slots produced a favorable effect on blade profile loss at incidence angles above the minimum loss incidence, particularly in the tip region. The fact that slotted Rotor 2 did not achieve the design pressure ratio calculated for the rotor without slots is attributed to the flow deterioration in the blade root region, although the specific cause of this deterioration has not yet been determined.

Further analysis of the results is in progress to fully evaluate the possible interaction effects between the slotted rotor and the unslotted stator. The results of this analysis as they are pertinent to the overall program objectives will be published in the final report under this program.

SECTION VII
ILLUSTRATIONS

This section contains the illustrations that have been referenced in the preceding sections.

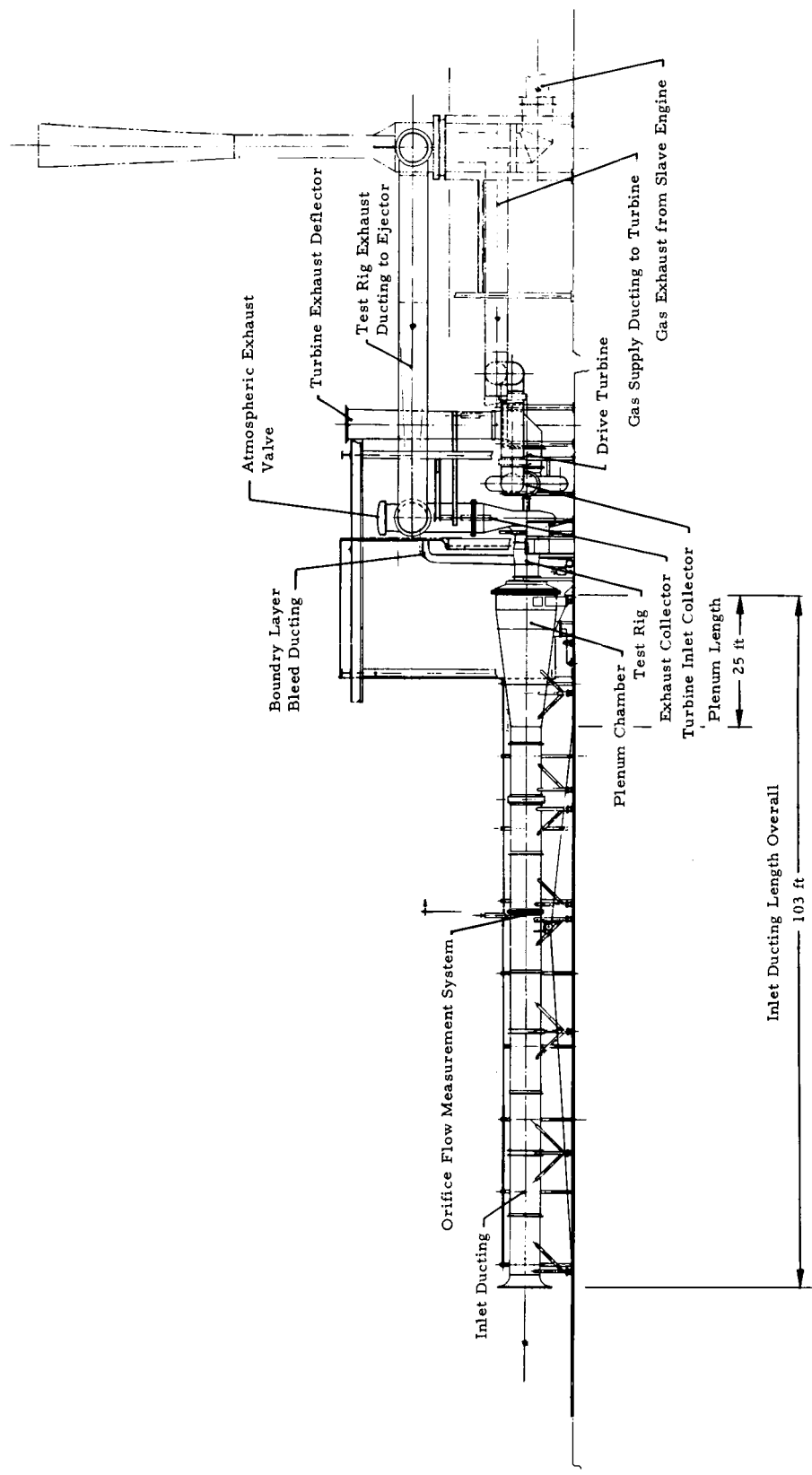


Figure III-1. Compressor Research Facility

FD 10891B

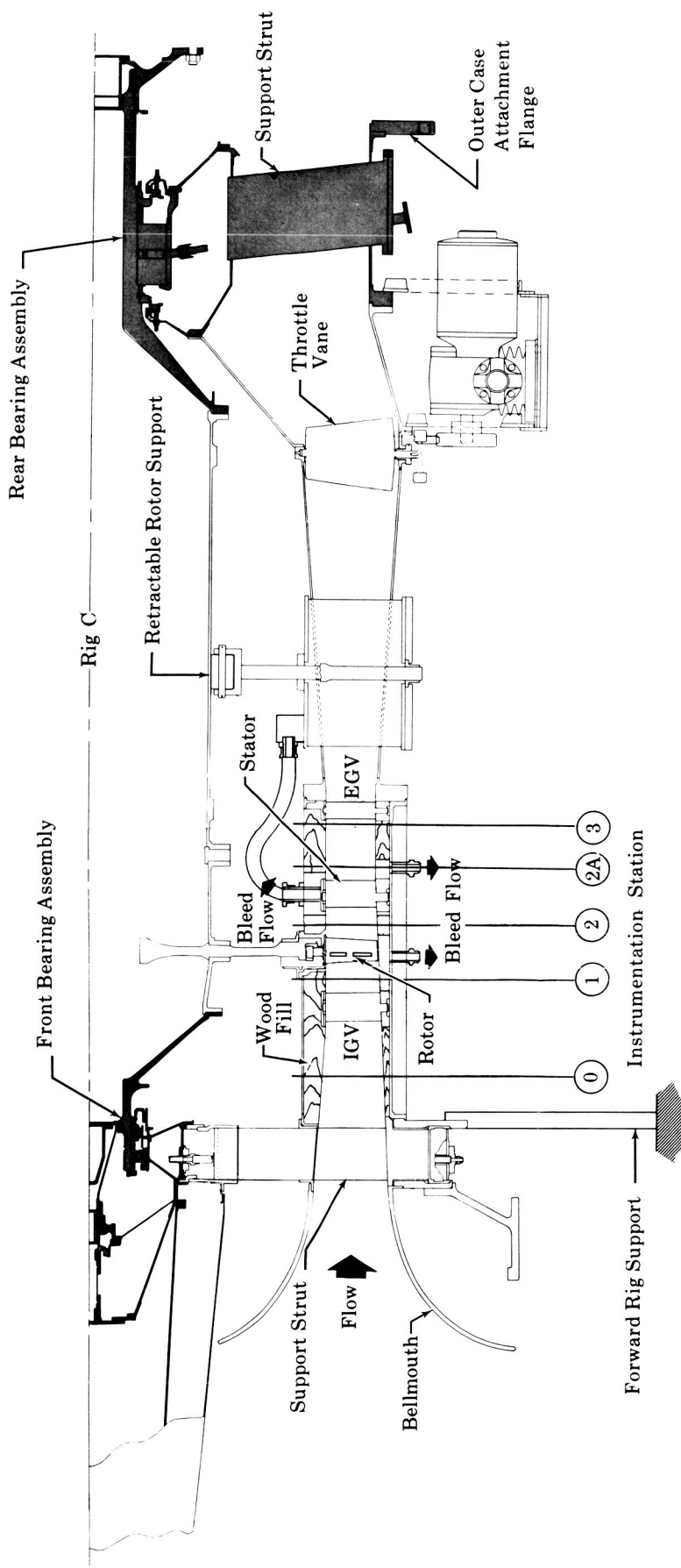
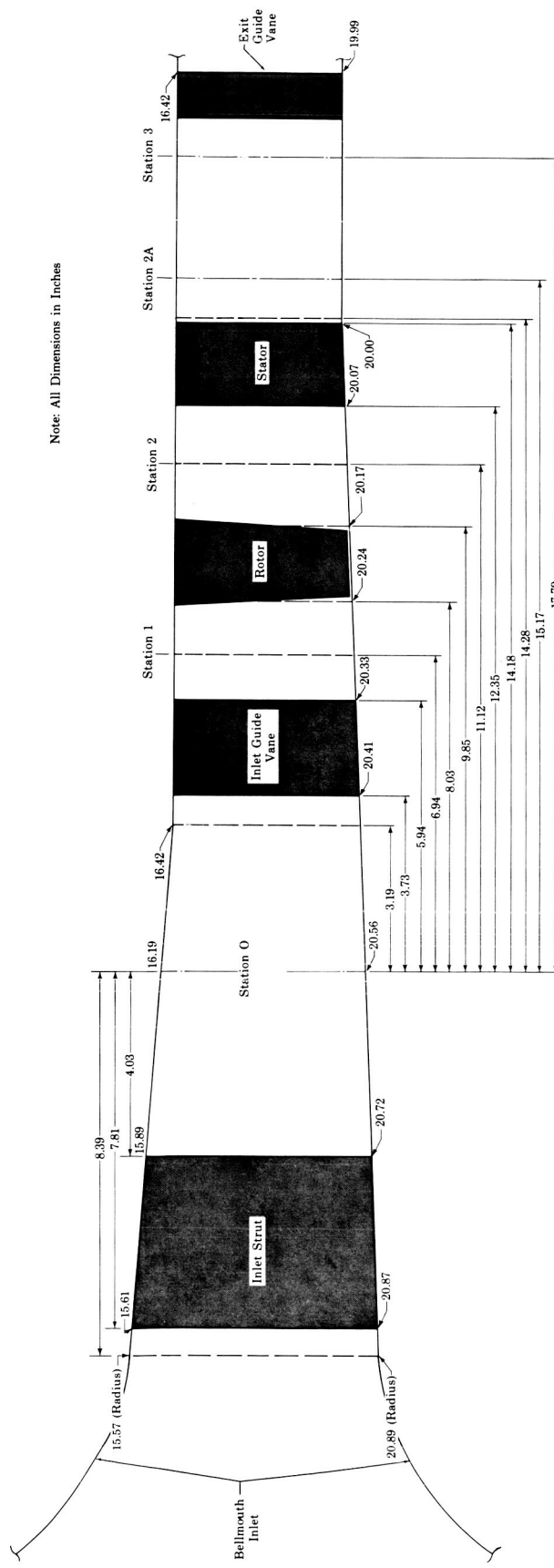


Figure III-2. Rotating Axial Flow Cascade Test Rig

FD 14685



VII-4

Figure III-3. Flow Path

Rig E

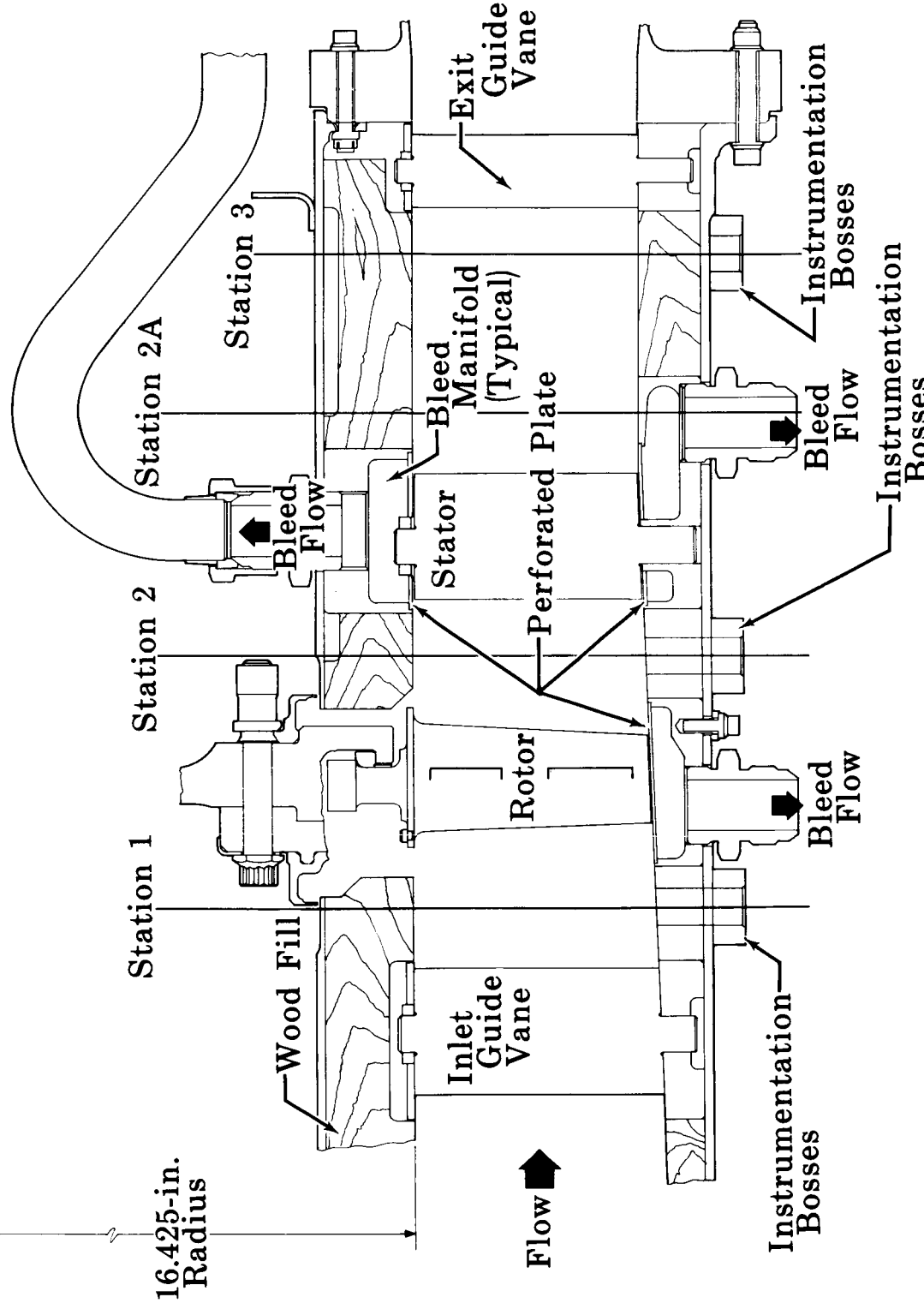


Figure III-4. Rotating Cascade Rig Bleed System

FD 14683

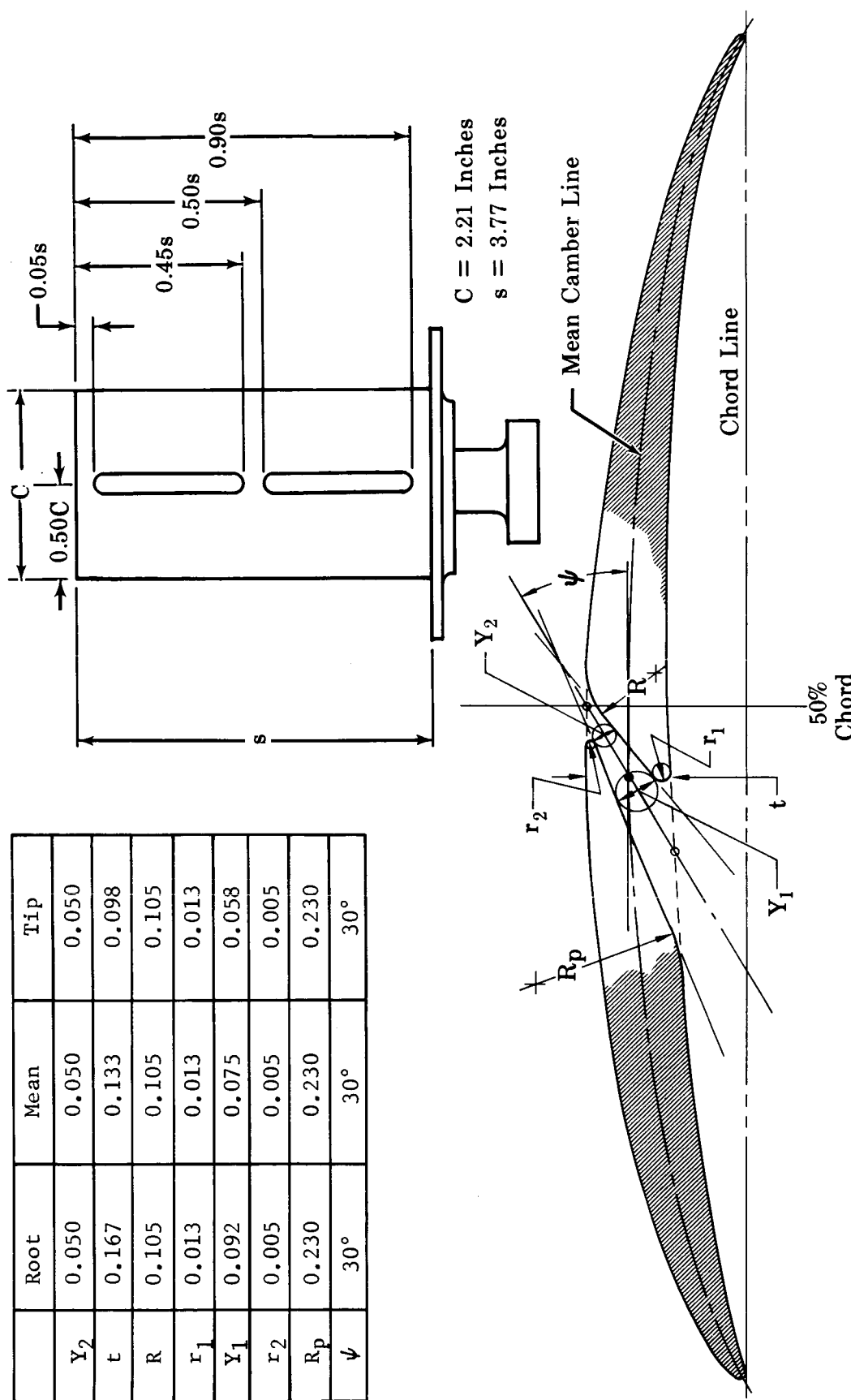


Figure III-5. Slot Geometry and Location

FD 19357

b. Pressure Surface

a. Suction Surface

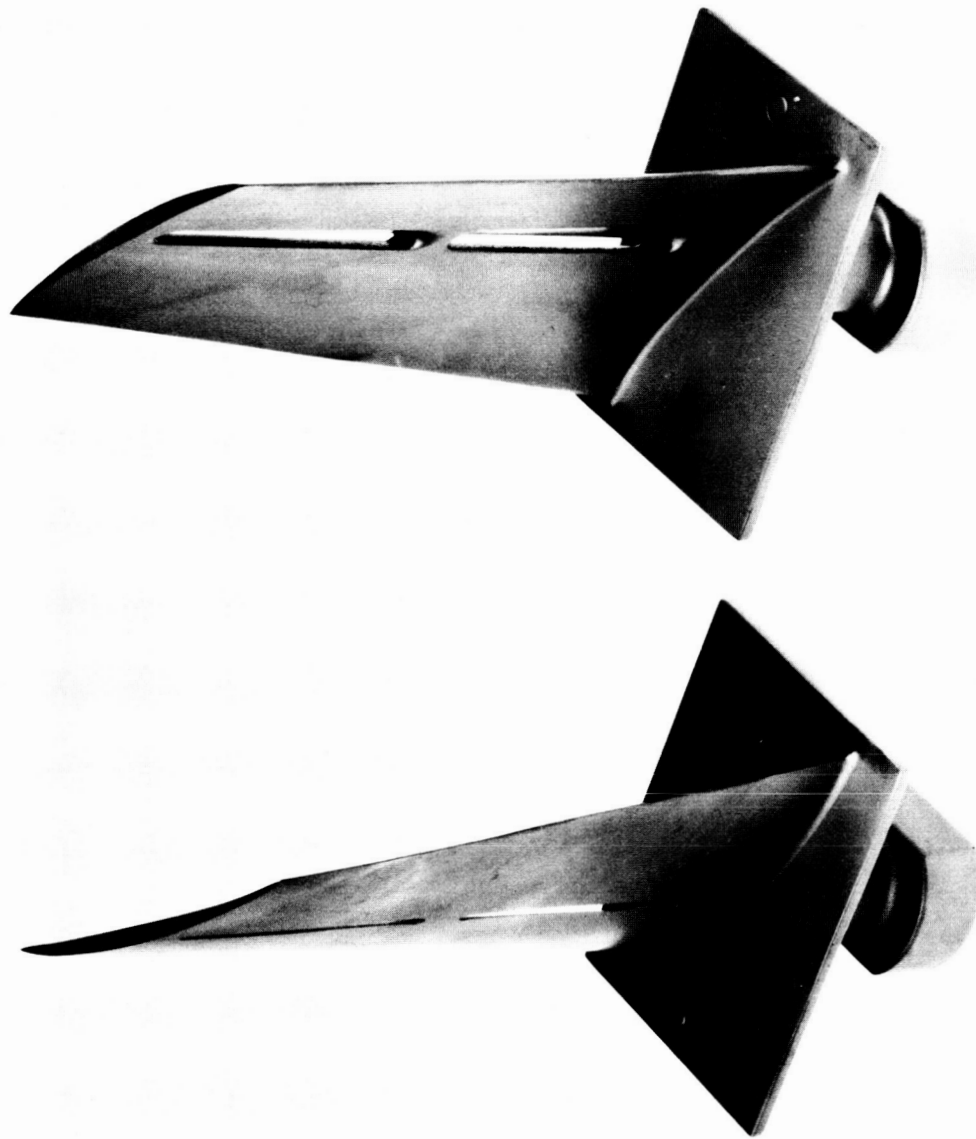
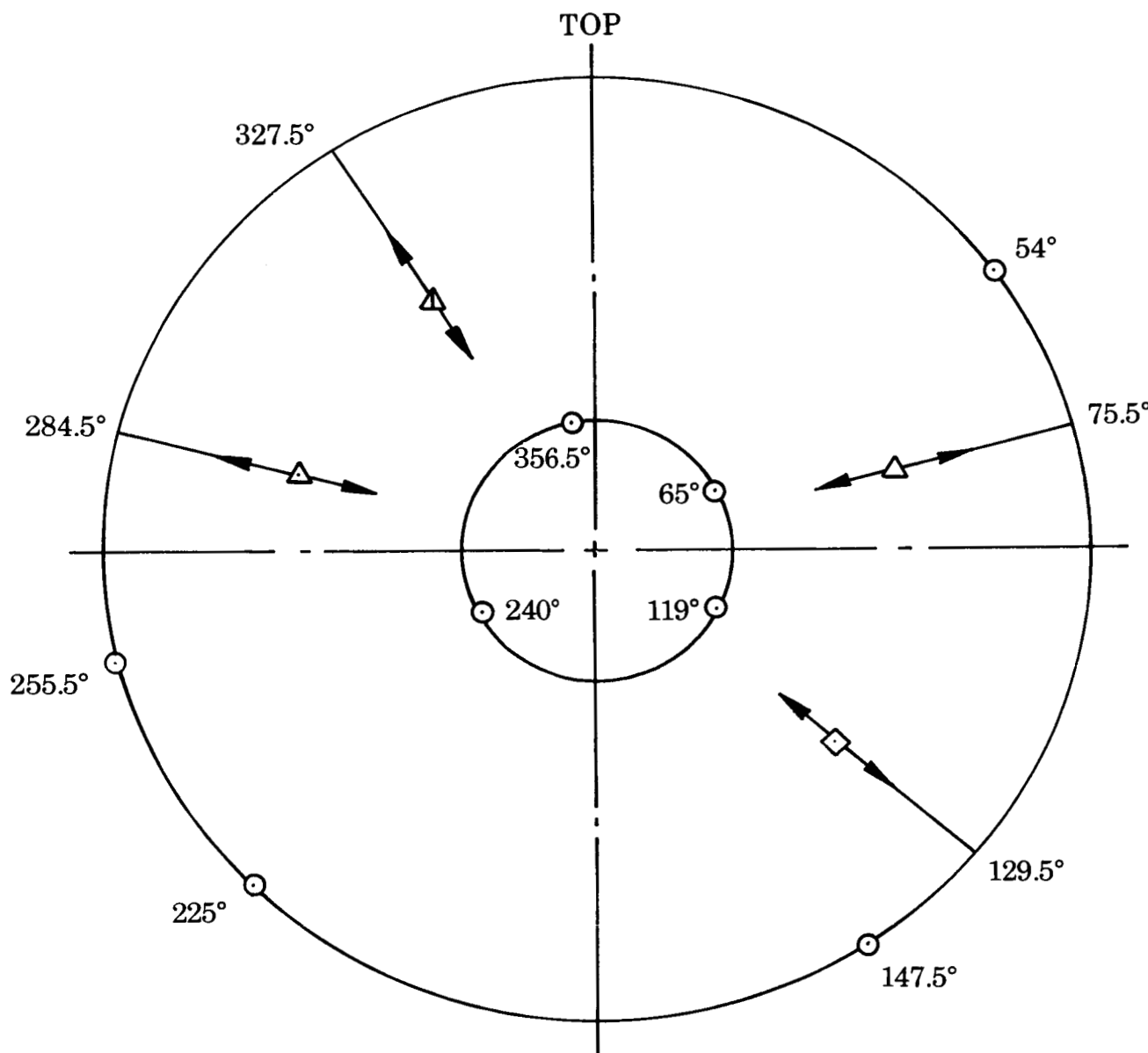


Figure III-6. Typical Slotted Rotor 2 Blade

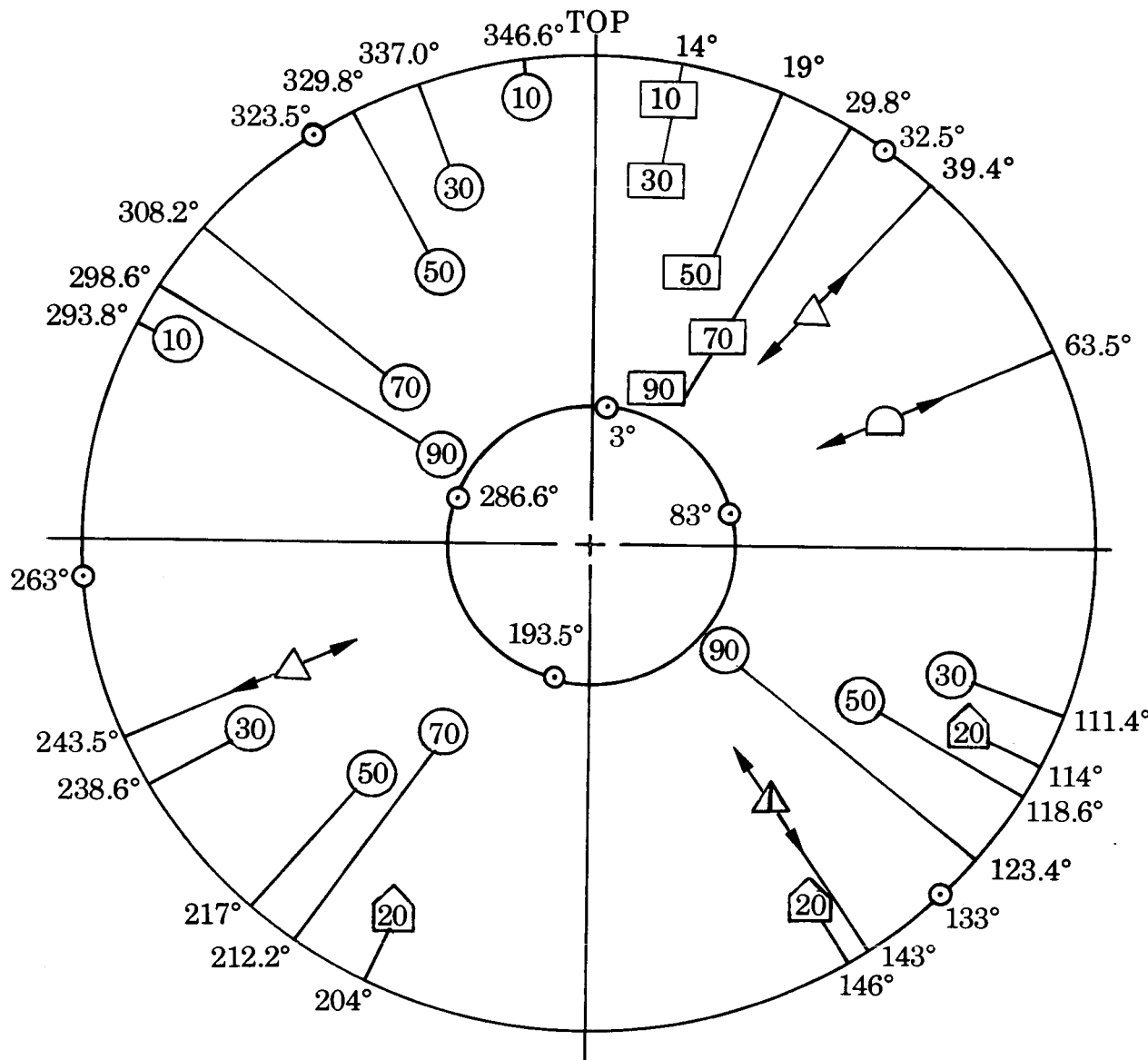


- Wall Static Pressure
- △ Traverse Wedge Probe, 20°
- ▲ Traverse Wedge Probe, 8°
- ◇ Traverse Wake Probe

Probe angular position is measured clockwise from the top.

Figure III-7. Instrumentation, Station 1
(View Looking Downstream)

FD 18596B



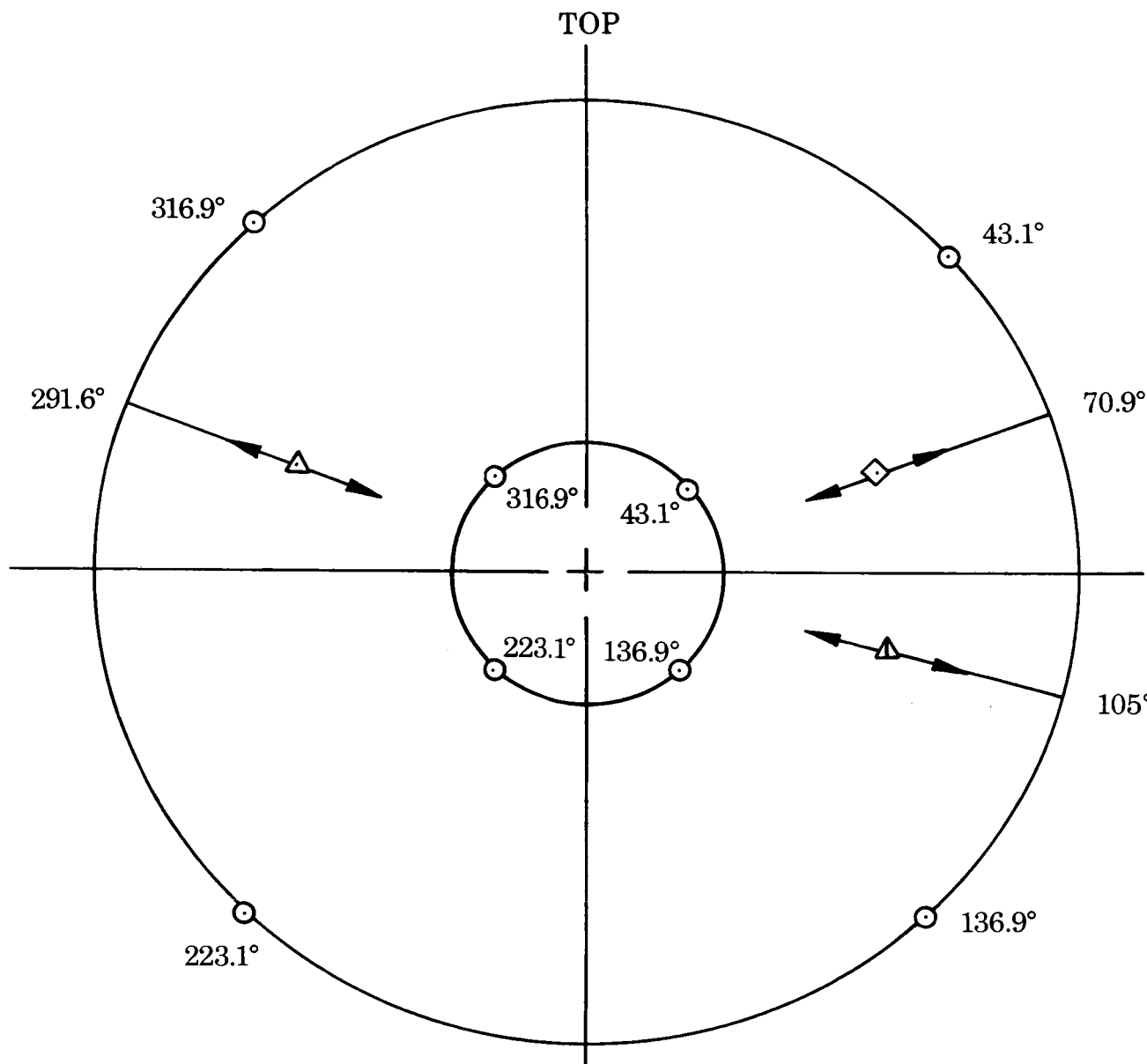
- Keil Probe *
- Wall Static Pressure
- △ Traverse Wedge Probe, 20°
- △ Traverse Wedge Probe, 8°
- Traverse Hot Film Probe
- Kiel Temperature Probe
- ◇ Kistler Probe *

Probe angular position is measured clockwise from the top.

*Radial location as a percent of span from tip is denoted by the number within the symbol

Figure III-8. Instrumentation, Station 2
(View Looking Downstream)

FD 18595C

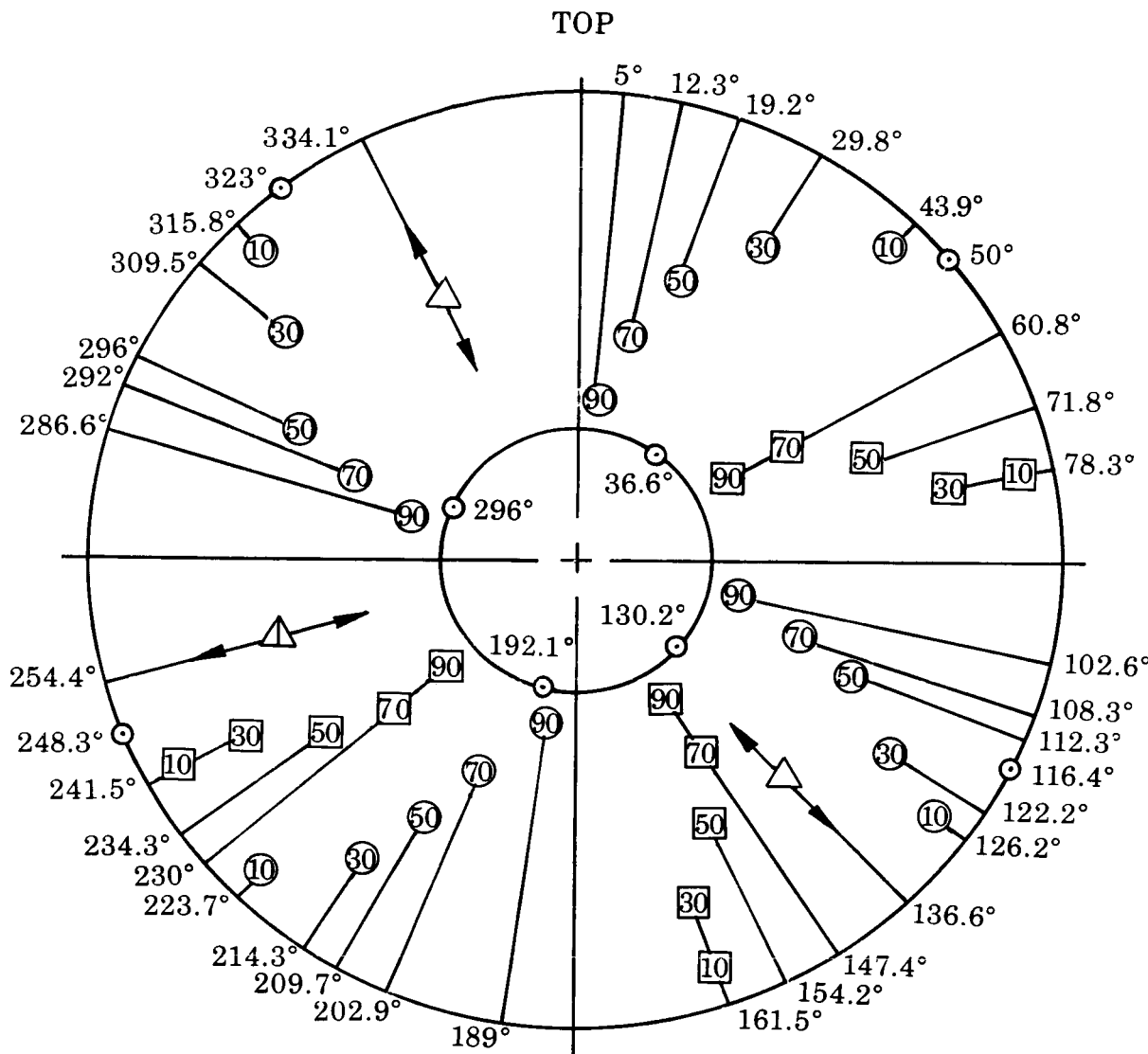


- Wall Static Pressure
- △ Traverse Wedge Probe, 20°
- ▲ Traverse Wedge Probe, 8°
- ◇ Traverse Wake Probe

Probe angular position is measured clockwise from the top.

Figure III-9. Instrumentation, Station 2A
(View Looking Downstream)

FD 18594B



- Wall Static
- △ Traverse Wedge Probe, 20°
- △ Traverse Wedge Probe, 8°
- Kiel Probe *
- Temperature *

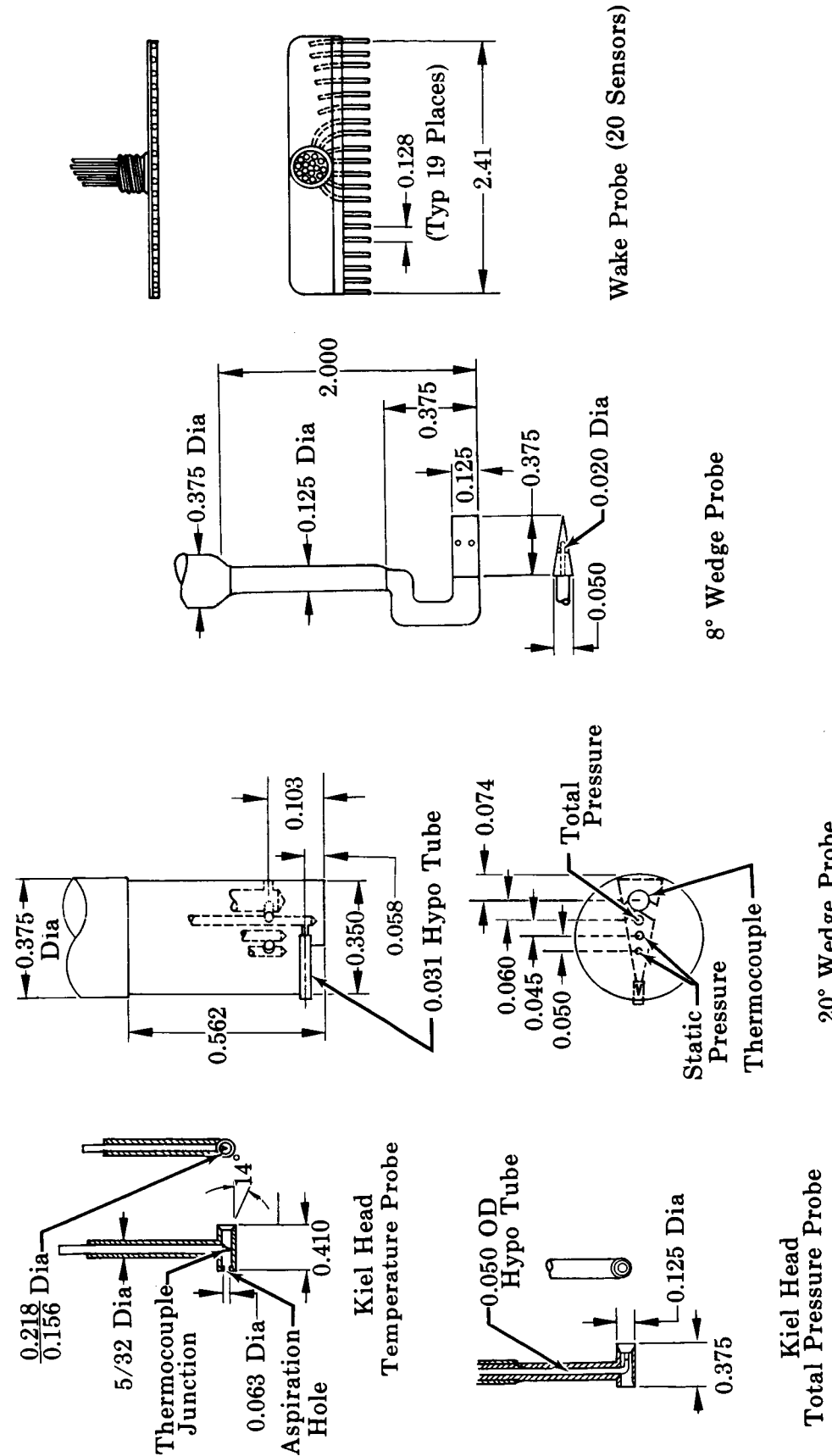
Probe angular position is measured clockwise from the top.

*Radial location as a percent of span from tip is denoted by the number within the symbol

Figure III-10. Instrumentation, Station 3
(View Looking Downstream)

FD 18597C

Note: All Dimensions Are in Inches.



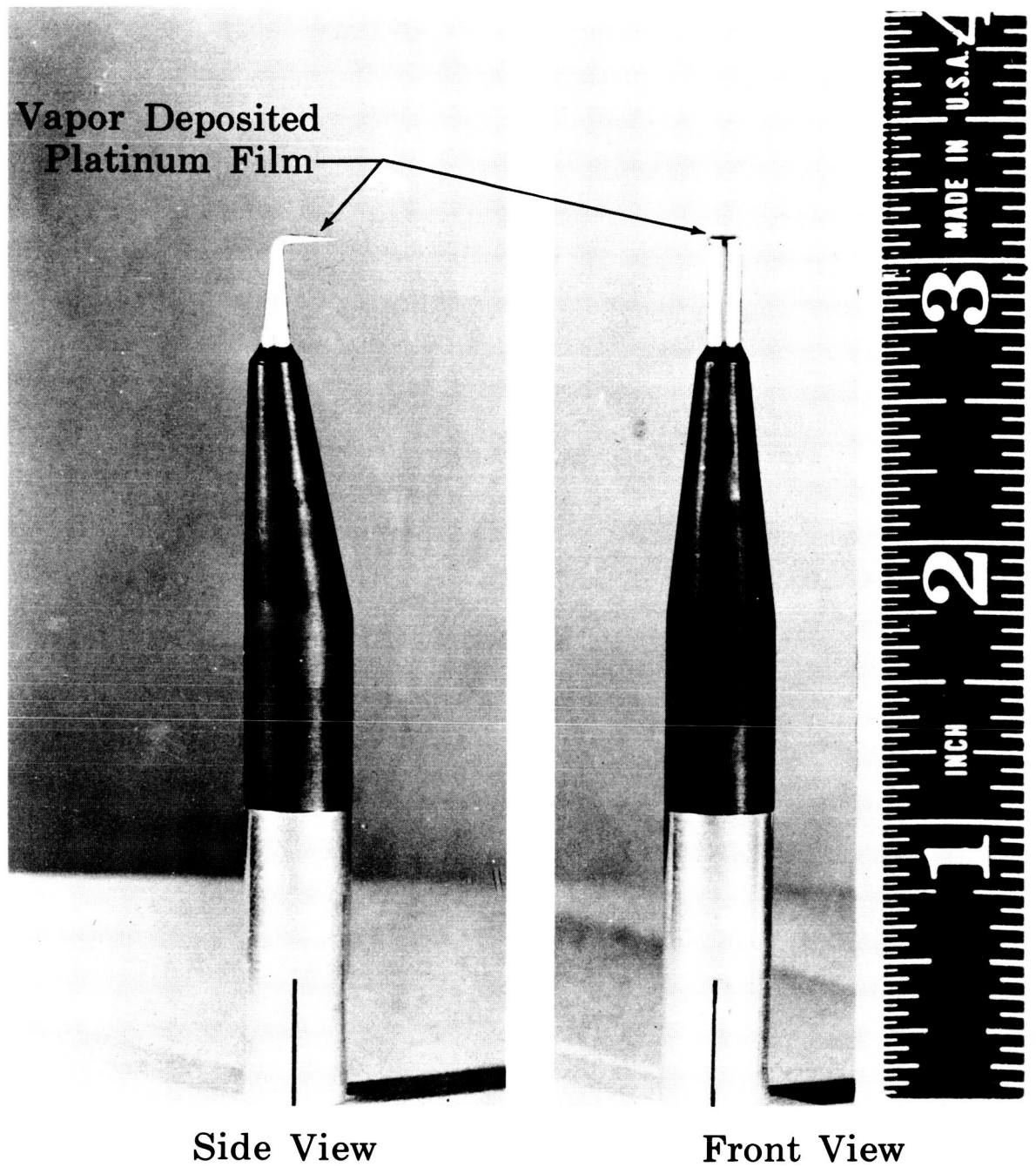


Figure III-12. Anemometer Probe

FD 18603

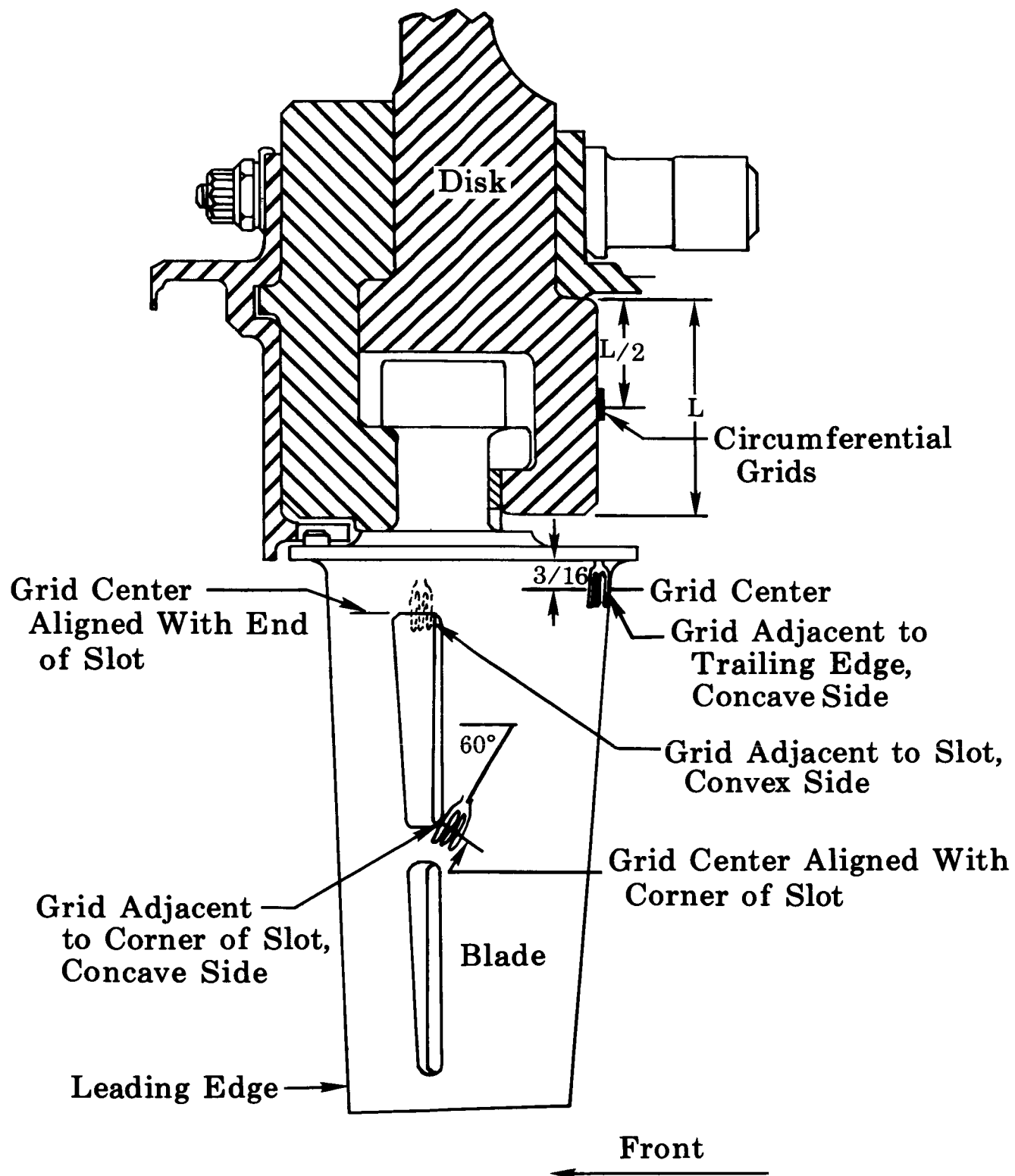


Figure III-13. Strain Gage Locations

FD 18598

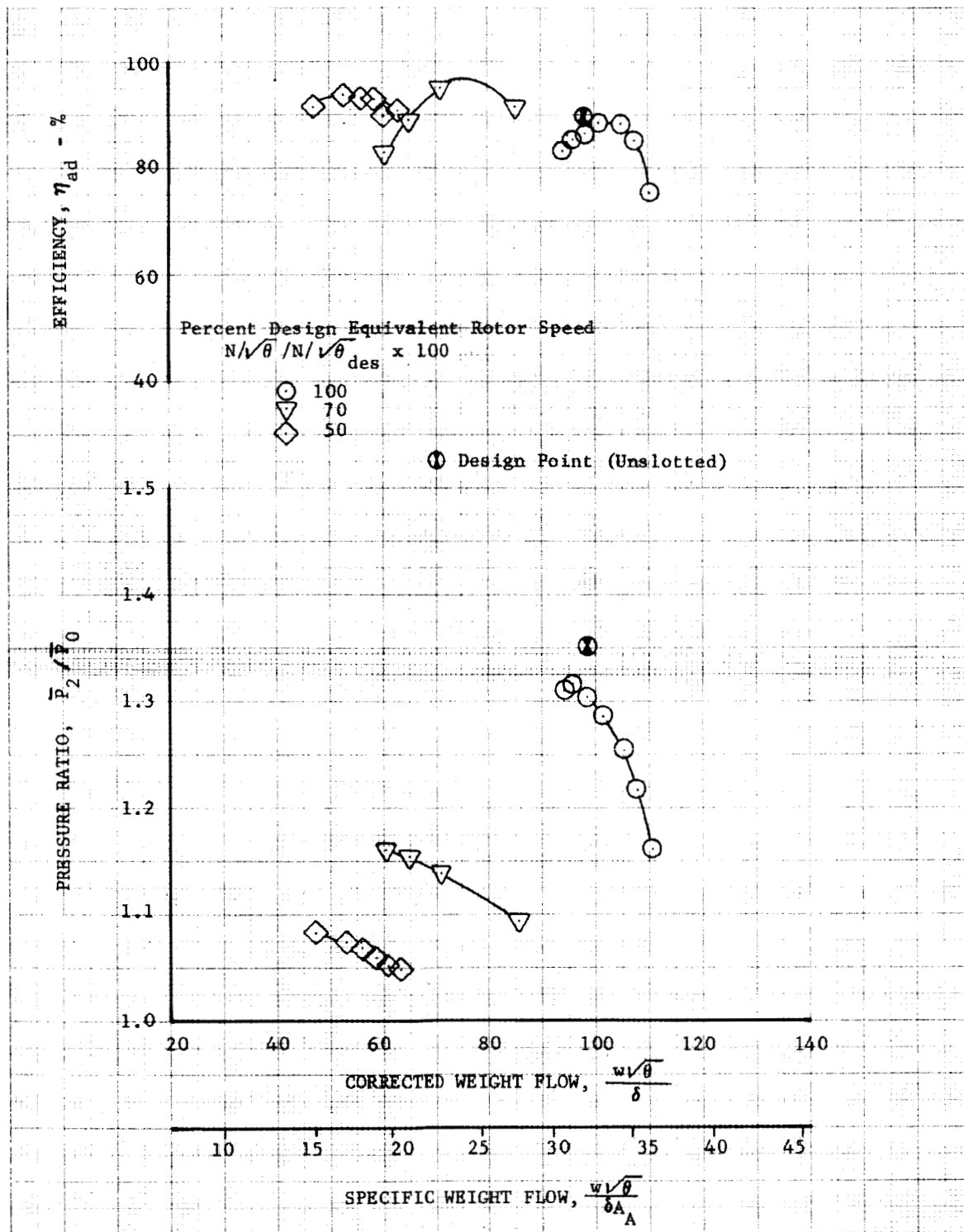


Figure V-1. Overall Performance; Slotted Rotor 2 Only

DF 52283

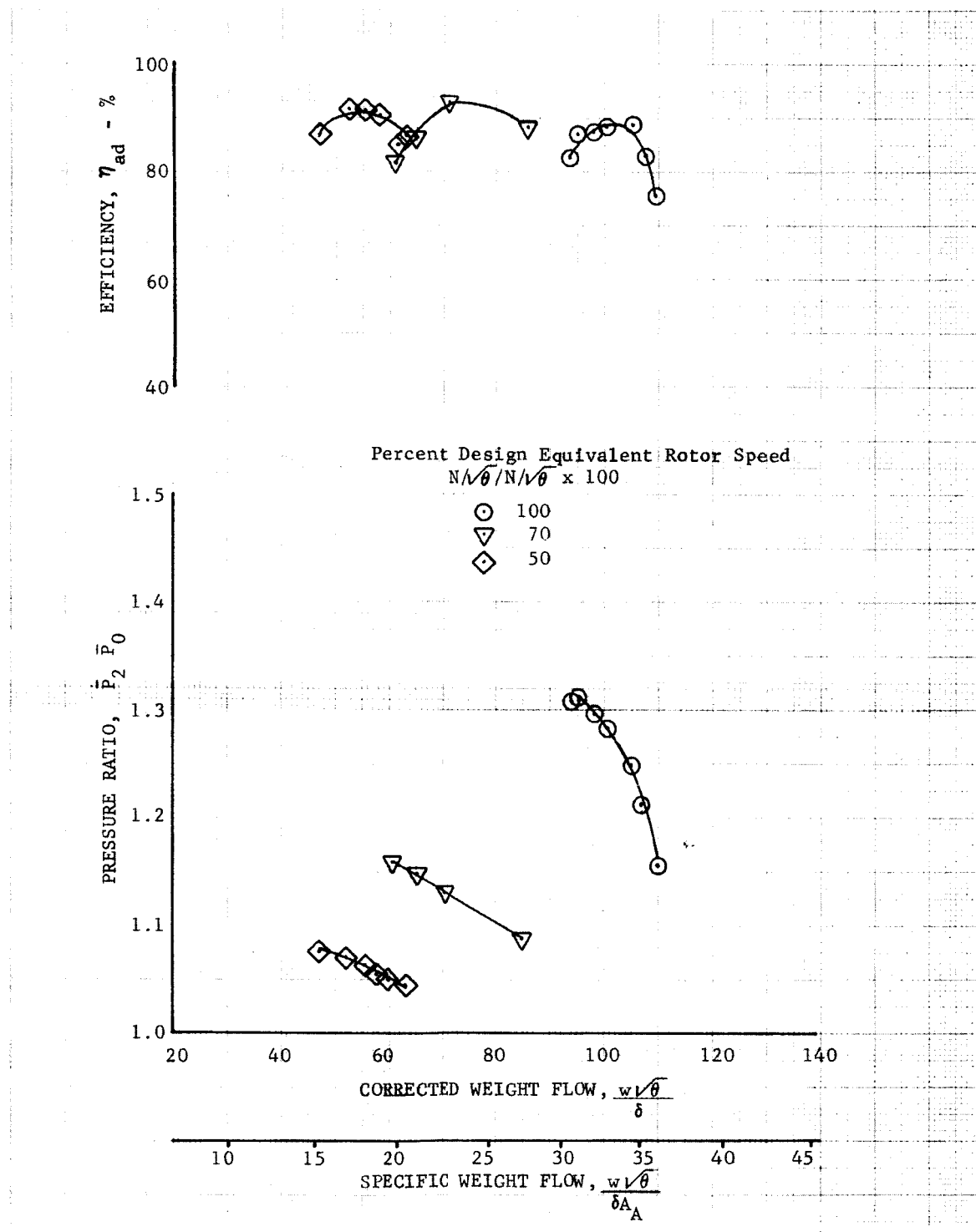


Figure V-2. Overall Performance; Inlet Guide Vane,
Slotted Rotor 2

DF 52284

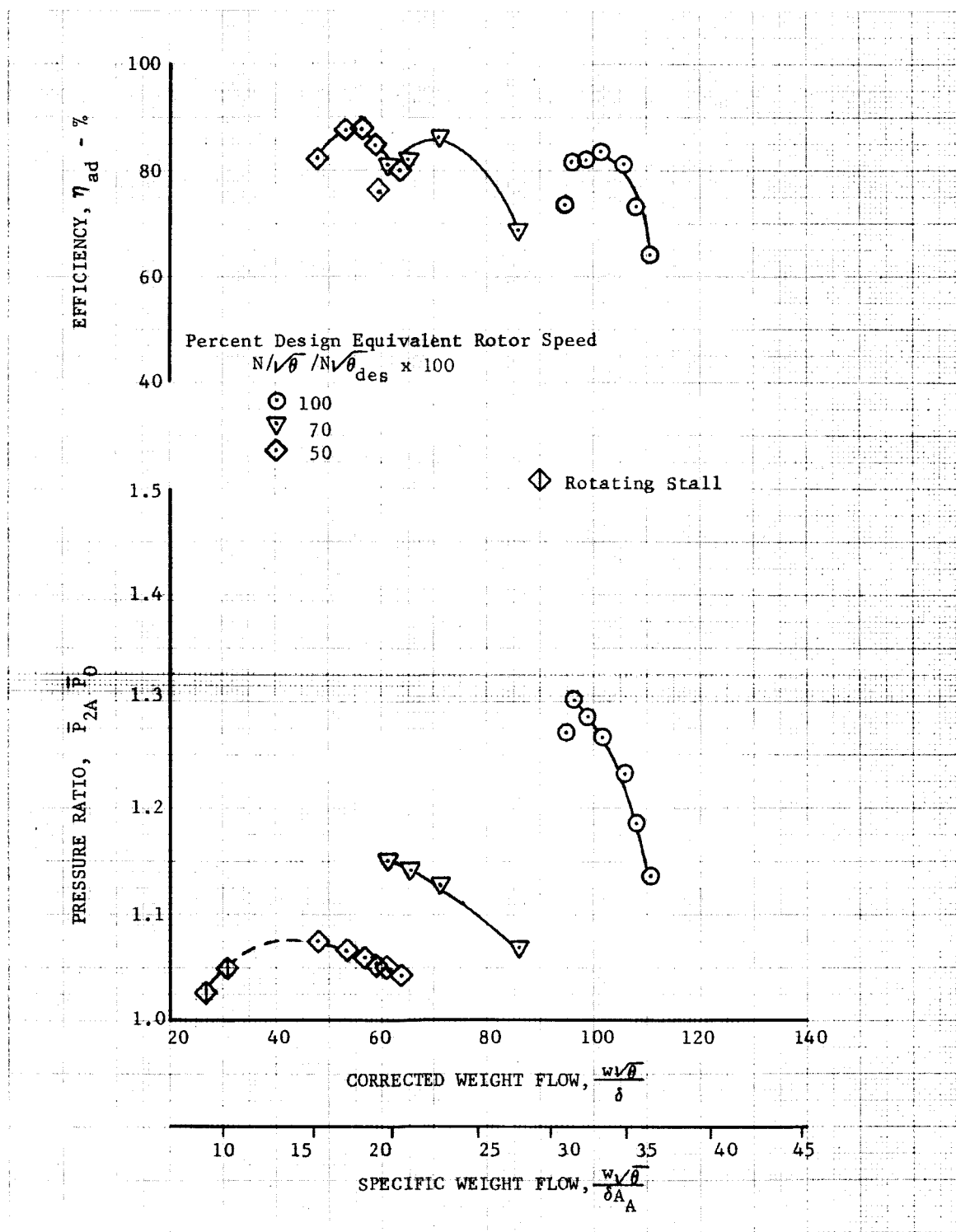


Figure V-3. Overall Performance; Inlet Guide Vane,
Slotted Rotor 2, Unslotted Stator 1

DF 52285

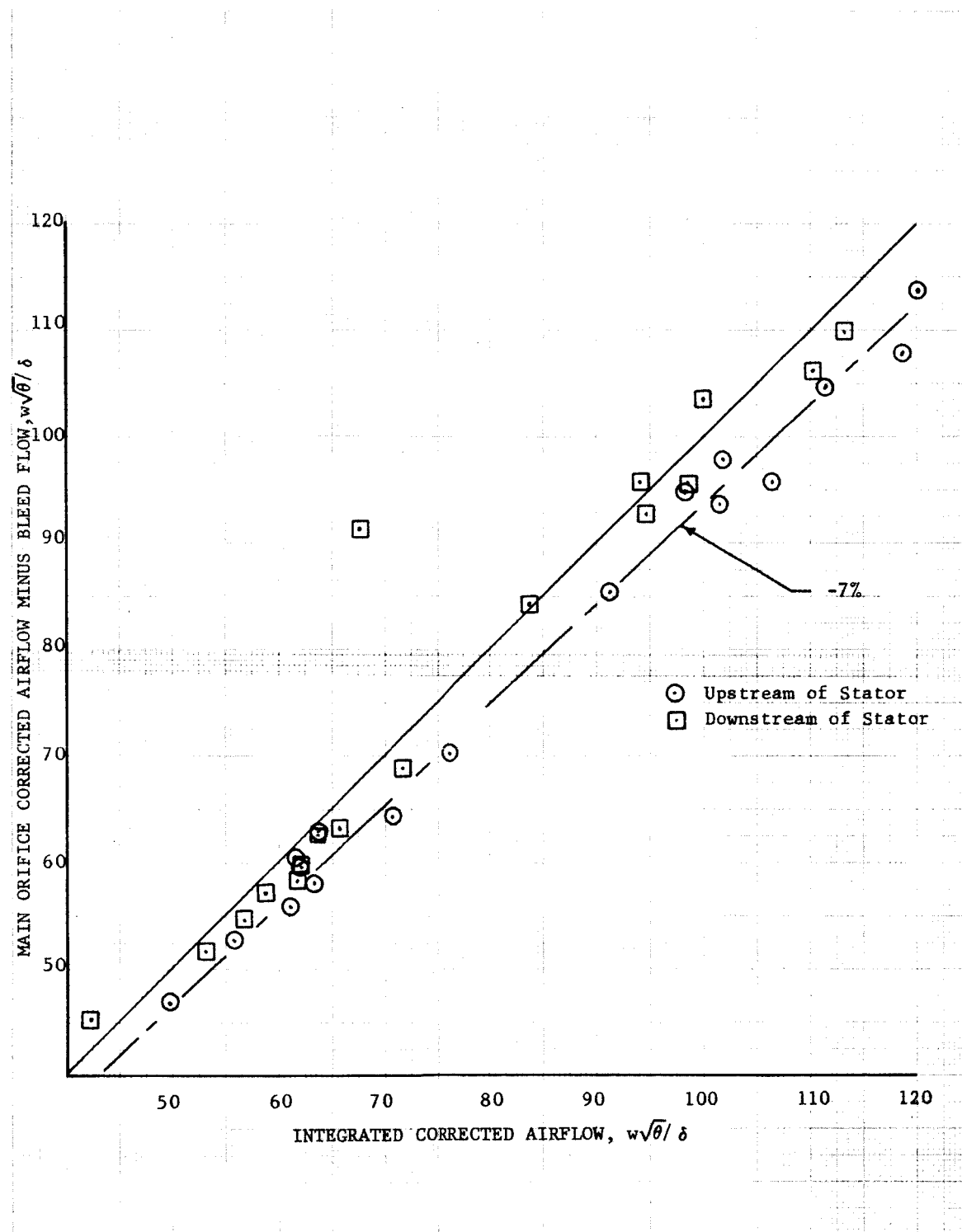


Figure V-4. Airflow Continuity Comparison

DF 52286

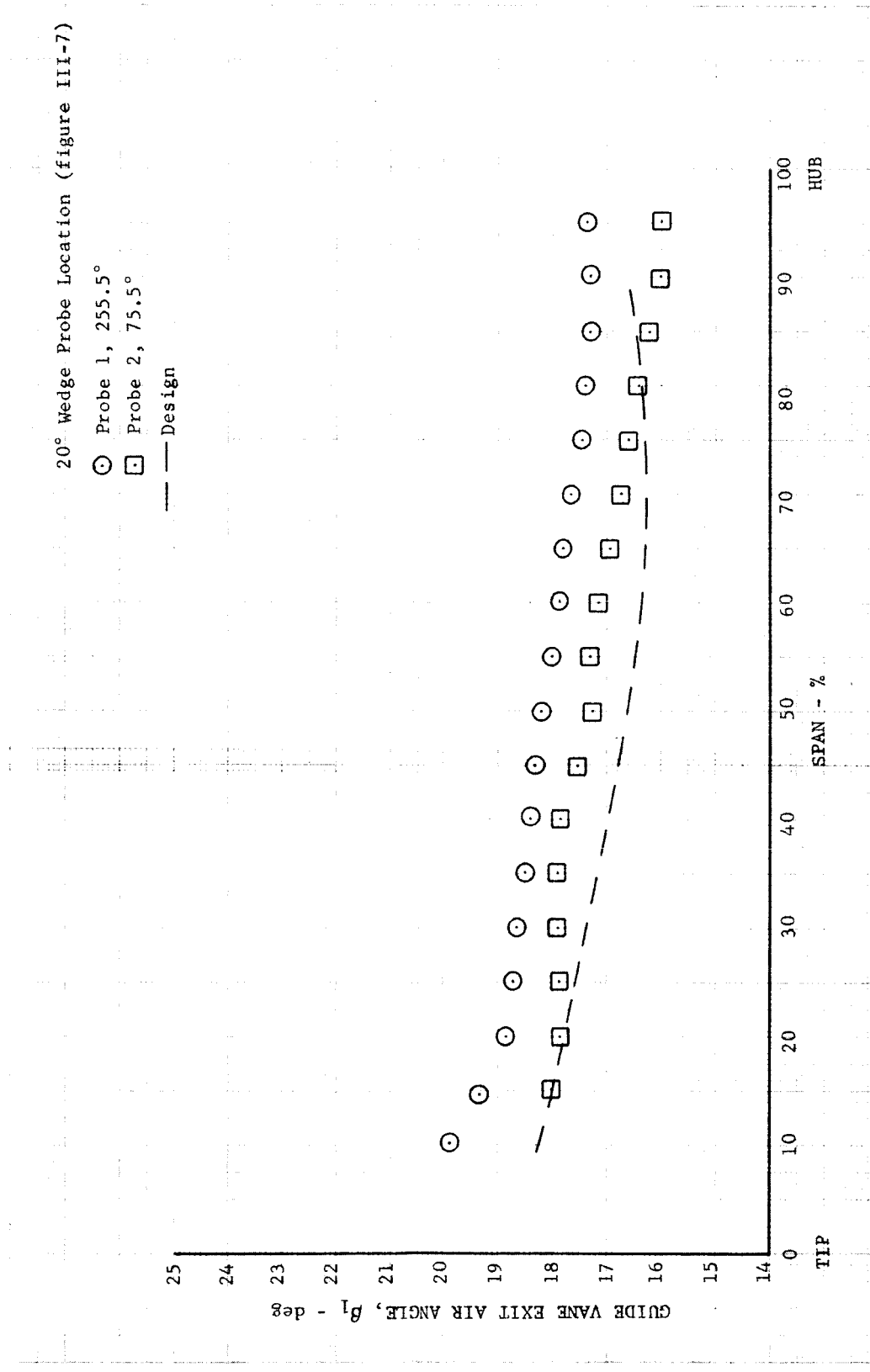


Figure V-5. Guide Vane Exit Air Angle Distribution - 100% Design Equivalent Rotor Speed

DF 52287

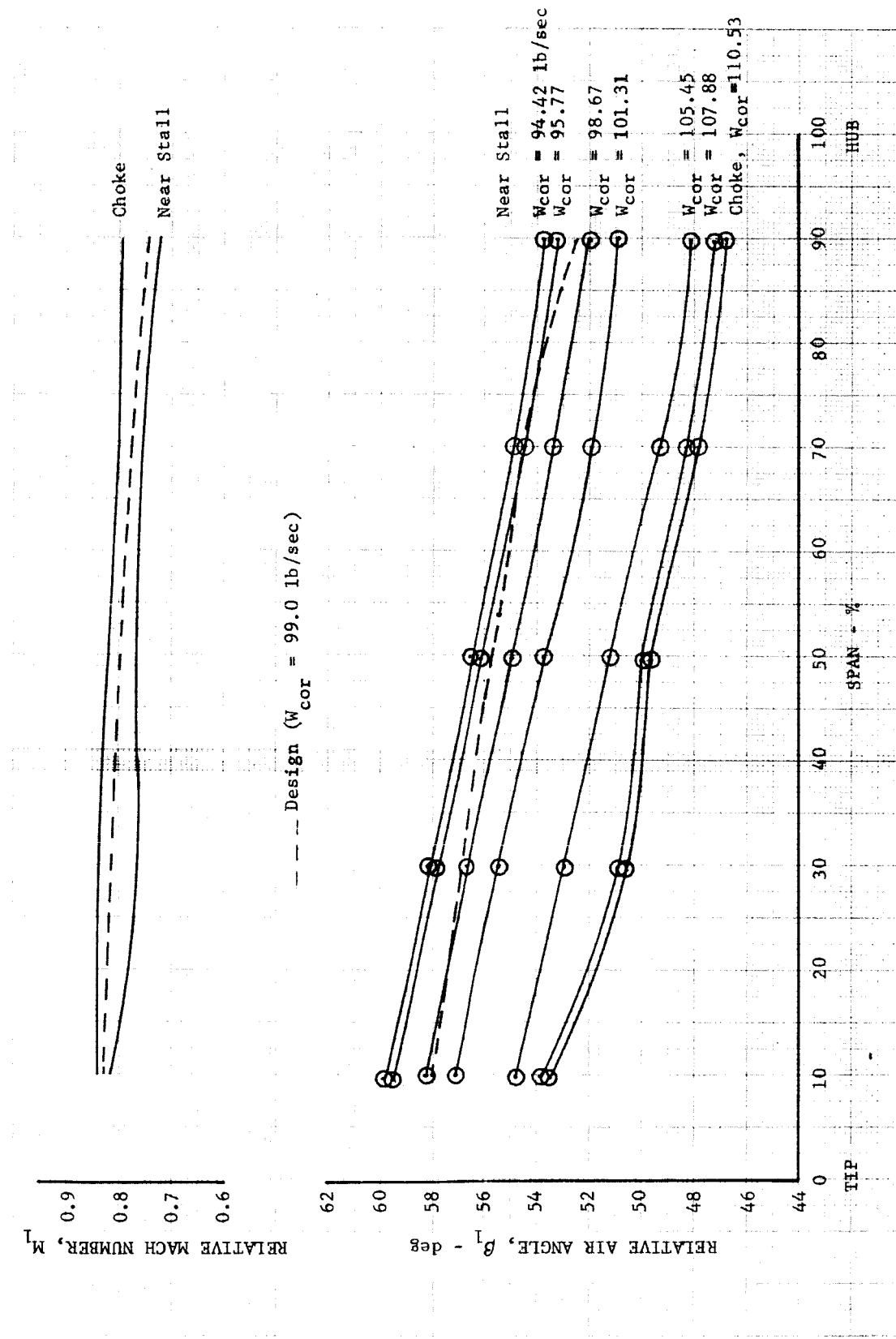


Figure V-6. Relative Air Angle and Mach Number Distribution Into Slotted Rotor 2 - 100% Design Equivalent Rotor Speed

DF 52289

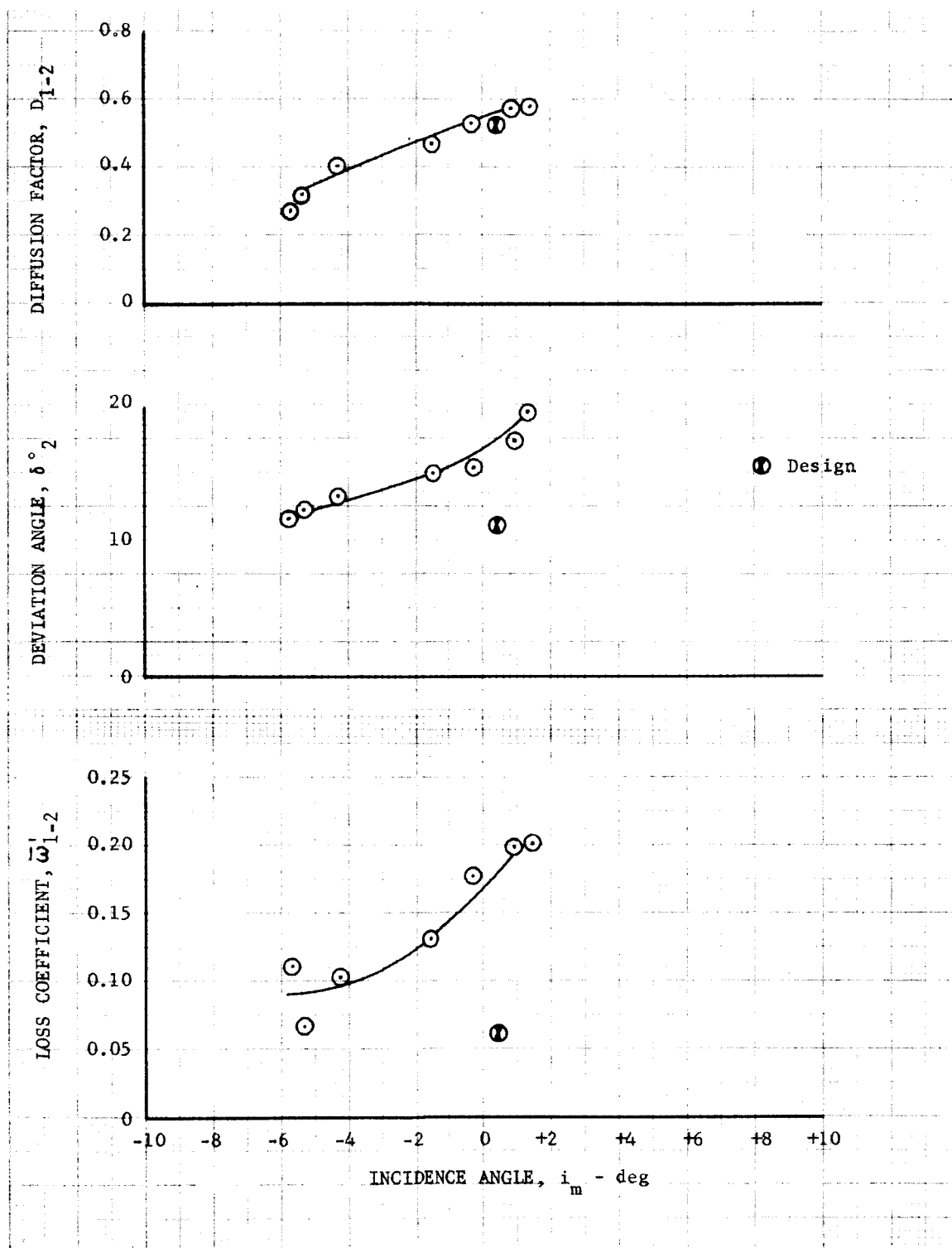


Figure V-7. Rotor Blade Element Performance - 100% Design
Equivalent Rotor Speed, 90% Span From Tip

DF 52290

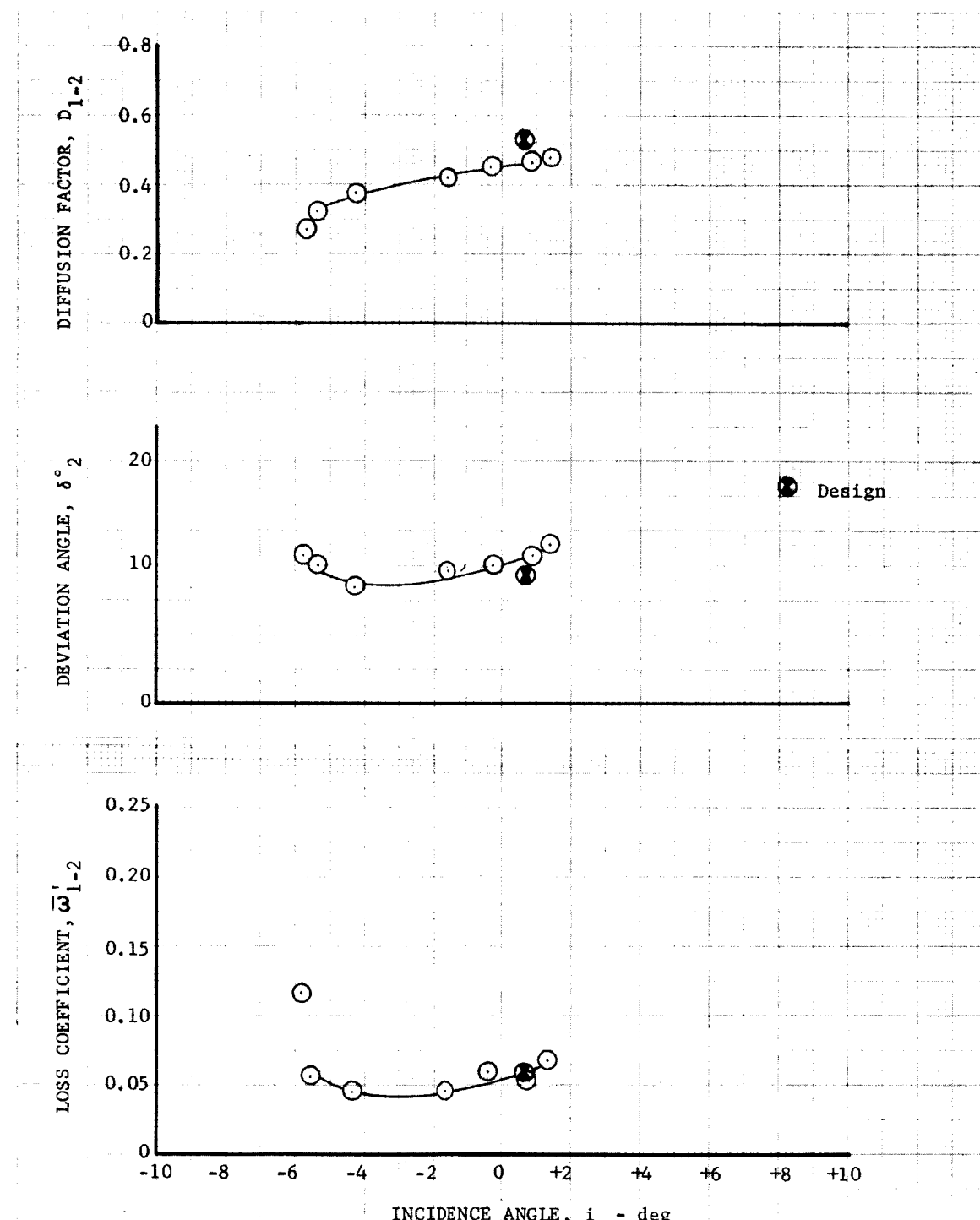


Figure V-8. Rotor Blade Element Performance - 100% Design
Equivalent Rotor Speed, 70% Span From Tip

DF 52291

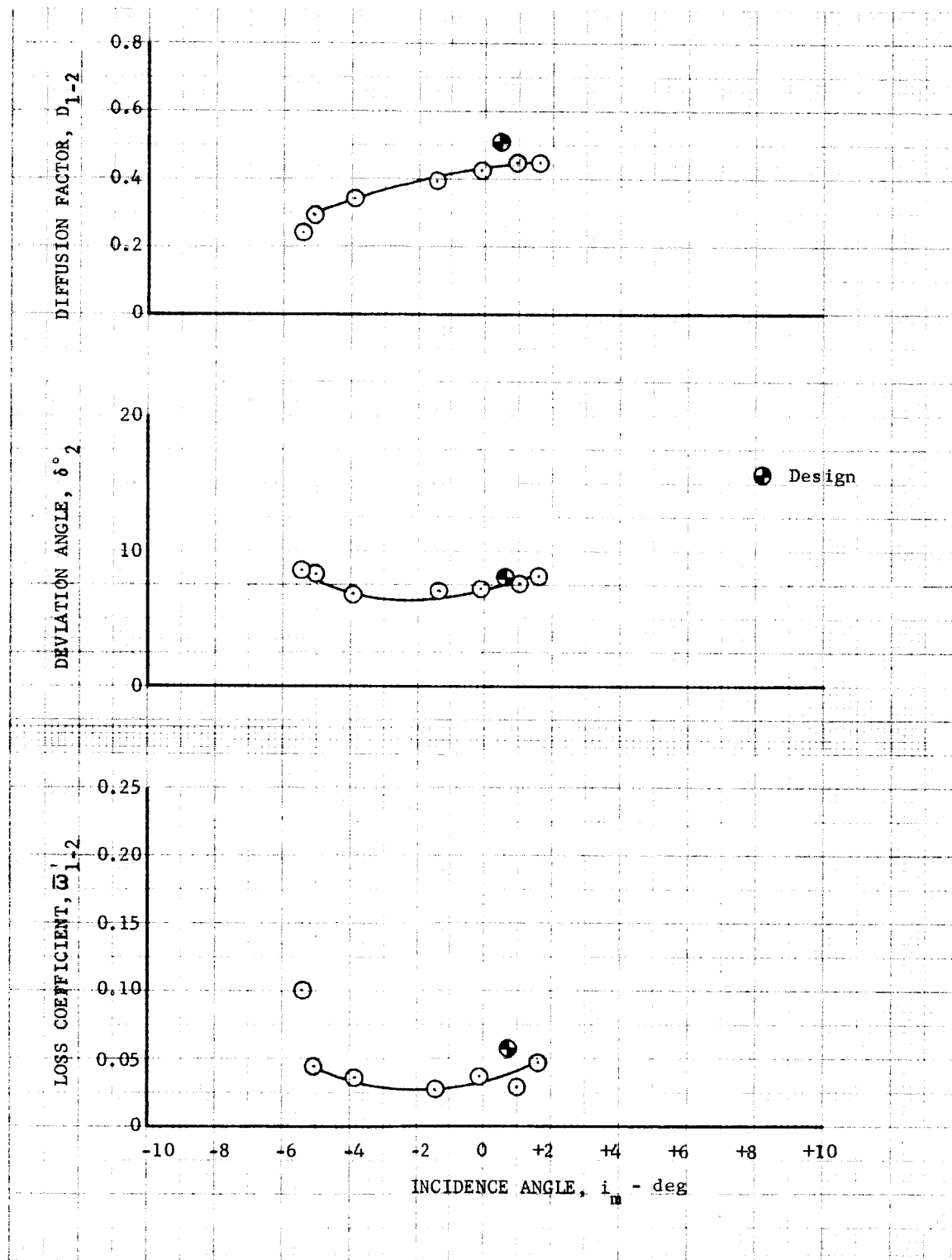


Figure V-9. Rotor Blade Element Performance - 100% Design
Equivalent Rotor Speed, 50% Span From Tip

DF 52292

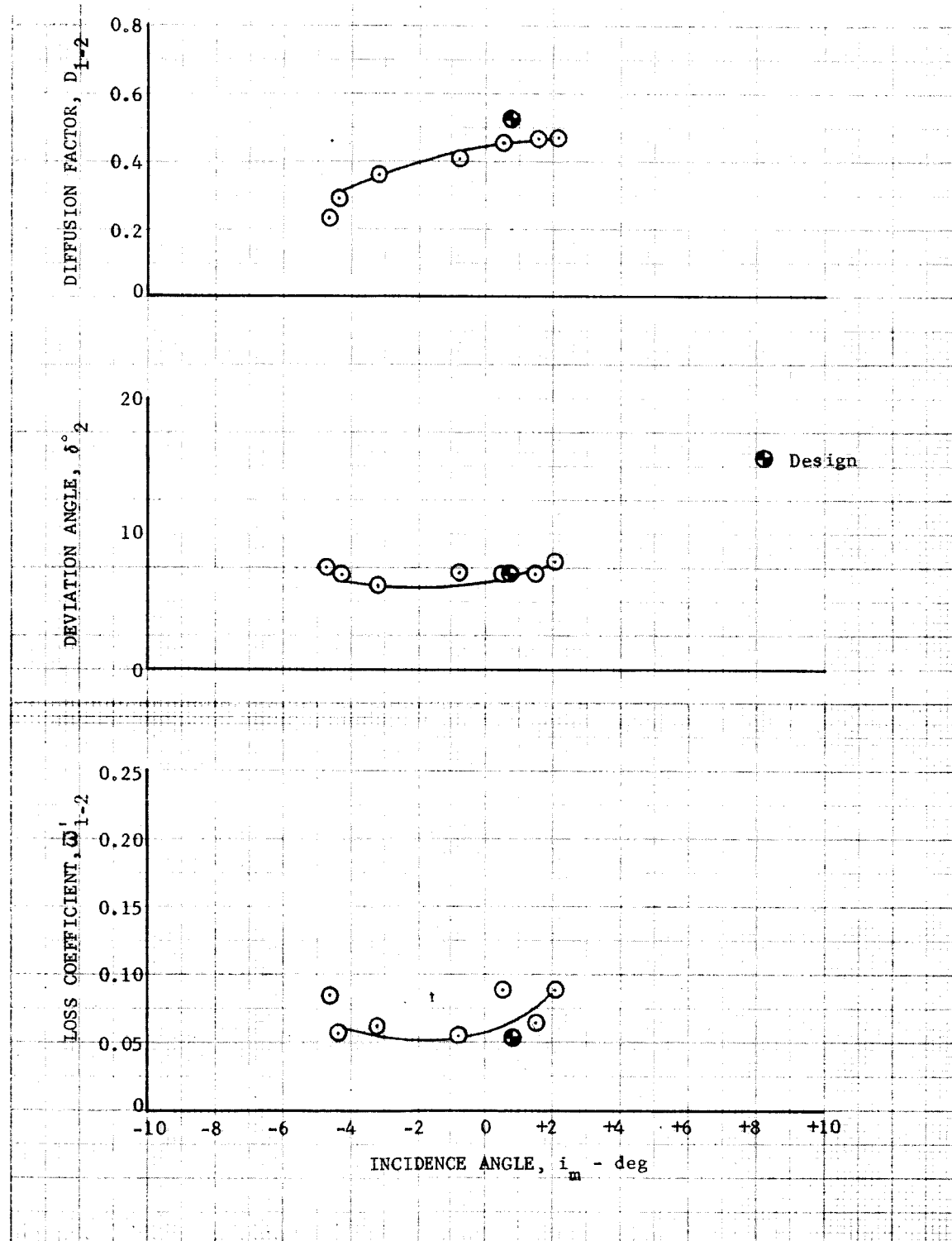


Figure V-10. Rotor Blade Element Performance - 100% Design
Equivalent Rotor Speed, 30% Span From Tip

DF 52293

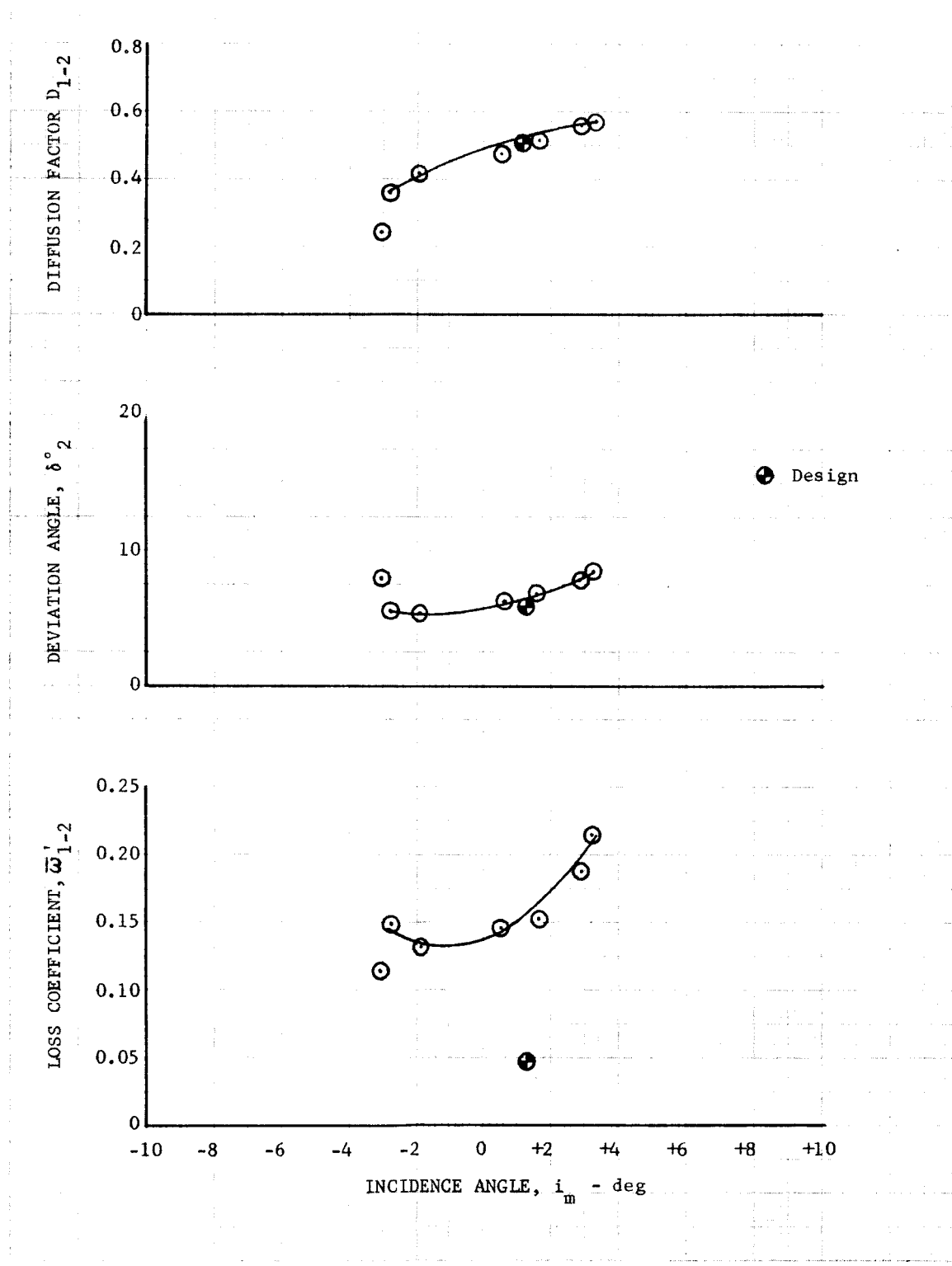


Figure V-11. Rotor Blade Element Performance - 100% Design
Equivalent Rotor Speed, 10% Span From Tip

DF 52294

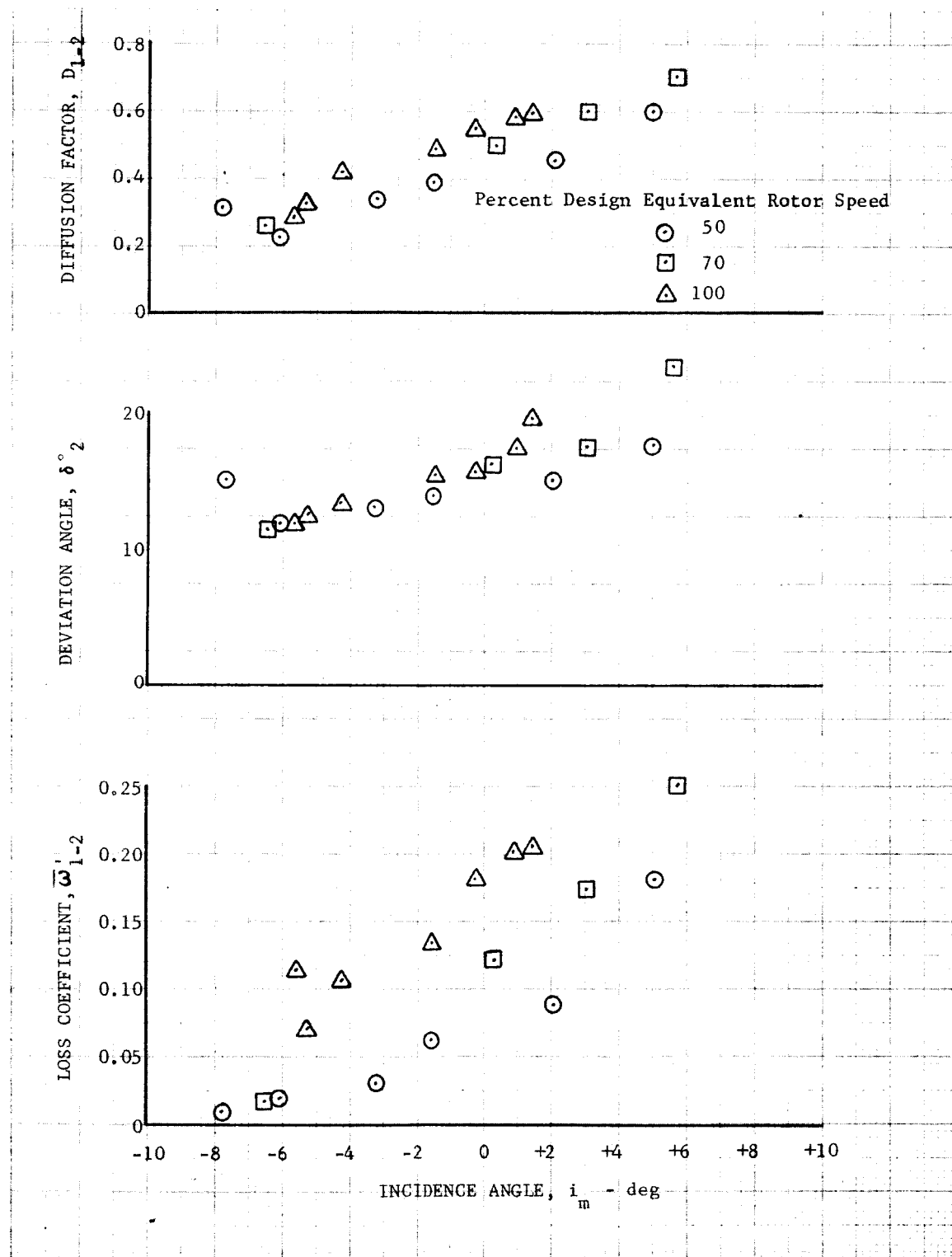


Figure V-12. Variation of Rotor Blade Element Parameters With Incidence, Slotted Rotor 2, 90% Span From Tip

DF 52295

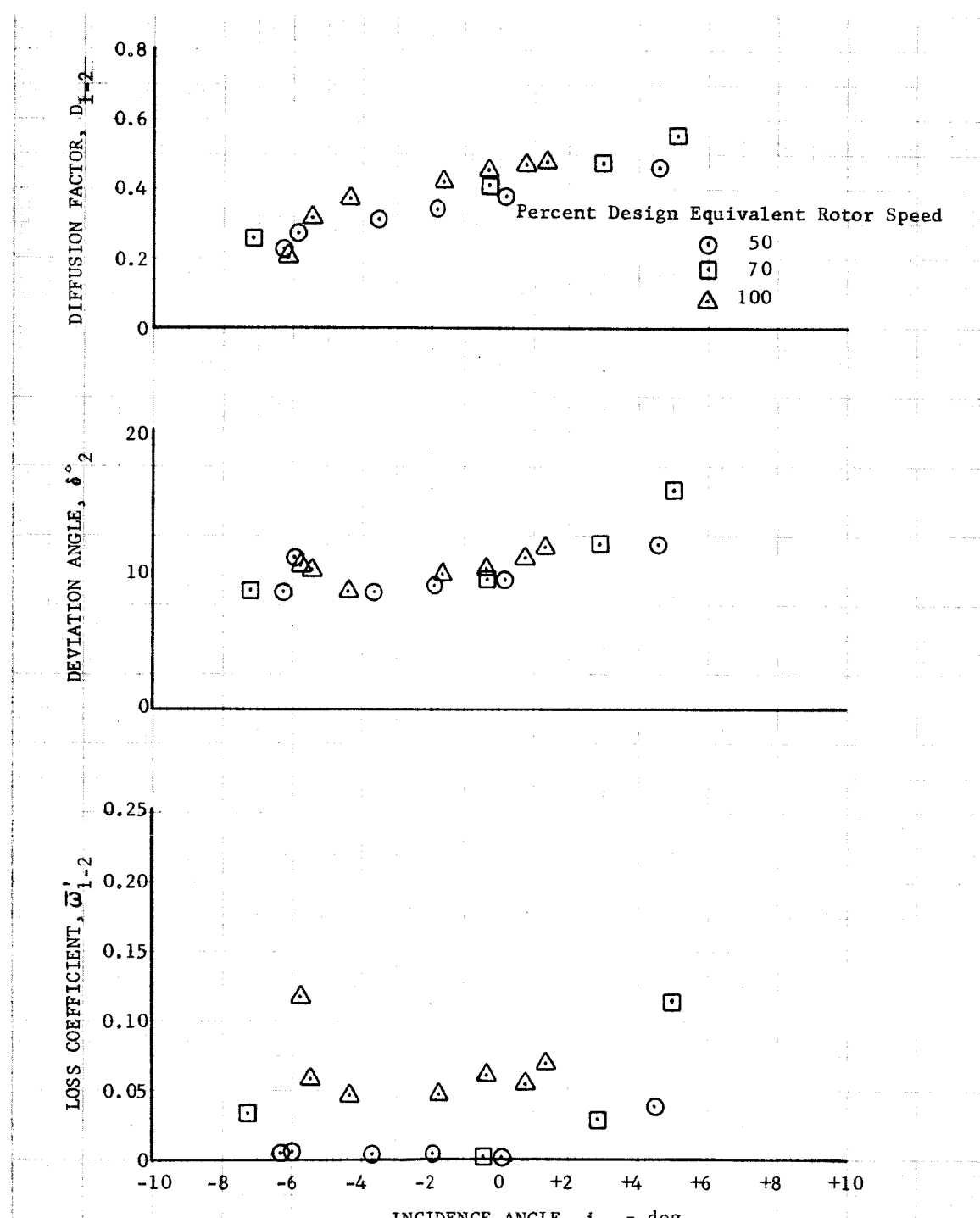


Figure V-13. Variation of Rotor Blade Element Parameters
With Incidence, Slotted Rotor 2, 70% Span
From Tip

DF 52296

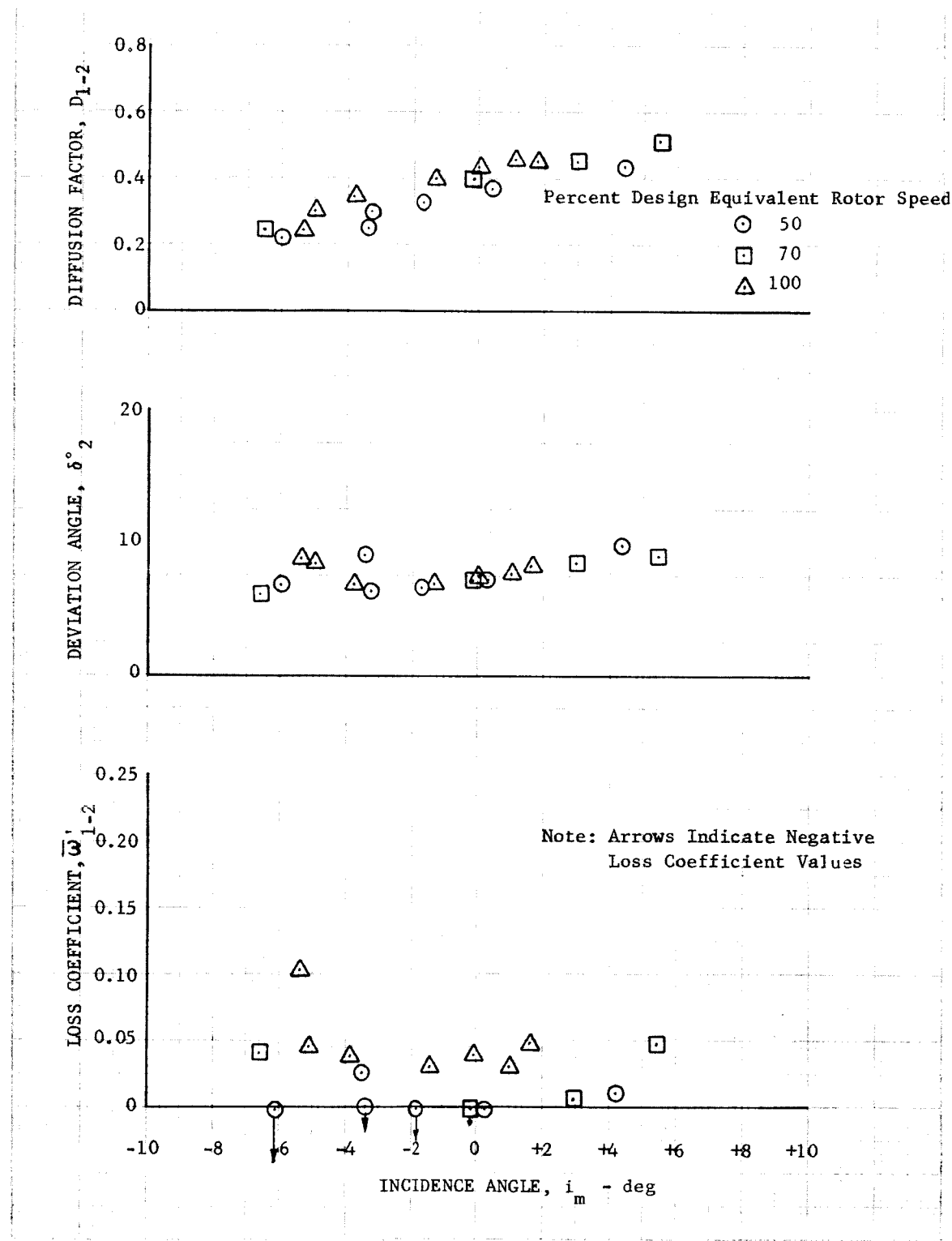


Figure V-14. Variation of Rotor Blade Element Parameters With Incidence, Slotted Rotor 2, 50% Span From Tip

DF 52297

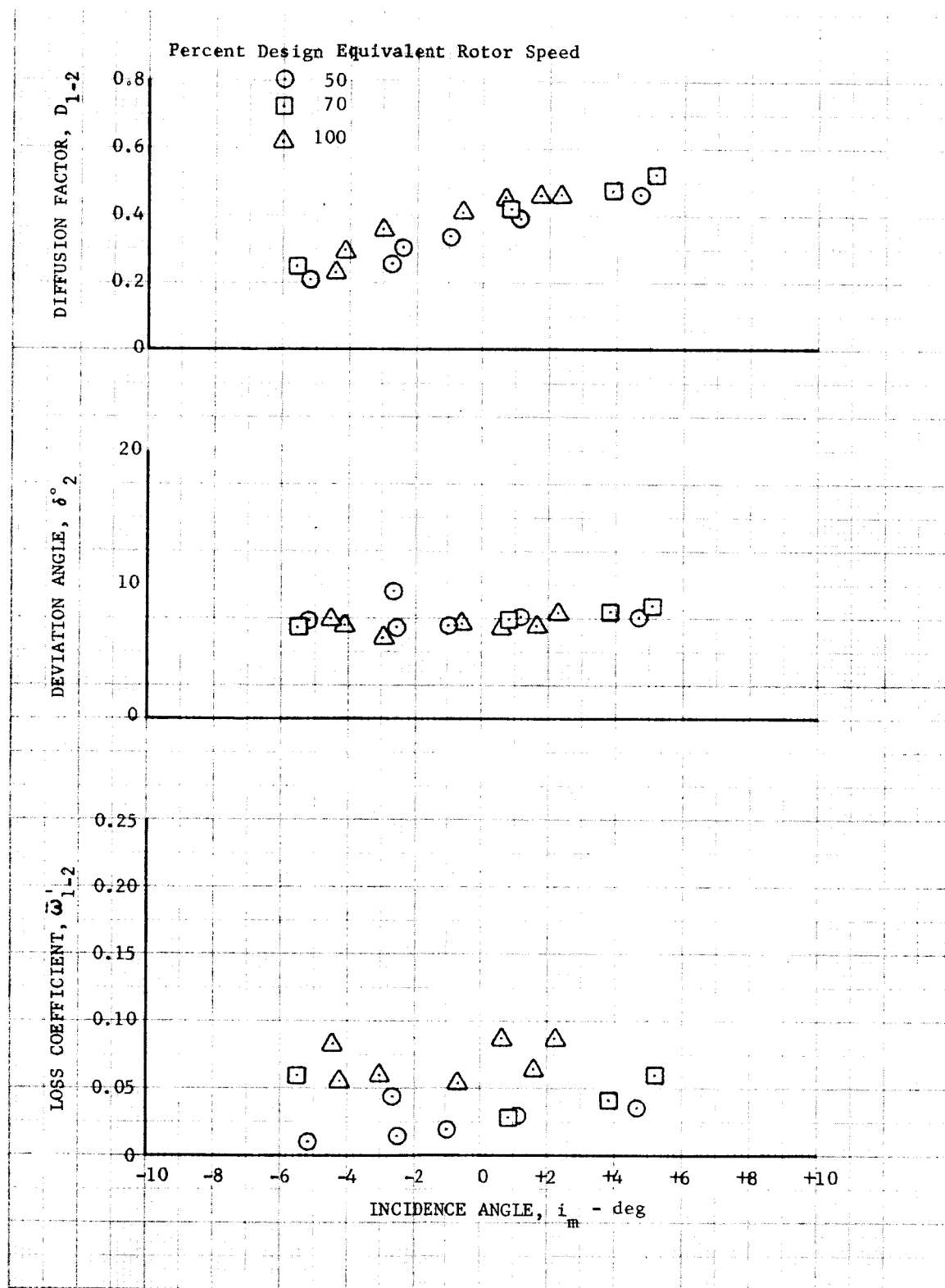


Figure V-15. Variation of Rotor Blade Element Parameters With Incidence, Slotted Rotor 2, 30% Span From Tip

DF 52298

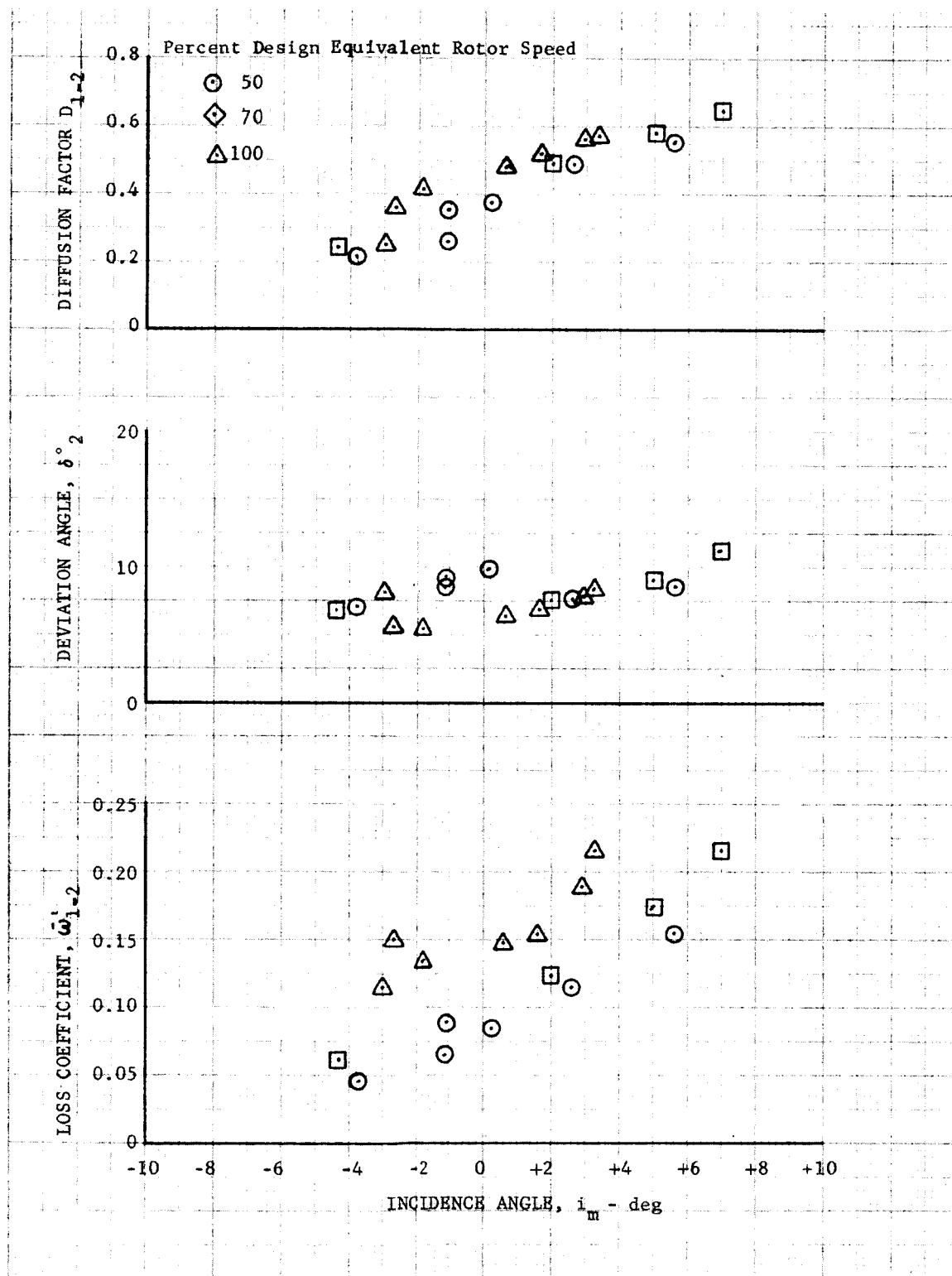


Figure V-16. Variation of Rotor Blade Element Parameters With Incidence, Slotted Rotor 2, 10% Span From Tip

DF 52299

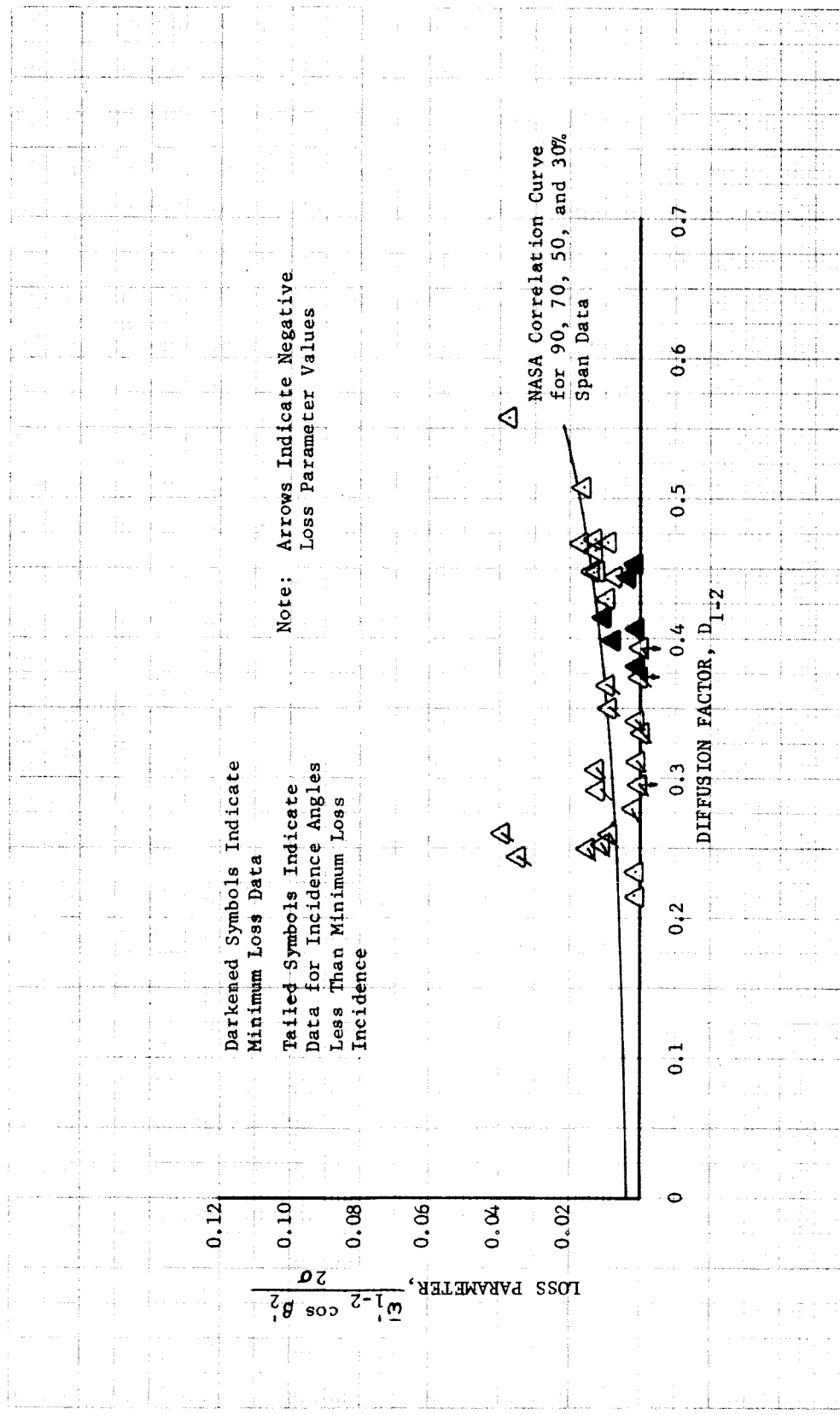


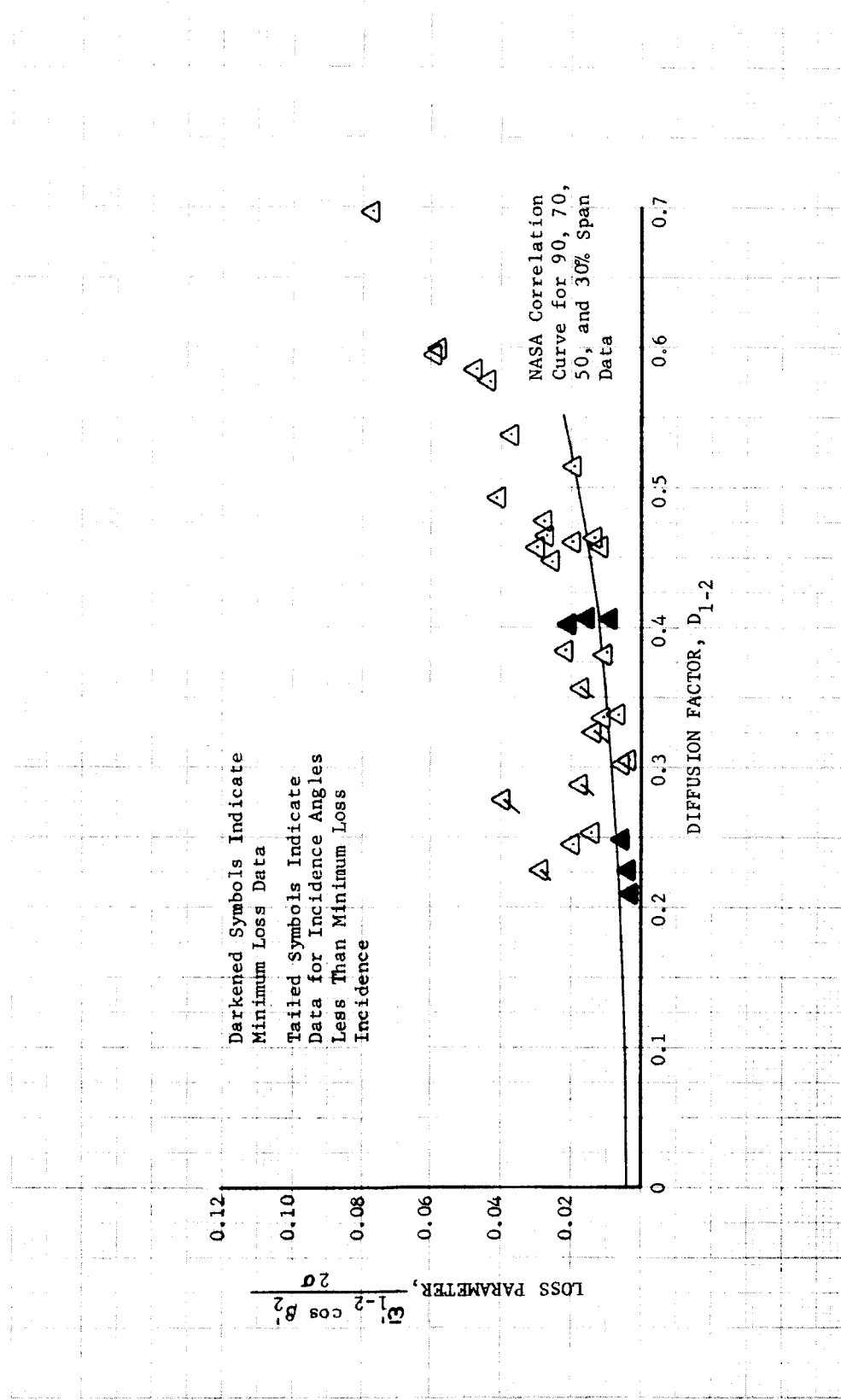
Figure V-17a.

Loss Parameter Versus Diffusion Factor at 70 and 50% Span (From Tip) -
90, 100, and 110% Design Equivalent Rotor Speed

DF 53230-1

DF 53230-2

Figure V-17b. Loss Parameter Versus Diffusion Factor at 90 and 30% Span (From Tip) -
90, 100, and 110% Design Equivalent Rotor Speed



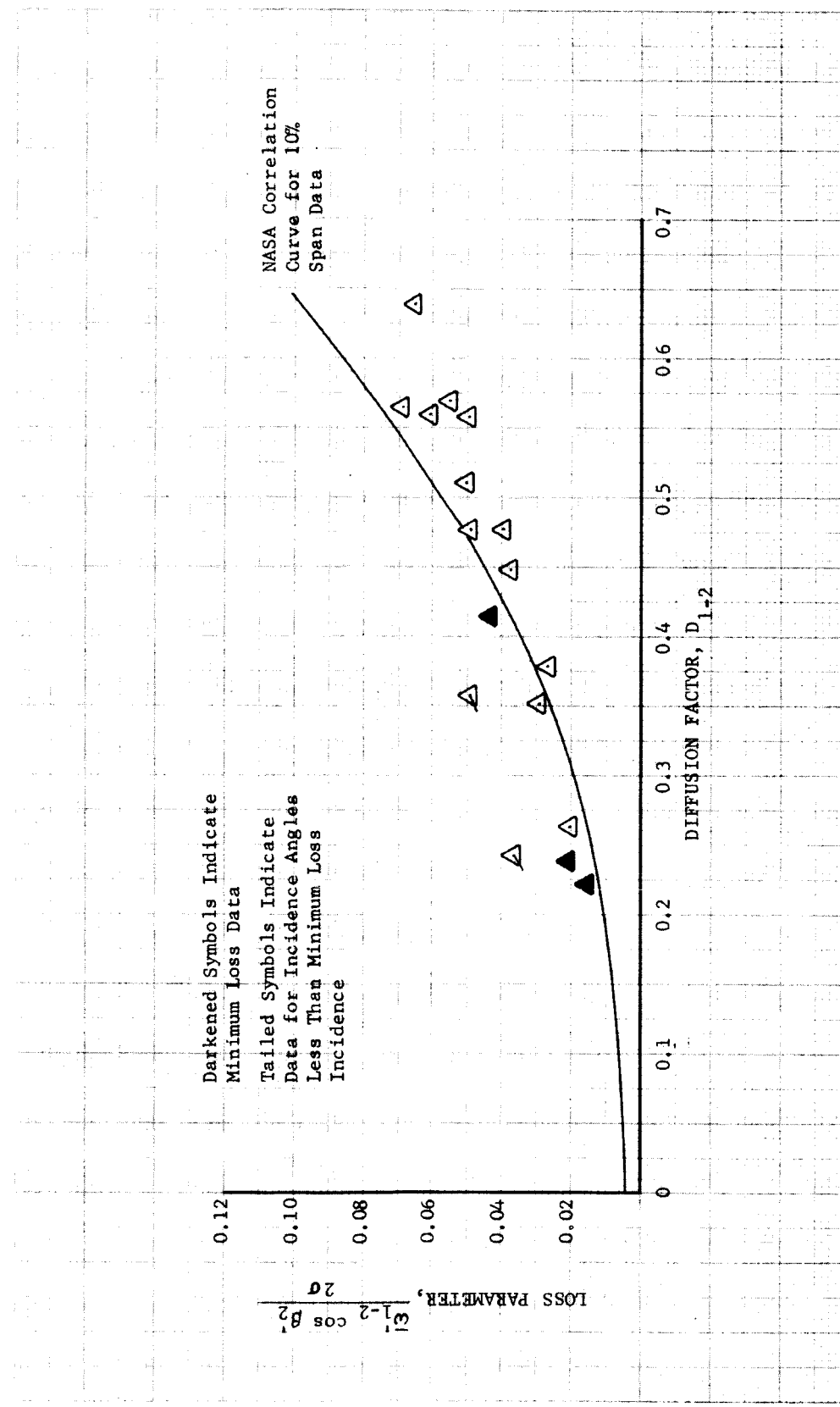


Figure V-17c. Loss Parameter Versus Diffusion Factor at 10% Span (From Tip)
90, 100, and 110% Design Equivalent Rotor Speed

DF 53230-3

DF 53231

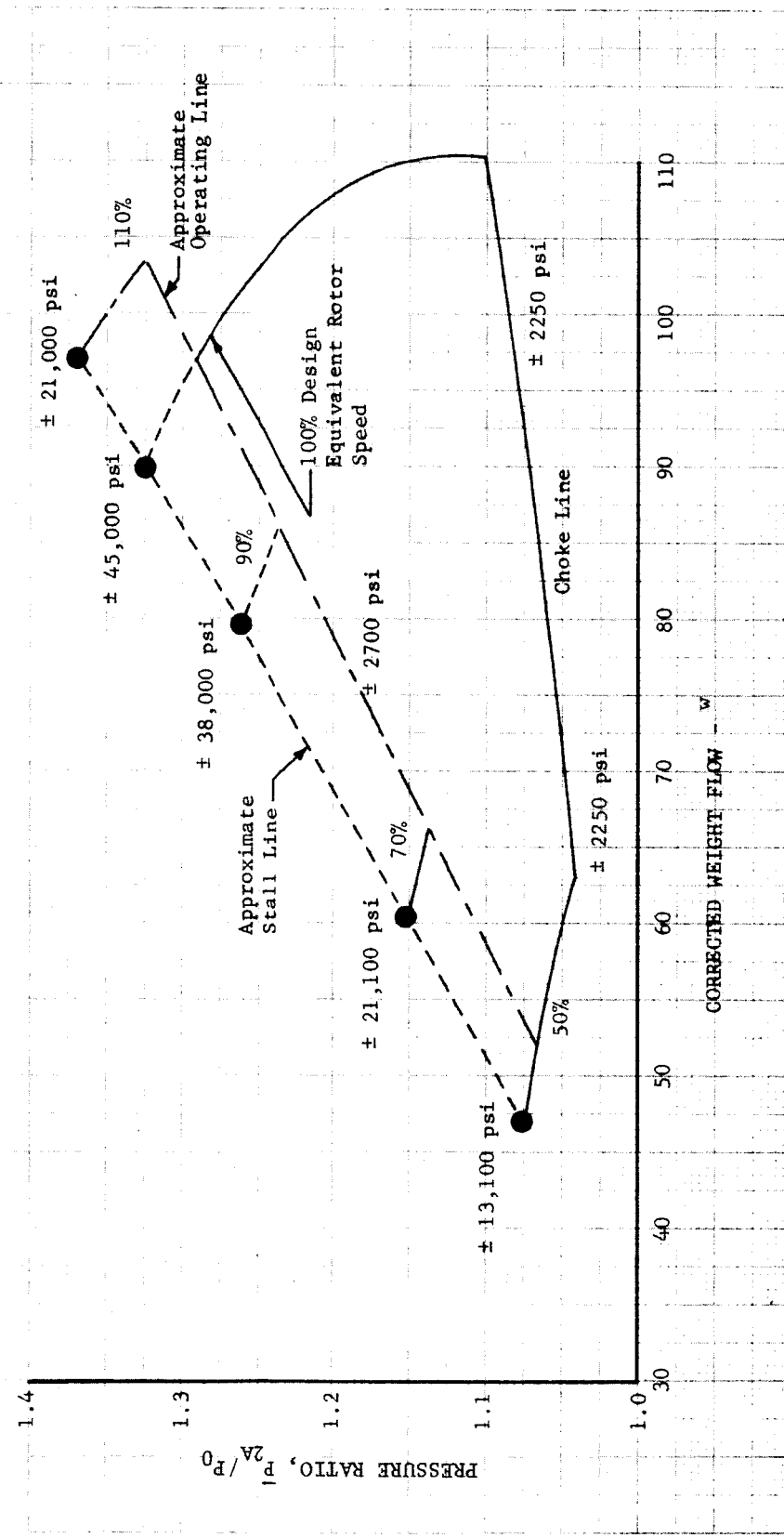


Figure V-18. Stress Survey Map

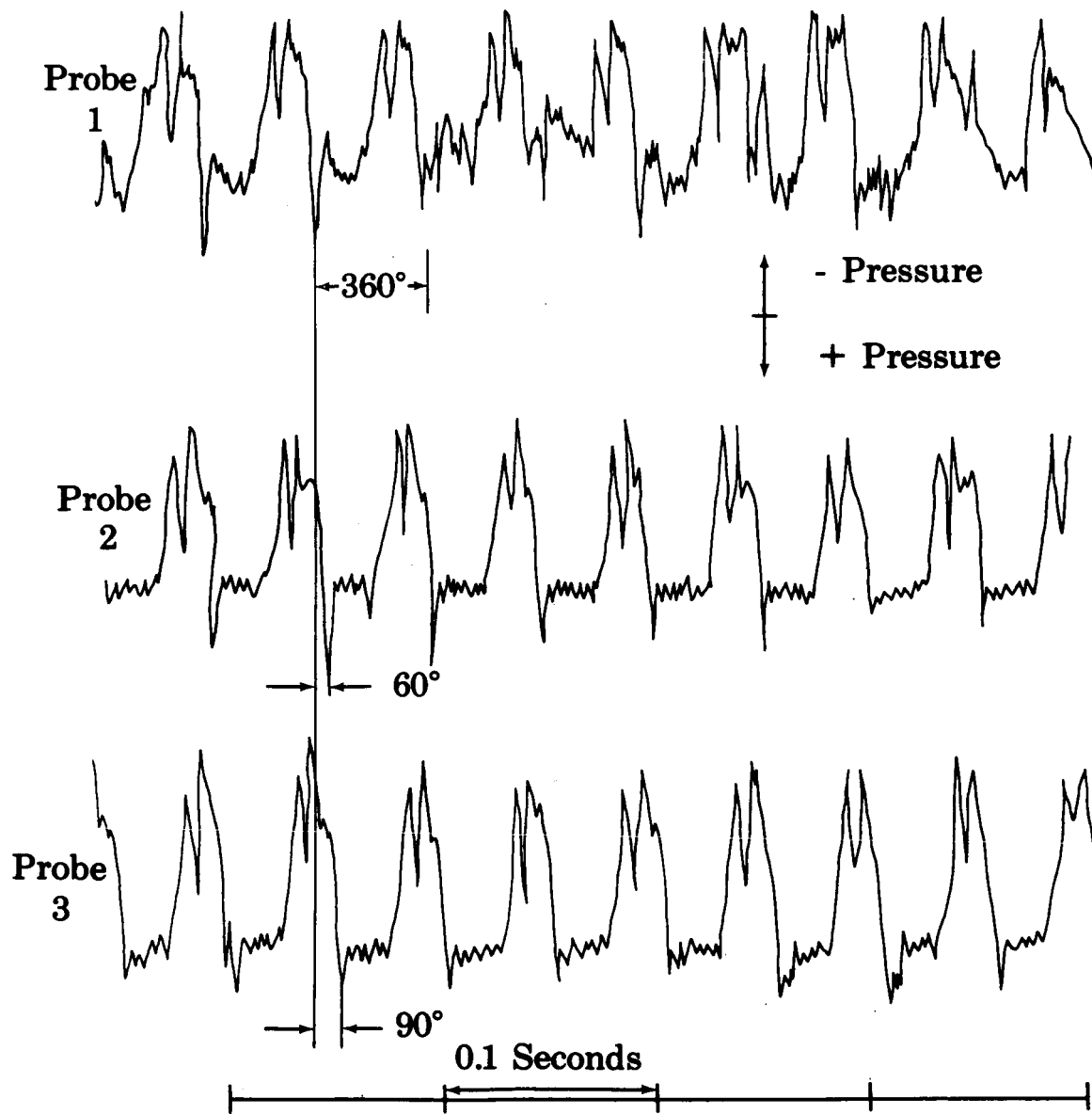


Figure V-19. Typical Rotating Stall Recording; FD 19356
Rotor Speed 6200 RPM

Major Scale Division: Vertical = 60 ft/sec

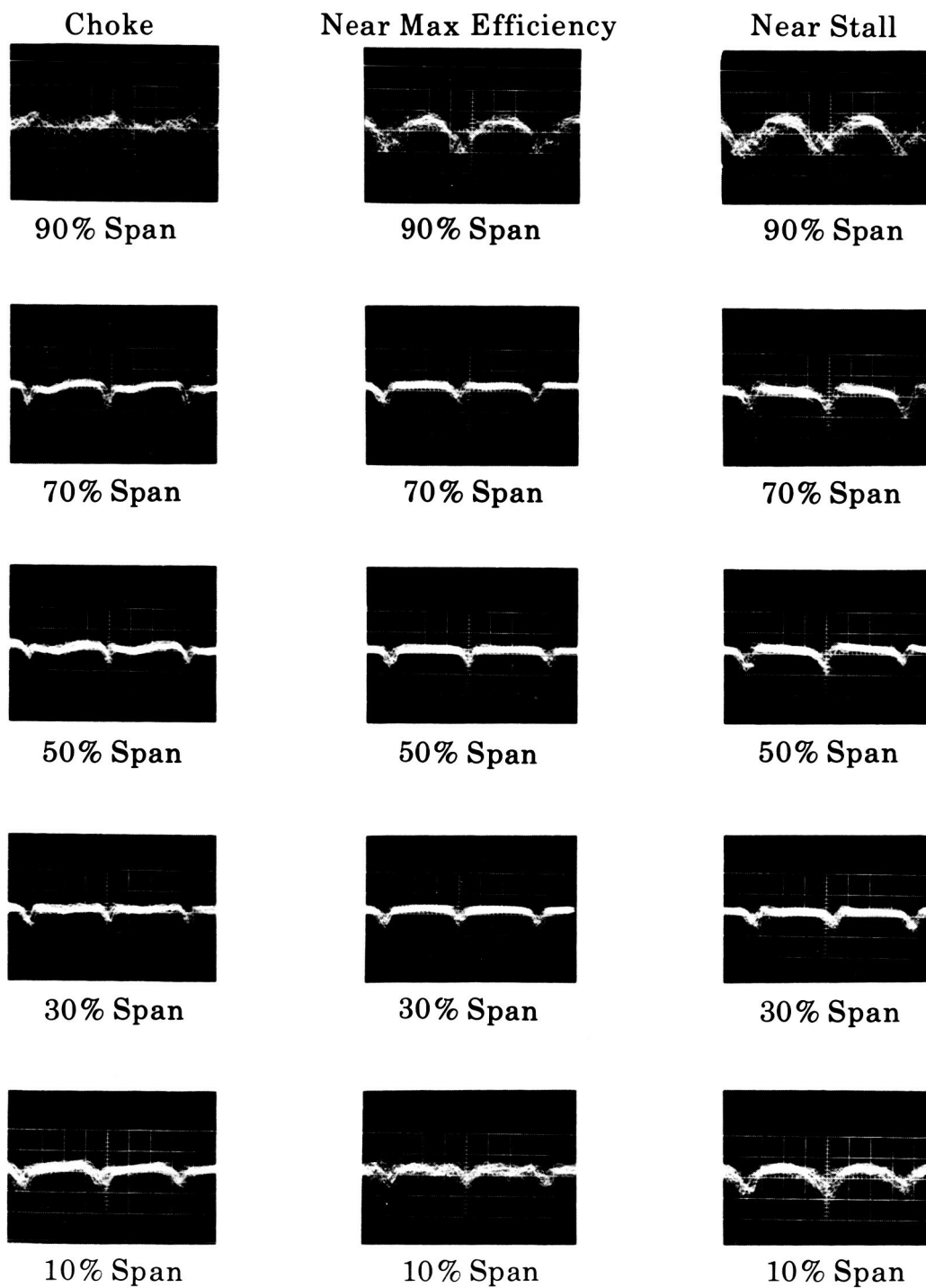


Figure V-20. Rotor Wake Surveys - 50% Design
Equivalent Rotor Speed

FD 19353

Major Scale Division: Vertical = 60 ft/sec

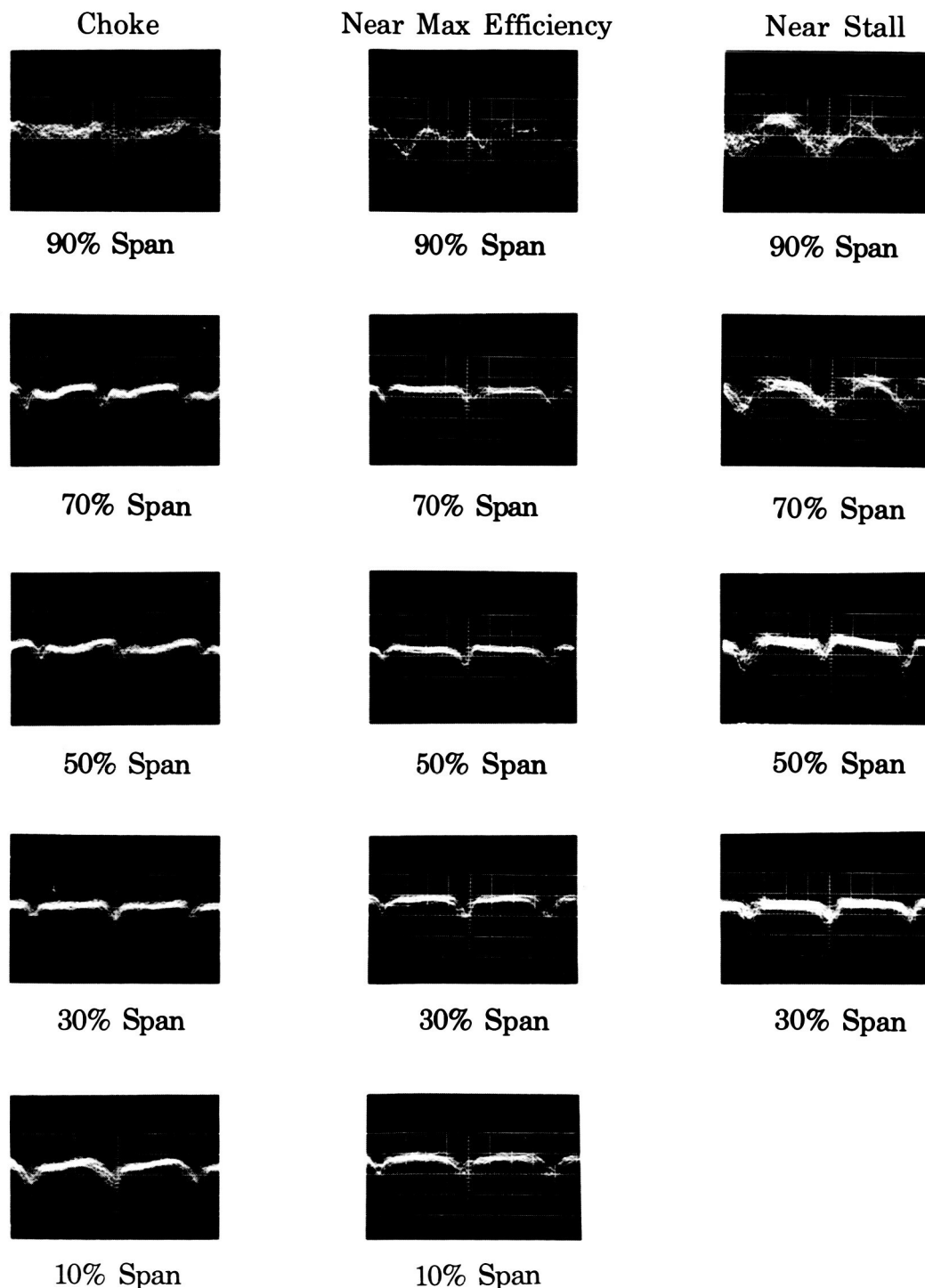


Figure V-21. Rotor Wake Surveys - 70% Design
Equivalent Rotor Speed

FD 19354

Major Scale Division: Vertical = 60 ft/sec sec

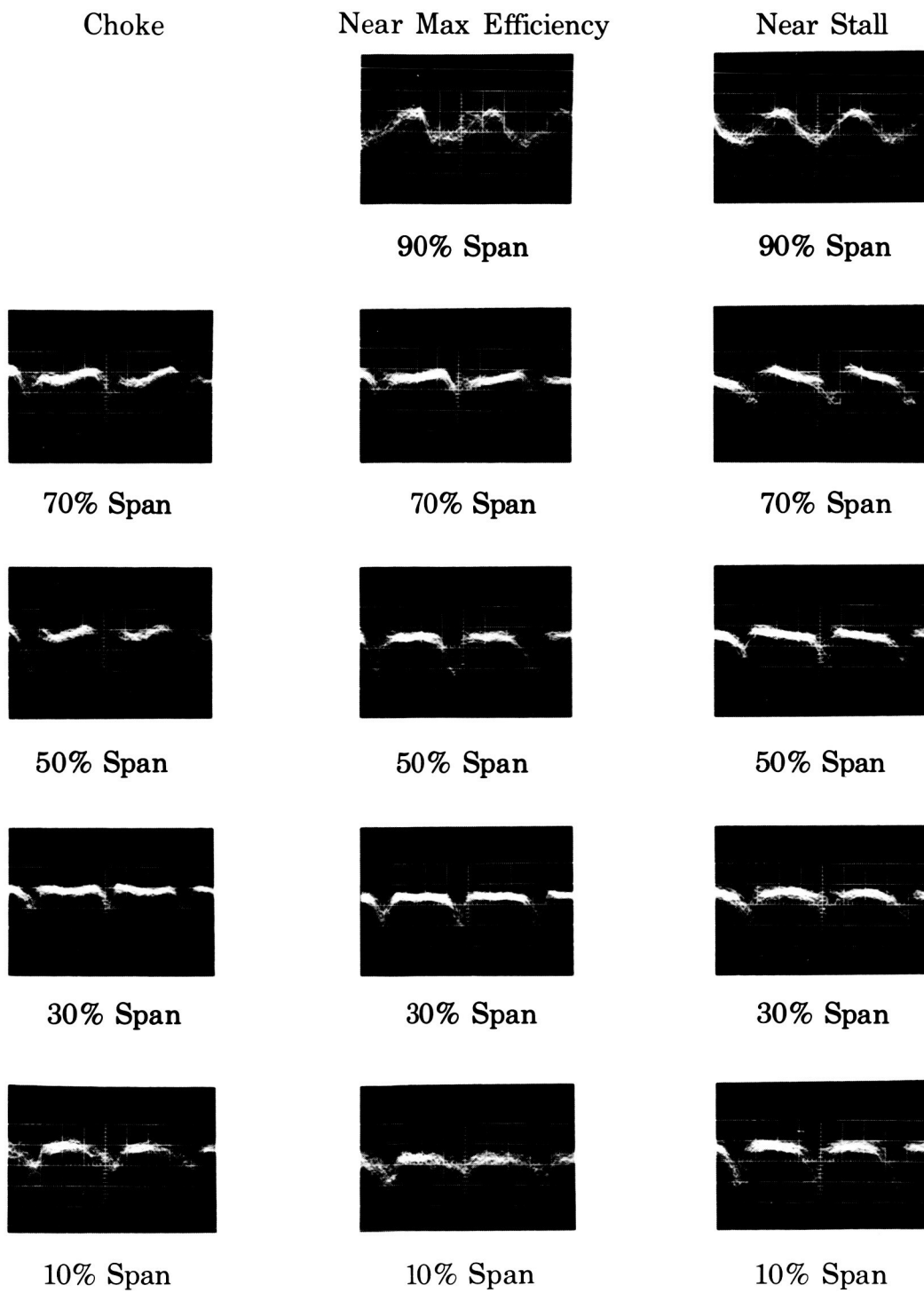
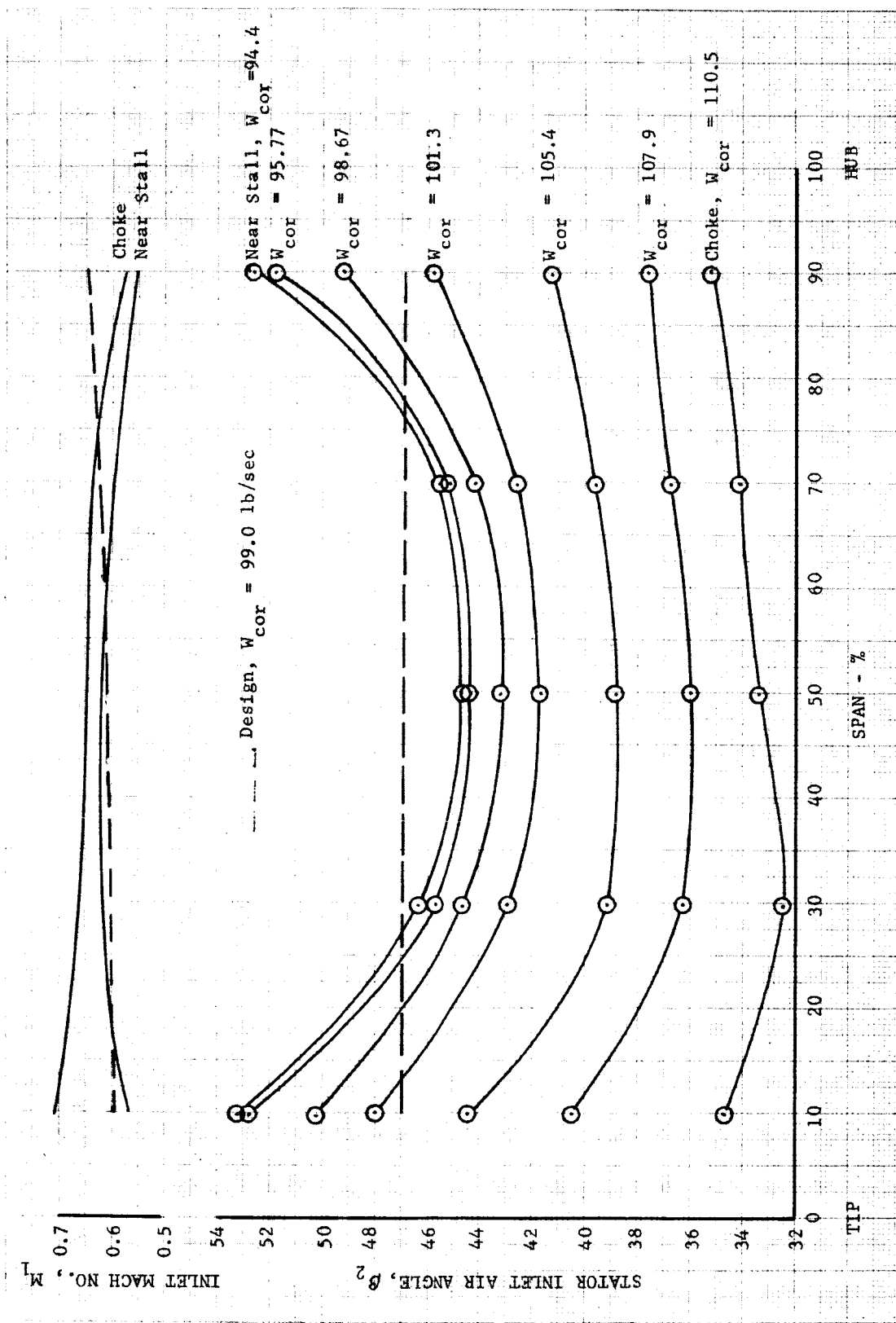


Figure V-22. Rotor Wake Surveys - 100% Design
Equivalent Rotor Speed

FD 19355

DF 52302

Figure V-23. Stator Inlet Air Angle and Mach Number Distribution, Slotted Rotor 2
Configuration, Design Rotor Speed



APPENDIX A
DEFINITION OF SYMBOLS

A. GENERAL NOMENCLATURE

A_A	Flow path annular area, in. ²
c	Chord length, in.
D	Diffusion factor
i_m	Incidence angle, deg
M	Absolute Mach number
o	Minimum blade passage gap, in.
o^*	Critical blade passage gap, in.
P	Total pressure, psia
p	Static pressure, psia
q	Pressure equivalent of the velocity head, psia
R	Reynolds number based on chord length
s	Blade spacing, in.
s	Blade span, in.
t	Blade maximum thickness, in.
U	Rotor speed, ft/sec
V	Absolute velocity, ft/sec
w	Actual flow rate, lb _m /sec
β	Absolute air angle, deg
γ	Ratio of specific heats
γ°	Blade-chord angle, deg
δ	Ratio of total pressure to NASA standard sea level pressure of 2116 psf
δ°	Deviation angle, deg
η_{ad}	Adiabatic efficiency
θ	Ratio of total temperature to NASA standard sea level temperature of 518.7°R

κ	Blade metal angle, deg
ρ	Density, lb_m/ft^3
σ	Solidity, c/S
ϕ	Blade camber angle, $\kappa_1 - \kappa_2$, deg
$\bar{\omega}$	Total pressure loss coefficient

Subscripts:

0	Guide vane inlet
1	Rotor inlet
2	Rotor exit
2A	Stator exit
z	Axial component
θ	Tangential component

Superscripts:

'	Related to rotor blade
-	Mass average value

B. SLOT NOMENCLATURE

A_2	Slot throat area, in. ²
R	Coanda radius, in.
R_p	Pressure surface edge radius, in.
r_1	Slot leading edge radius, in.
r_2	Slot trailing edge radius, in.
t	Blade thickness at intersection of slot centerline and mean camber line, in.
Y_1	Slot capture dimension, in.
Y_2	Slot throat dimension, in.
ψ	Angle formed by slot centerline and mean camber line, deg

C. BLADE ELEMENT TABULATION NOMENCLATURE FOR TABLE B-2

PCT SPAN	Percent span
DIA	Diameter, inches
BETA	Absolute air angle, degrees
BETA(PR)	Relative air angle, degrees
V	Absolute velocity, ft/sec
VZ	Axial component of velocity, ft/sec
V-THETA	Tangential components of absolute velocity, ft/sec
V(PR)	Relative velocity, ft/sec
V-THETA PR	Tangential component of relative velocity, ft/sec
U	Wheel speed, ft/sec
M	Absolute Mach number
M(PR)	Relative Mach number
TURN	Air turning, degrees
TURN(PR)	Relative air turning, degrees
UUBAR	Loss coefficient
DFAC	Diffusion factor
EFFP	Polytropic efficiency
EFF	Adiabatic efficiency
INCID	Incidence, degrees
DEV	Deviation, degrees
LOSS PARA	Loss parameter

APPENDIX B
TABULATED PERFORMANCE

The overall performance and percent rotor and stator bleed flow rates for each test point are presented in table B-1.

Table B-2 presents blade element data for each test point. Definition of the blade element parameters as tabulated in the computer printouts is presented in Appendix A.

Table B-1. Tabulation of Overall Performance and Percent Bleed Flows

50% Design Equivalent Rotor Speed						
Corrected Main Orifice Weight Flow $w\sqrt{\theta/\delta}$, 1b/sec	P_2/\bar{P}_1	Overall Performance		\bar{P}_{2a}/P_0	η_{ad} Percent	Percent Bleed Rotor Stator
		Rotor	η_{ad} Percent			
47.41	1.08	91.7	1.07	82.1	1.34	3.40
53.15	1.07	93.8	1.07	87.6	1.08	1.96
56.18	1.06	93.2	1.06	87.2	0.96	1.44
58.38	1.06	93.3	1.05	84.7	0.86	1.46
60.60	1.05	89.3	1.05	76.7	0.70	0.61
63.28	1.05	90.6	1.04	79.6	0.57	0.58
70% Design Equivalent Rotor Speed						
60.76	1.16	87.0	1.15	80.1	1.30	2.55
65.06	1.15	88.6	1.14	82.1	1.16	1.89
70.98	1.14	94.9	1.13	86.3	0.98	2.11
85.62	1.09	91.6	1.07	68.9	0.69	0.97
100% Equivalent Design Rotor Speed						
94.42	1.31	83.2	1.30	81.0	0.82	2.45
95.77	1.32	85.2	1.30	81.6	0.75	2.24
98.67	1.30	86.2	1.29	82.0	0.73	2.17
101.31	1.29	88.5	1.27	83.5	0.67	2.05
105.45	1.25	87.9	1.23	81.0	0.57	1.67
107.88	1.22	85.0	1.19	73.1	0.25	1.18
110.53	1.16	74.9	1.14	64.0	0.13	0.51

Table B-2. Blade Element Performance

PERCENT DESIGN SPEED = 100.00
 CORRECTED WEIGHT FLOW = 110.53
 CORRECTED ROTOR SPEED = 5400.00

INLET GUIDE VANE 2		STATION 0 - STATION 1				STATION 1 - STATION 2				SLOTTED ROTOR 2	
PCT SPAN	90	70	50	30	10	PCT SPAN	90	70	50	30	10
DIA	33.622	35.167	36.711	38.256	39.801	DIA	33.589	35.067	36.545	38.023	39.501
BETA 0	0.000	0.000	0.000	0.000	0.000	BETA 1	17.095	18.074	18.743	18.790	20.636
BETA 1	17.095	18.074	18.743	18.790	20.636	BETA 2	35.362	34.277	33.446	32.467	34.782
V 0	495.82	495.82	495.82	495.82	495.82	BETA(PR) 1	46.526	47.855	49.603	51.480	53.676
V 1	608.41	608.95	603.14	576.39	576.99	BETA(PR) 2	27.965	33.983	41.02	46.725	
VZ 0	495.82	495.82	495.82	495.82	495.82	V 1	608.41	608.95	603.14	596.39	576.99
VZ 1	581.53	578.90	571.15	564.60	539.97	V 2	782.26	737.59	716.27	699.55	645.08
V-THETA 0	-0.00	-0.00	-0.00	-0.00	-0.00	VZ 1	581.53	578.90	571.15	564.60	539.97
V-THETA 1	178.85	188.92	193.00	192.10	203.35	VZ 2	637.94	609.49	596.97	590.21	529.82
M 0	0.4532	0.4532	0.4532	0.4532	0.4532	V-THETA 1	178.85	188.92	193.80	192.10	203.35
M 1	0.5620	0.5625	0.5568	0.5502	0.5313	V-THETA 2	452.73	415.40	395.82	375.53	367.99
TURN	-17.10	-18.07	-18.74	-18.79	-20.64	V(PR) 1	845.2	862.7	881.3	906.6	911.6
UUBAR	0.0386	0.0028	0.0002	0.0013	0.0696	V(PR) 2	722.3	735.0	756.9	786.8	772.9
DFAC	-0.053	-0.033	-0.0052	-0.002	-0.0052	VTHETA PRI	-613.4	-639.7	-671.2	-709.3	-736.4
EFFP	0.9440	1.0041	1.0092	1.0078	0.8593	VTHETA PR2	-338.7	-410.8	-465.3	-522.4	-562.7
INCID	0.0000	0.0000	0.0000	0.0000	0.0000	U 1	792.20	828.60	864.98	901.39	937.79
DEV	6.945	5.896	6.097	7.810	8.244	M 1	0.5620	0.5625	0.5950	0.5313	0.5717
STATOR 1											
PCT SPAN	90	70	50	30	10	M 2	0.7081	0.6695	0.6500	0.5313	0.5199
STATION 2 - STATION 2A											
PCT SPAN	90	70	50	30	10	M 1(PR) 1	0.7807	0.7970	0.8136	0.8394	
BETA 2	35.362	34.277	33.546	32.467	34.782	M 1(PR) 2	0.6538	0.6671	0.7143	0.6948	
BETA 2A	26.300	23.400	23.100	25.000	27.900	TURN(PR)	18.561	13.872	11.672	10.778	6.951
V 2	782.26	737.59	716.27	699.55	645.08	UUBAR	0.1125	0.1142	0.1017	0.0930	0.1133
V 2A	683.49	659.88	636.01	650.10	612.41	DFAC	0.2766	0.2601	0.2445	0.2284	0.2432
VZ 2	637.94	609.49	596.97	590.21	529.82	EFFP	0.7543	0.7945	0.8088	0.8561	0.6463
V-THETA 2	452.73	415.40	395.82	375.53	367.99	EFF	0.7474	0.7896	0.8045	0.8529	0.6396
V-THETA 2A	302.83	262.07	249.53	274.74	286.56	INCID	-5.63	-5.75	-5.43	-4.56	-3.11
M 2	0.7081	0.6695	0.6500	0.6350	0.5799						
M 2A	0.6115	0.5952	0.5737	0.5871	0.5478						
TURN	9.062	10.877	10.446	7.467	6.882						
UUBAR	0.1436	0.0989	0.1267	0.0689	0.0684						
DFAC	0.2063	0.1962	0.2053	0.1396	0.1138						
EFFP	0.4954	0.7872	0.6935	0.6054	0.2815						
INCID	-11.59	-12.67	-13.40	-14.48	-12.17						
DEV	9.36	6.46	6.16	8.06	10.96						
DIA	33.564	34.992	36.420	37.848	39.276						

Table B-2. Blade Element Performance (Continued)

PERCENT DESIGN SPEED = 100.07
 CORRECTED WEIGHT FLOW = 95.77
 CORRECTED ROTOR SPEED = 5370.00

INLET GUIDE VANE 2		STATION 0 - STATION 1					STATION 1 - STATION 2					SLOTTED Rotor	
PCT SPAN		90	70	50	30	10	PCT SPAN		90	70	50	30	10
DIA	33.622	35.167	36.711	38.256	39.801	DIA	33.589	35.067	36.545	38.023	39.501		
BETA 0	0.000	0.000	0.000	0.000	0.000	BETA 1	17.119	17.640	18.227	19.452	19.940	18.227	19.452
BETA 1	17.119	17.640	18.227	18.706	19.452	BETA 2	51.940	45.368	44.474	45.775	52.944		
V 0	4.16.71	4.16.71	4.16.71	4.16.71	4.16.71	BETA(PR) 1	53.145	54.417	56.026	57.631	59.650		
V 1	502.00	503.98	499.42	493.86	479.88	BETA(PR) 2	33.657	34.265	36.866	40.948	46.570		
VZ 0	416.71	416.71	416.71	416.71	416.71	V 1	502.00	503.98	499.42	493.86	479.88		
VZ 1	479.76	480.29	474.36	467.78	452.49	V 2	657.03	690.32	692.97	674.02	645.16		
V-THETA 0	-0.00	-0.00	-0.00	-0.00	-0.00	VZ 1	479.76	480.29	474.36	467.78	452.49		
V-THETA 1	147.77	152.72	156.21	158.39	159.81	VZ 2	405.05	484.98	494.48	470.12	388.77		
M 0	0.3786	0.3786	0.3786	0.3786	0.3786	V-THETA 1	147.77	152.72	156.21	158.39	159.81		
M 1	0.4591	0.4610	0.4566	0.4513	0.4381	V-THETA 2	517.32	491.25	485.48	483.01	514.87		
TURN	-17.12	-17.64	-18.23	-18.71	-19.45	V(PR) 1	79.9	82.54	84.89	87.38	89.55		
UUBAR	0.0356	-0.0027	-0.0034	0.0010	0.0529	V(PR) 2	486.6	586.8	618.1	622.4	565.5		
DFAC	-0.033	-0.022	-0.006	0.012	0.050	VTHETA PR1	-640.0	-671.3	-704.0	-738.0	-772.8		
EFFP	0.9452	1.0199	1.0227	1.0143	0.8859	VTHETA PR2	-269.7	-330.4	-370.8	-407.9	-410.7		
INCID	0.0000	0.0000	0.0000	0.0000	0.0000	U 1	787.80	824.00	860.18	896.38	932.58		
DEV	6.921	6.330	6.613	7.894	9.428	U 2	787.03	821.66	856.29	890.92	925.55		
						M 1	0.4591	0.4610	0.4566	0.4513	0.4381		
						M 2	0.5740	0.6113	0.6151	0.5961	0.5639		
						M(PR) 1	0.7315	0.7750	0.7761	0.7985	0.8175		
						M(PR) 2	0.4252	0.5197	0.5487	0.5505	0.4943		
						TURN(PR)	19.488	20.152	19.161	16.684	13.080		
						UUBAR	0.1982	0.0521	0.0280	0.0644	0.1881		
						DFAC	0.5784	0.4631	0.4444	0.4607	0.5609		
						EFFP	0.6253	0.8522	0.9293	0.8854	0.7395		
BETA 2	51.940	45.368	44.474	45.775	52.944	EFF	0.6119	0.8461	0.9262	0.8806	0.7288		
BETA 2A	29.700	27.900	26.100	28.800	32.900	INCID	0.99	0.81	1.00	1.59	2.86		
V 2	657.03	690.32	692.97	674.02	645.16	DEV	17.507	10.665	7.626	7.038	7.920		
V 2A	414.07	475.97	500.54	496.08	459.71	LOSS PARA	0.043984	0.012273	0.007315	0.01909	0.060338		
VZ 2	405.05	484.98	494.48	470.12	388.77								
VZ 2A	359.67	420.64	449.50	434.72	385.98								
V-THETA 2	517.32	491.25	485.48	483.01	514.87								
V-THETA 2A	205.15	222.72	220.21	238.99	249.70								
M 2	0.5740	0.6113	0.6151	0.5961	0.5639								
M 2A	0.3581	0.4153	0.4379	0.4326	0.3982								
TURN	22.240	17.468	18.374	16.975	20.044								
UUBAR	0.0636	0.0852	0.0759	0.0648	0.1073								
DFAC	0.5680	0.4802	0.4519	0.4358	0.4902								
EFFP	1.7233	1.1039	1.0505	0.9879	1.3565								
INCID	4.99	-1.58	-2.48	-1.17	5.99								
DEV	12.76	10.96	9.16	11.86	15.96								
DIA	33.564	34.992	36.420	37.848	39.276								

Table B-2. Blade Element Performance (Continued)

INLET GUIDE VANE		STATION 0 - STATION 1		STATION 1 - STATION 2		SLOTTED ROTOR		ROTOR	
PCT SPAN		90	70	50	30	10	PCT SPAN	90	70
DIA	33.622	35.167	36.711	38.256	39.801	DIA	33.589	35.067	36.545
BETA 0	0.000	0.000	0.000	0.000	0.000	BETA 1	16.808	17.389	18.042
BETA 1	16.8C8	17.389	18.042	17.784	20.244	BETA 2	49.327	44.167	43.316
V 0	431.64	431.64	431.64	431.64	431.64	BETA(PR) 1	51.953	53.281	54.907
V 1	521.07	522.26	517.41	499.21	499.21	BETA(PR) 2	31.819	32.530	36.637
VZ 0	431.64	431.64	431.64	431.64	431.64	V 1	521.07	522.26	517.41
VZ 1	498.81	498.39	491.97	487.25	468.37	V 2	677.02	701.25	698.03
V-THETA C	-C.0C	-0.00	-0.00	-0.00	-0.00	VZ 1	498.81	498.39	491.97
V-THETA 1	15C.67	15C.08	16C.25	15C.29	17C.74	VZ 2	441.24	503.01	480.46
M 0	0.3926	0.3926	0.3926	0.3926	0.3926	V-THETA 1	150.67	156.08	166.25
M 1	0.4773	0.4784	0.4738	0.4683	0.4564	V-THETA 2	513.48	488.60	478.86
TURN	-16.81	-17.39	-18.04	-17.78	-20.24	V(PRI) 1	809.3	833.6	855.7
UUBAR	0.C342	-0.0022	0.0012	0.0079	0.0537	V(PRI) 2	519.3	603.4	632.9
DFAC	-0.C42	-0.025	-0.008	0.003	0.054	VTHETA PR1	-637.4	-668.2	-700.2
EFFP	0.5478	1.0179	1.0117	0.9973	0.8869	VTHETA PR2	-273.8	-333.3	-377.7
INC10	0.0000	0.0000	0.0000	0.0000	0.0000	U 1	788.04	824.25	860.44
DEV	7.232	6.581	6.798	8.816	8.636	U 2	787.27	821.91	856.55
STATOR		STATOR 1		STATOR 2		STATOR		STATOR	
PCT SPAN	90	70	50	30	10	M(PRI) 1	0.7414	0.7636	0.7836
BETA 2	49.327	44.167	43.316	44.619	50.246	M(PRI) 2	0.4552	0.5357	0.5629
BETA 2A	29.200	27.600	25.900	28.900	32.900	TURN(PRI)	20.134	19.751	18.270
V 2	677.02	701.25	698.03	674.99	650.22	UUBAR	0.1790	0.0590	0.0376
V 2A	425.56	502.28	503.34	494.99	453.52	DFAC	0.5396	0.4454	0.4261
VZ 2	441.24	503.01	507.87	480.46	415.81	DEV	15.669	9.930	6.4738
VZ 2A	371.48	445.12	452.78	433.34	380.78	LOSS PARA	0.03733	0.015612	0.009755
V-THETA 2	512.48	488.60	478.86	474.11	499.89				
V-THETA 2A	207.61	232.70	219.86	239.22	246.34				
M 2	0.5935	0.6225	0.6208	0.5996	0.5701				
M 2A	0.3695	0.4400	0.4415	0.4331	0.3940				
TURN	20.127	16.567	17.416	15.719	17.346				
UUBAR	0.1078	0.0604	0.0818	0.0720	0.1354				
DFAC	0.5599	0.4429	0.4478	0.4318	0.4949				
EFFP	1.7817	1.2324	1.1007	0.9311	1.3409				
INC10	2.38	-2.78	-3.63	-2.33	3.30				
DEV	12.26	10.66	8.96	11.96	15.96				
DIA	33.564	34.992	36.420	37.848	39.276				

Table B-2. Blade Element Performance (Continued)

PERCENT DESIGN SPEED = 99.89
 CORRECTED WEIGHT FLOW = 101.31
 CORRECTED ROTOR SPEED = 5360.00

	INLET GUIDE VANE 2				STATION 0 - STATION 1				STATION 1 - STATION 2				SLOTTED ROTOR 2				
	PCT SPAN	90	70	50	30	PCT SPAN	90	70	50	PCT SPAN	90	70	50	PCT SPAN	90	70	50
DIA	33.622	35.167	36.711	38.256	39.801	DIA	33.589	35.067	36.545	DIA	33.589	35.067	36.545	DIA	33.589	35.067	36.545
BETA 0	0.000	0.000	0.000	0.000	0.000	BETA 1	17.216	17.755	18.318	BETA 2	42.653	41.920	42.882	BETA 3	45.946	42.653	41.920
BETA 1	17.216	17.755	18.318	18.942	20.005	BETA 2	45.946	42.653	41.920	BETA 3	42.653	41.920	42.882	BETA 4	48.045	45.946	42.882
V 0	445.48	445.48	445.48	445.48	445.48	BETA(PR) 1	50.650	51.975	53.619	BETA(PR) 2	31.645	33.197	36.384	BETA(PR) 3	31.645	33.197	36.384
V 1	538.24	540.08	535.66	528.93	515.23	V 1	538.24	540.08	535.66	V 2	484.76	707.75	702.67	V 3	484.76	707.75	702.67
VZ 0	445.48	445.48	445.48	445.48	445.48	V 4	484.76	707.75	702.67	VZ 1	514.13	514.13	514.13	VZ 2	514.13	514.13	508.52
VZ 1	514.13	514.36	508.52	500.29	484.15	VZ 2	514.13	514.13	508.52	VZ 3	520.53	522.84	494.74	VZ 4	520.53	522.84	494.74
V-THETA 0	0.000	-0.000	-0.000	-0.000	-0.000	V-THETA 1	159.31	171.70	176.26	V-THETA 2	159.31	164.70	168.35	V-THETA 3	159.31	164.70	176.26
V-THETA 1	159.31	164.70	168.35	171.70	176.26	V-THETA 2	492.12	479.54	469.45	V-THETA 3	492.12	479.54	469.45	V-THETA 4	492.12	479.54	469.45
M 0	0.4056	0.4056	0.4056	0.4056	0.4056	V(PR) 1	810.9	835.0	857.3	V(PR) 2	622.1	649.4	655.4	V(PR) 3	622.1	649.4	655.4
M 1	0.4938	0.4956	0.4913	0.4848	0.4717	V(PR) 4	559.3	559.3	559.3	VTHETA PR1	-627.0	-657.8	-690.2	VTHETA PR2	-627.0	-657.8	-754.6
TURN	-17.22	-17.32	-18.32	-18.94	-20.01	VTHETA PR3	-293.4	-340.6	-385.2	VTHETA PR4	-293.4	-340.6	-429.8	VTHETA PR1	-293.4	-340.6	-438.1
UBAR	0.0439	0.0008	-0.0030	0.0065	0.0528	U 1	786.33	822.47	858.58	U 2	785.56	820.13	854.69	U 3	785.56	820.13	854.69
DFAC	-0.036	-0.023	-0.008	0.013	0.052	U 4	820.13	854.69	889.26	U 5	820.13	854.69	889.26	U 6	820.13	854.69	889.26
EFFP	0.9305	1.0109	1.0195	0.9996	0.9895	U 7	854.69	889.26	923.83	U 8	854.69	889.26	923.83	U 9	854.69	889.26	923.83
INCID	0.0000	0.0000	0.0000	0.0000	0.0000	U 10	923.83	941.93	948.0	U 11	923.83	941.93	948.0	U 12	923.83	941.93	948.0
DEV	6.824	6.215	6.522	7.658	8.875	M 1	0.6021	0.6263	0.6013	M 2	0.6021	0.6263	0.6013	M 3	0.6021	0.6263	0.6013
						STATOR 1	0.7439	0.7662	0.7863	STATOR 2	0.7439	0.7662	0.7863	STATOR 3	0.7439	0.7662	0.7863
						M(PR) 1	0.4918	0.5542	0.5789	M(PR) 2	0.4918	0.5542	0.5789	M(PR) 3	0.4918	0.5542	0.5789
						TURN(PR)	19.005	18.778	17.236	TURN(PR)	19.005	18.778	17.236	TURN(PR)	19.005	18.778	17.236
						UBAR	0.1326	0.0443	0.0285	UBAR	0.1326	0.0443	0.0285	UBAR	0.1326	0.0443	0.0285
						DFAC	0.4762	0.4152	0.3990	DFAC	0.4762	0.4152	0.3990	DFAC	0.4762	0.4152	0.3990
						EFFP	0.6367	0.8666	0.9031	EFFP	0.6367	0.8666	0.9031	EFFP	0.6367	0.8666	0.9031
BETA 2	45.946	42.653	41.920	42.882	48.045	INC ID	-1.51	-1.63	-1.41	INC ID	-1.51	-1.63	-1.41	INC ID	-1.51	-1.63	-1.41
BETA 2A	28.900	26.700	25.400	28.100	33.200	DEV	15.495	9.597	7.144	DEV	15.495	9.597	7.144	DEV	15.495	9.597	7.144
V 2	6.8476	7.0775	7.0267	6.7517	6.5321	LOSS PARA	0.027792	0.010141	0.007359	LOSS PARA	0.027792	0.010141	0.007359	LOSS PARA	0.027792	0.010141	0.007359
V 2A	450.26	517.90	510.37	510.59	463.35												
VZ 2	476.14	520.53	522.84	494.74	436.70												
VZ 2A	394.19	461.03	455.41	455.41	387.72												
V-THETA 2	492.12	479.54	469.45	459.45	485.77												
V-THETA 2A	217.60	23.70	216.92	240.49	253.71												
M 2	0.6021	0.6305	0.6263	0.6013	0.5752												
M 2A	0.3914	0.4554	0.4491	0.4484	0.442												
TURN	17.046	15.953	16.520	14.782	14.845												
UBAR	0.0939	0.0587	0.0934	0.0483	0.1315												
DFAC	0.5097	0.4204	0.4360	0.3977	0.4661												
EFFP	1.4855	1.2196	1.1577	0.9409	1.3007												
INCID	-1.00	-4.30	-5.03	-4.07	1.10												
DEV	11.96	9.76	8.46	11.16	16.26												
DIA	33.564	34.992	36.420	37.848	39.276												

Table B-2. Blade Element Performance (Continued)

PFRGENT DESIGN SPEED = 99.33

CORRECTED WEIGHT FLOW = 105.45

CORRECTED ROTOR SPEED = 5330.00

INLET GUIDE VANE 2				STATION 0 - STATION 1				STATION 1 - STATION 2				SLOTTED ROTOR 2			
PCT SPAN	90	70	50	30	10	PCT SPAN	90	70	50	30	10	PCT SPAN	90	70	50
DIA	33.622	35.167	36.711	38.256	39.801	DIA	33.589	35.067	36.545	38.023	39.501				
BETA 0	0.000	0.000	0.000	0.000	0.000	BETA 1	16.541	17.548	18.048	18.048	18.048				
BETA 1	16.541	17.548	17.930	18.048	20.287	BETA 2	41.357	39.704	38.832	39.181	44.404				
V 0	467.71	467.71	467.71	467.71	467.71	BETA(PR) 1	47.958	49.290	51.110	52.953	54.826				
V 1	580.16	580.20	574.01	566.90	551.75	BETA(PR) 2	29.420	31.970	36.201	40.240	44.321				
VZ 0	467.71	467.71	467.71	467.71	467.71	V 1	580.16	580.20	574.01	566.90	551.75				
VZ 1	556.15	553.20	546.13	539.01	517.52	V 2	720.61	728.81	709.92	686.69	657.40				
V-THETA 0	-0.00	-0.00	-0.00	-0.00	-0.00	VZ 1	556.15	553.20	546.13	539.01	517.52				
V-THETA 1	165.17	174.93	176.71	175.63	191.30	VZ 2	560.90	560.71	553.02	532.29	469.66				
M 0	0.4265	0.4265	0.4265	0.4265	0.4265	V-THETA 1	165.17	174.93	176.71	175.63	191.30				
M 1	0.5344	0.5344	0.5284	0.5215	0.5068	V-THETA 2	476.14	465.58	465.14	453.83	459.99				
TURN	-16.54	-17.55	-17.93	-18.05	-20.29	V(PR) 1	830.5	848.2	869.9	894.7	898.4				
UUBAR	0.0407	0.0026	0.0008	0.0055	0.0517	V(PR) 2	621.0	661.0	685.3	697.3	656.5				
DFAC	-0.070	-0.049	-0.033	-0.017	0.035	VTHETA PR1	-616.8	-642.9	-642.9	-714.1	-734.3				
EFFP	0.9444	1.0054	1.0089	1.0006	0.9038	VTHETA PR2	-350.0	-350.0	-350.0	-450.5	-458.7				
INCID	0.0000	0.0000	0.0000	0.0000	0.0000	U 1	781.93	817.86	853.77	889.70	925.63				
DEV	7.499	6.422	6.910	8.552	8.593	U 2	781.16	815.54	849.91	884.28	918.66				
						M 1	0.5344	0.5344	0.5284	0.5215	0.5068				
						M 2	0.6383	0.6383	0.6370	0.6149	0.5824				
						M(PR) 1	0.7649	0.7812	0.807	0.8230	0.8252				
						M(PR) 2	0.5501	0.5929	0.6149	0.6245	0.5816				
						TURN(PR)	18.538	17.320	14.908	12.713	10.504				
						UBAR	0.1044	0.0439	0.0370	0.0615	0.1319				
						DFAC	0.4037	0.3664	0.3500	0.3559	0.4158				
						EFFP	0.6446	0.8775	0.9069	0.8900	0.7264				
						EFF	0.8732	0.9037	0.8864	0.7176					
						INCID	-4.20	-4.32	-3.92	-3.09	-1.96				
						DEV	13.270	8.370	6.961	6.330	5.671				
						LOSS PARA	0.020500	0.009725	0.009509	0.01798	0.043006				
BETA 2	41.357	39.704	38.832	39.181	44.404										
BETA 2A	28.500	25.400	23.700	27.100	33.300										
V 2	720.61	728.81	709.92	686.69	657.40										
V 2A	513.09	544.58	532.32	533.46	493.93										
VZ 2	540.90	560.71	553.02	532.29	469.66										
VZ 2A	450.91	491.94	497.43	474.89	412.83										
V-THETA 2	476.14	465.58	445.14	433.83	459.99										
V-THETA 2A	244.82	233.59	213.96	243.02	271.18										
M 2	0.6383	0.6538	0.6370	0.6149	0.5824										
M 2A	0.4491	0.4818	0.4713	0.4714	0.4338										
TURN	12.857	14.304	15.132	12.081	11.104										
UUBAR	0.0953	0.0857	0.0878	0.0497	0.1039										
DFAC	0.4219	0.3917	0.3984	0.3552	0.3908										
EFFP	1.3505	1.4042	1.0627	0.9850	1.3047										
INCID	-5.59	-7.25	-8.12	-7.77	-2.55										
DEV	11.56	8.46	6.76	10.16	16.36										
DIA	33.564	34.992	36.420	37.848	39.276										

Table B-2. Blade Element Performance (Continued)

PERCENT DESIGN SPEED = 100.07

CORRECTED WEIGHT FLOW = 107.88

CORRECTED ROTOR SPEED = 5370.00

INLET GUIDE VANE		STATION 0 - STATION 1		STATION 1 - STATION 2		SLOTTED ROTOR	
PCT SPAN		90	70	50	30	10	PCT SPAN
DIA	33.622	35.167	36.711	38.256	39.801	DIA	33.589
BETA 0	0.000	0.000	0.000	0.000	0.000	BETA 1	35.067
BETA 1	17.182	18.082	18.717	19.162	19.704	BETA 2	36.545
V 0	481.02	481.02	481.02	481.02	481.02	BETA(PR) 1	38.023
V 1	598.81	60.56	593.92	587.23	571.29	BETA(PR) 2	39.501
VZ 0	481.02	481.02	481.02	481.02	481.02	EFF	19.62
VZ 1	572.09	570.90	562.51	554.69	537.84	EFF	19.704
V-THETA 0	-0.00	-0.00	-0.00	-0.00	-0.00	V 1	18.182
V-THETA 1	176.89	186.40	190.58	192.75	192.62	V 2	18.082
M 0	0.4391	0.4391	0.4391	0.4391	0.4391	VZ 1	36.116
M 1	0.5525	0.5542	0.5477	0.5412	0.5257	VZ 2	40.565
TURN	-17.18	-18.08	-18.72	-19.16	-19.70	V(PRI) 1	43.444
UBAR	0.0477	0.0007	0.0018	0.0062	0.0543	V(PRI) 2	43.444
DFAC	-0.067	-0.050	-0.031	-0.013	0.023	V(THETA PR1)	43.444
EFFP	0.9266	0.9989	0.9969	0.9887	0.8920	V(THETA PR2)	43.444
INCID	0.0000	0.0000	0.0000	0.0000	0.0000	U 1	46.155
DEV	6.858	5.888	6.123	7.438	9.176	U 2	46.155
STATOR		STATOR 1		STATOR 2		STATOR 2A	
PCT SPAN		90	70	50	30	10	PCT SPAN
BETA 2	37.702	36.823	36.035	36.116	40.566	M(PRI) 1	46.547
BETA 2A	27.400	24.400	22.700	25.400	32.200	M(PRI) 2	46.547
V 2	754.71	728.39	706.37	689.13	666.51	TURN(PR)	46.547
V 2A	573.93	585.49	561.12	573.62	531.56	U(BAR)	46.547
VZ 2	597.13	583.07	571.21	556.70	506.32	DFAC	46.547
VZ 2A	509.55	533.19	517.66	518.17	449.81	EFFP	46.547
V-THETA 2	461.55	436.56	415.54	406.19	433.45	EFF	46.547
V-THETA 2A	264.12	241.87	216.54	246.05	283.26	INCID	46.547
M 2	0.6756	0.6579	0.6368	0.6200	0.5956	DEV	46.547
M 2A	0.5081	0.5223	0.5006	0.5098	0.4701	EFF	46.547
TURN	10.302	12.423	13.335	10.716	8.366	INCID	46.547
UBAR	0.1507	0.0843	0.1038	0.0477	0.1309	LOSS PARA	46.547
DFAC	0.3487	0.3129	0.3340	0.2782	0.3142		46.547
EFFP	1.1436	0.9543	1.0458	0.8307	0.8345		46.547
INCID	-9.25	-10.13	-10.91	-10.83	-6.38		46.547
DEV	10.46	7.46	5.76	9.46	15.26		
DIA	33.564	34.992	36.420	37.848	39.276		

Table B-2. Blade Element Performance (Continued)

PERCENT DESIGN SPEED = 99.94
 CORRECTED WEIGHT FLOW = 94.42
 CORRECTED ROTOR SPEED = 5363.00

INLET GUIDE VANE 2		STATION 0 - STATION 1				STATION 1 - STATION 2				SLOTTED ROTOR 2			
PCT SPAN		90	70	50	30	10	PCT SPAN	90	70	50	30	10	
DIA	33.622	35.167	36.711	38.256	39.801	39.801	DIA	33.589	35.067	36.545	38.023	39.501	
BETA 0	0.000	0.000	0.000	0.000	0.000	0.000	BETA 1	17.060	17.664	18.313	18.738	19.173	
BETA 1	17.060	17.664	18.313	18.738	19.173	19.173	BETA 2	52.657	45.781	44.775	46.314	53.347	
V 0	409.86	409.36	409.86	409.86	409.86	409.86	BETA(PR) 1	53.601	54.995	56.648	58.196	59.954	
V 1	494.79	494.55	489.32	474.85	474.85	474.85	BETA(PR) 2	35.819	37.507	41.499	47.222		
VZ 0	409.86	409.86	409.86	409.86	409.86	409.86	V 1	494.79	494.55	489.05	484.32	474.86	
VZ 1	473.02	471.23	464.28	458.65	448.52	448.52	V 2	637.57	681.24	684.59	662.05	638.61	
V-THETA 0	0.00	0.00	0.00	0.00	0.00	0.00	VZ 1	473.02	471.23	464.28	458.65	448.52	
V-THETA 1	145.16	150.66	155.58	155.95	155.95	155.95	VZ 2	386.74	475.10	435.98	457.28	381.23	
M 0	0.3722	0.3722	0.3722	0.3722	0.3722	0.3722	V-THETA 1	145.16	150.06	153.66	155.58	155.95	
M 1	0.4522	0.4514	0.4467	0.4422	0.4333	0.4333	V-THETA 2	506.98	489.23	482.17	478.75	512.34	
TURN	-17.06	-17.66	-18.31	-18.74	-19.17	-19.17	V(PRI) 1	797.1	821.5	844.5	870.3	895.8	
UUBAR	0.0351	0.03922	0.0112	0.0149	0.0383	0.0383	V(PRI) 2	476.9	579.8	612.6	614.9	561.3	
DFAC	-0.039	-0.015	0.015	0.015	0.015	0.015	VTHETA PR1	-641.6	-672.9	-705.4	-739.6	-775.4	
EFFP	0.9331	0.9955	0.9760	0.9660	0.9040	0.9040	VTHETA PR2	-279.1	-332.4	-373.0	-411.0	-412.0	
INCID	0.0001	0.0001	0.0001	0.0001	0.0001	0.0001	U 1	786.77	922.93	859.06	895.21	931.36	
DEV	6.980	6.306	6.527	7.862	9.707	9.707	U 2	786.00	820.59	855.17	889.76	924.34	
STATOR 1													
PCT SPAN		90	70	50	30	10	M(PRI) 1	0.7285	0.7507	0.7714	0.7947	0.8173	
BETA 2	52.657	45.781	44.775	46.314	53.347	53.347	M(PRI) 2	0.4152	0.5114	0.5420	0.5421	0.4891	
BETA 3	29.700	28.200	26.300	28.900	33.000	33.000	TURN(PR)	17.782	20.020	19.141	16.247	12.732	
V 2	637.57	681.24	684.59	662.05	638.61	638.61	UUBAR	0.2033	0.0672	0.0468	0.0385	0.2159	
V 2A	416.96	468.45	501.96	482.31	454.77	454.77	DFAC	0.5851	0.4689	0.4476	0.4422	0.4333	
VZ 2	346.74	475.10	485.98	457.28	391.23	391.23	M(PRI) 2	0.7285	0.7507	0.7714	0.7947	0.8173	
V-THETA 2	506.88	488.23	482.17	478.75	512.34	512.34	M(PRI) 2	0.4152	0.5114	0.5420	0.5421	0.4891	
V-THETA 2A	206.59	221.37	222.40	233.09	247.59	247.59	TURN(PR)	17.782	20.020	19.141	16.247	12.732	
M 1	0.9550	0.6008	0.6056	0.5837	0.5564	0.5564	UUBAR	0.2033	0.0672	0.0468	0.0385	0.2159	
M 2A	C*36C4	C*4CB4	0.4391	0.4197	0.3932	0.3932	DFAC	0.5888	0.7884	0.8638	0.8253	0.6847	
TURN	22.957	17.581	18.475	17.414	20.347	20.347	M(PRI) 2	0.4152	0.5114	0.5420	0.5421	0.4891	
UUBAR	0.0142	0.0725	0.0318	0.0446	0.0762	0.0762	TURN(PR)	17.782	20.020	19.141	16.247	12.732	
DFAC	0.9425	0.4832	0.4395	0.4475	0.4923	0.4923	UUBAR	0.2033	0.0672	0.0468	0.0385	0.2159	
EFFP	2.3709	1.4082	1.3651	1.0903	1.6494	1.6494	DFAC	0.5888	0.7884	0.8638	0.8253	0.6847	
INCID	5.71	-1.17	-2.17	-0.64	6.40	6.40	INCID	1.44	1.38	1.62	2.16	3.16	
DEV	12.76	11.26	9.36	11.96	16.06	16.06	DEV	19.669	11.375	8.267	8.039	8.572	
DIA	33.564	34.997	36.420	37.848	39.276	39.276	INCID	0.047572	0.016114	0.012398	0.026645	0.058478	

Table B-2. Blade Element Performance (Continued)

INLET GUIDE VANE		STATION 0 - STATION 1		STATION 1 - STATION 2		SLOTTED ROTOR	
PCT SPAN		90	70	50	30	10	
DIA	33.622	35.167	36.711	38.256	39.801		
BETA 0	0.000	0.000	0.000	0.000	0.000	DIA	33.589
BETA 1	17.782	17.417	18.083	18.503	18.997	BETA 1	17.782
V 0	263.87	263.87	263.87	263.87	263.87	BETA 2	33.484
V 1	305.60	310.38	307.94	305.09	297.62	BETA(PR) 1	46.122
VZ 0	263.87	263.87	263.87	263.87	263.87	BETA(PR) 2	47.327
VZ 1	291.00	296.15	292.73	289.32	281.41	V 1	28.091
V-THETA 0	-0.00	-0.00	-0.00	-0.00	-0.00	V 2	305.60
V-THETA 1	93.33	92.91	95.58	96.82	96.88	VZ 1	306.60
M 0	0.2377	0.2377	0.2377	0.2377	0.2377	V-THETA 1	93.33
M 1	0.2158	0.2802	0.2780	0.2753	0.2685	V-THETA 2	218.92
TURN	-17.78	-17.42	-18.08	-18.50	-19.00	V(PR) 1	419.8
UUBAR	0.0564	0.0036	0.0018	0.0005	0.0005	V(PR) 2	375.1
DFAC	0.009	0.004	0.019	0.024	0.0265	VTHETA PR1	-302.6
EFFP	0.8614	0.9910	0.9951	0.9848	0.8638	VTHETA PR2	-176.6
INCID	0.0000	0.0000	0.0000	0.0000	0.0000	U 1	395.95
DEV	6.258	6.553	6.757	8.097	9.883	U 2	395.56
STATOR 1							
PCT SPAN		90	70	50	30	10	
BETA 2	33.484	32.665	31.660	31.211	32.211	M(PRI) 1	0.3789
BETA 2A	23.900	22.4300	22.000	23.000	26.500	M(PRI) 2	0.3363
V 2	396.80	381.73	374.95	355.08	331.21	TURN(PR)	18.030
VZ 2A	350.36	350.76	342.64	339.30	298.59	UUBAR	0.0177
VZ 2A	330.95	326.40	319.15	303.69	280.23	DFAC	0.2276
V-THETA 2	32.24	32.9.15	317.69	312.33	267.22	EFFP	0.6972
V-THETA 2A	218.92	209.27	196.80	184.00	176.55	EFF	0.6947
M 2	0.3557	0.3483	0.3483	0.3369	0.3369	INCID	-6.04
M 2A	0.3147	0.3197	0.3077	0.3047	0.2968	DEV	11.941
TURN	9.584	10.365	9.660	8.211	5.711	LOSS PARA	0.003334
UUBAR	0.1127	0.0655	0.0855	0.0153	0.1325		
DFAC	0.1951	0.1662	0.1696	0.1136	0.1638		
EFFP	1.3579	-4.2316	2.4835	-5.3364	0.8077		
INCID	-13.47	-14.28	-15.29	-15.74	-14.74		
DE.M	6.96	5.36	5.06	6.06	9.56		
DIA	33.564	34.992	36.420	37.848	39.276		

Table B-2. Blade Element Performance (Continued)

PERCENT DESIGN SPEED = 50.22
CORRECTED WEIGHT FLOW = 47.41
CORRECTED ROTOR SPEED = 2695.00

INLET GUIDE VANE 2			STATION 0 - STATION 1			STATION 1 - STATION 2			SLOTTED ROTOR 2		
PCT SPAN	90	70	50	30	10	PCT SPAN	90	70	50	30	10
DIA	33.622	35.167	36.711	38.256	39.801	DIA	33.589	35.067	36.545	38.023	39.501
BETA 0	0.000	0.000	0.000	0.000	0.000	BETA 1	16.671	17.214	17.809	18.263	18.622
BETA 1	16.671	17.214	17.869	18.263	18.622	BETA 2	52.709	45.726	44.368	45.496	52.506
V 0	19.5.34	19.5.34	19.5.34	19.5.34	19.5.34	BETA(PR) 1	57.241	58.108	59.258	60.607	62.320
V 1	222.66	225.85	226.36	225.02	220.16	BETA(PR) 2	33.762	35.560	39.320	41.567	47.281
V 2 0	19.5.34	19.5.34	19.5.34	19.5.34	19.5.34	V 1	222.66	225.85	226.36	225.02	220.16
V 2 1	213.30	215.73	215.44	213.68	208.63	V 2	328.99	339.38	334.48	334.97	319.77
V-THETA 0	-0.00	-0.00	-0.00	-0.00	-0.00	VZ 1	223.30	215.73	213.68	208.63	208.63
V-THETA 1	63.87	66.84	69.46	70.52	70.30	VZ 2	199.32	236.92	239.11	234.80	194.64
M 3	0.1755	0.1755	0.1755	0.1755	0.1755	V-THETA 1	63.87	66.84	69.46	70.52	70.30
M 1	0.2002	0.2031	0.2036	0.2024	0.1980	V-THETA 2	261.74	243.00	233.89	238.90	253.71
TURN	-16.67	-17.21	-17.87	-18.26	-18.62	V(PR) 1	394.2	408.3	421.5	435.4	449.1
UUBAR	0.0519	0.0662	-0.0065	0.0540	0.0540	V(PR) 2	239.8	291.2	309.1	313.8	286.9
DFAC	0.015	0.019	0.024	0.036	0.062	VTHETA PR1	-331.5	-346.7	-362.2	-379.3	-397.7
EFFP	0.8565	0.9822	1.0192	0.9910	0.8353	VTHETA PR2	-133.2	-169.4	-195.8	-208.2	-210.8
INCID	0.0000	0.0000	0.0000	0.0000	0.0000	U 1	395.37	413.53	431.69	449.86	468.33
DEV	7.369	6.756	6.971	8.337	10.258	U 2	394.98	412.36	429.74	447.12	464.50
						M 1	0.2002	0.2031	0.2074	0.224	0.1980
						M 2	0.2918	0.3018	0.2982	0.2843	
						M(PR) 1	0.3545	0.3673	0.3791	0.3916	
						M(PR) 2	0.2127	0.2590	0.2756	0.2917	
						TURN(PR)	23.479	22.549	19.938	19.041	15.100
						UUBAR	0.1781	0.0407	0.0111	0.0352	0.1569
						DFAC	0.5946	0.4698	0.4402	0.4592	0.5592
						EFFP	0.5605	0.6757	0.8247	0.8448	0.7317
						EFF	0.5560	0.6721	0.8228	0.8430	0.7286
						INCIDM	5.08	4.50	4.23	4.57	5.53
						LOSS PARA	0.0553	0.0539	0.0372	0.09582	0.04967
						DEV	17.612	11.960	10.080	7.657	8.431
						DIA	36.420	37.848	34.992	39.276	

Table B-2. Blade Element Performance (Continued)

INLET GUIDE VANE 2										SLOTTED ROTOR 2									
STATION 0 - STATION 1										STATION 1 - STATION 2									
PCT SPAN	90	70	50	30	10	PCT SPAN	90	70	50	30	PCT SPAN	90	70	50	30	10			
DIA	33.622	35.167	36.711	38.256	39.801	DIA	33.589	35.067	36.545	38.023	39.501								
BETA 0	0.000	0.000	0.000	0.000	0.000	BETA 1	16.037	16.950	17.623	17.709	19.201	16.037	16.950	17.623	17.709	19.201			
BETA 1	16.037	16.950	17.623	17.709	19.201	BETA 2	44.525	44.286	45.225	46.126	46.218	40.126	40.855	41.507	41.507	46.218			
V 0	219.87	219.87	219.87	219.87	219.87	BETA(PR) 1	54.286	53.737	55.249	57.069	59.256								
V 1	245.83	259.96	258.26	254.20	244.92	BETA(PR) 2	31.151	33.024	36.821	41.507	46.623								
VZ 0	219.87	219.87	219.87	219.87	219.87	V 1	245.83	259.96	258.26	254.20	244.92								
VZ 1	236.27	248.67	242.16	231.30	231.30	V 2	349.90	361.67	354.18	338.84	320.36								
V-THETA 0	-0.00	-0.00	-0.00	-0.00	-0.00	VZ 1	236.27	248.67	246.14	242.16	231.30								
V-THETA 1	67.91	75.79	78.19	77.32	80.55	VZ 2	249.46	270.82	256.28	221.66									
M 0	0.1977	0.1977	0.1977	0.1977	0.1977	V-THETA 1	67.91	75.79	78.19	77.32	80.55								
M 1	0.2213	0.2341	0.2326	0.2205	0.2289	V-THETA 2	245.16	234.74	228.26	221.65	231.29								
TURN	-16.04	-16.95	-17.62	-17.71	-19.20	V(PR) 1	404.47	420.47	431.8	445.4	452.5								
UUBAR	0.1838	0.0702	-0.0003	0.0173	0.0627	V(PR) 2	291.5	328.2	338.3	342.2	322.7								
DFAC	0.028	-0.006	0.008	0.026	0.079	VTHETA PR1	-328.6	-339.0	-354.8	-373.9	-388.9								
EFFP	0.5803	0.9825	1.0008	0.9519	0.7963	VTHETA PR2	-150.8	-178.8	-202.8	-226.8	-234.6								
INCID	0.0000	0.0000	0.0000	0.0000	0.0000	U 1	396.54	414.76	432.97	451.19	469.42								
DEV	8.003	7.020	7.217	8.891	9.679	M 1	0.2213	0.2341	0.2326	0.2289	0.2205								
						STATOR 1	M 2	0.3115	0.3231	0.3164	0.3025	0.2855							
							M (PR) 1	0.3643	0.3786	0.3889	0.4011	0.4172							
							M (PR) 2	0.2595	0.2932	0.3055	0.3055	0.2876							
							TURN(PR)	23.134	20.713	18.427	15.561	12.633							
							UUBAR	0.0869	0.0011	-0.0012	0.0298	0.1164							
							EFFAC	0.4571	0.3800	0.3715	0.3832	0.4494							
							EFFP	0.6343	0.8103	0.8243	0.8020	0.7251							
BETA 2	44.525	40.469	40.126	40.855	46.218	EFF	0.6306	0.8083	0.8224	0.8000	0.7224								
BETA 2A	27.400	23.300	23.600	26.000	30.500	INCID	2.13	0.13	0.22	1.03	2.47								
V 2	349.90	361.67	354.18	338.84	320.36														
V 2A	253.84	283.17	279.10	271.75	247.93	DEV	15.001	9.424	7.581	7.597	7.973								
VZ 2	249.46	275.15	270.82	256.28	221.66	LOSS PARA	0.02975	0.00038	-0.00418	0.01006	0.03733								
VZ 2A	225.36	258.08	255.76	244.25	213.62														
V-THETA 2	245.36	234.74	228.26	221.65	231.29														
V-THETA 2A	116.82	116.53	111.74	119.13	125.83														
M 2	0.3115	0.3231	0.3164	0.3025	0.2855														
M 2A	0.2258	0.2528	0.2491	0.2424	0.2207														
TURN	17.125	16.169	16.526	14.855	15.718														
UUBAR	0.850	0.0569	0.0677	0.0525	0.1005														
DFAC	0.4278	0.3597	0.3618	0.3417	0.3887														
EFFP	4.4364	4.5474	3.4459	2.7819	1.9080														
INCID	-2.42	-6.48	-6.82	-6.09	-0.73														
DEV	1C.46	7.36	6.66	9.06	13.56														
DIA	33.564	34.992	36.420	37.848	39.276														

Table B-2. Blade Element Performance (Continued)

INLET GUIDE VANE		STATION 0 - STATION 1		STATION 1 - STATION 2		SLOTTED ROTOR					
PCT SPAN	90	70	50	30	10	PCT SPAN	90	70	50	30	10
DIA	33.622	35.167	36.711	38.256	39.801	DIA	33.589	35.067	36.545	38.023	39.501
BETA 0	0.000	0.000	0.000	0.000	0.000	BETA 1	16.209	16.826	17.632	17.889	19.348
BETA 1	16.209	16.826	17.632	17.889	19.348	BETA 2	40.512	38.268	37.955	38.201	42.610
V 0	232.9C	232.90	232.90	232.90	232.90	BETA(PR) 1	50.719	51.721	53.216	54.992	56.885
V 1	272.59	275.76	274.15	270.55	263.74	BETA(PR) 2	30.035	32.628	36.053	40.772	48.459
VZ 0	232.90	232.90	232.90	232.90	232.90	V 1	272.59	275.76	274.15	270.55	263.74
VZ 1	261.75	263.95	261.47	257.47	248.85	V 2	363.32	368.21	362.09	345.62	308.66
V-THETA 0	-C.CC	-0.00	-0.00	-0.00	-0.00	VZ 1	261.75	263.95	261.27	257.47	248.85
V-THETA 1	76.59	79.82	83.04	83.10	87.38	VZ 2	276.22	289.09	285.50	271.60	227.17
M 0	0.2095	0.2095	0.2095	0.2095	0.2095	V-THETA 1	76.09	79.82	83.04	83.10	87.38
M 1	0.2456	0.2485	0.2471	0.2438	0.2376	V-THETA 2	236.01	228.05	222.70	213.74	208.96
TURN	-16.21	-16.83	-17.63	-17.89	-19.35	V(PR) 1	413.4	426.1	436.3	448.8	455.5
UUBAR	0.c629	0.0066	-0.0001	0.0134	0.0584	V(PR) 2	319.1	343.3	353.1	358.6	342.6
DFAC	-0.016	-0.009	0.006	0.024	0.065	V(THETA PR1	-320.0	-334.5	-349.5	-367.6	-381.5
EFFP	0.e572	0.9841	1.0003	0.9638	0.8315	V(THETA PR2	-159.7	-185.7	-207.8	-234.2	-256.4
INCID	0.c00C	0.0000	0.0000	0.0000	0.0000	U 1	396.10	414.30	432.49	450.69	468.89
DEV	7.831	7.144	7.208	8.711	9.532	U 2	395.71	413.12	430.54	447.95	465.36
						M 1	0.2456	0.2485	0.2471	0.2438	0.2376
						M 2	0.3241	0.3295	0.3092	0.2752	
						M(PR) 1	0.3726	0.3840	0.3932	0.4044	0.4103
						M(PR) 2	0.2846	0.3072	0.316C	0.3208	0.3354
						TURN(PR)	20.684	19.093	17.163	14.220	8.426
						UUBAR	0.0608	0.0648	-0.0027	0.0181	0.0857
						DFAC	0.3847	0.3423	0.3336	0.3374	0.3795
BETA 2	4C.512	38.268	37.955	38.201	42.610	EFFP	0.6401	0.8370	0.8568	0.8549	0.6446
BETA 2A	26.70C	23.800	23.100	25.400	29.300	EFF	0.6368	0.8354	0.8555	0.8536	0.6418
V 2	362.32	368.21	362.09	345.62	308.66	INCID	-1.44	-1.89	-1.81	-1.05	C.10
V 2A	275.49	298.00	287.47	275.96	252.06	DEV	13.885	9.028	6.813	6.862	9.809
VZ 2	276.22	289.09	285.50	271.60	227.17	LOSS PARA	0.02106	0.00168	0.00095	0.00317	0.02655
V-THETA 2	236.01	228.05	222.70	213.74	208.96						
V-THETA 2A	125.58	120.26	112.78	118.37	123.35						
M 2	0.2241	0.3295	0.3240	0.3092	0.2752						
M 2A	0.2492	0.2664	0.2568	0.2464	0.2246						
TURN	13.812	14.468	14.855	12.801	13.310						
UUBAR	0.C95C	0.0761	0.1164	0.1153	0.0690						
DFAC	0.2576	0.3184	0.3443	0.3326	0.3206						
EFFP	5.889C	2.8798	1.5550	1.1501	3.6832						
INCID	-t.44	-8.68	-8.99	-8.75	-4.34						
DEV	5.76	6.86	6.16	8.46	12.36						
DIA	33.564	34.992	36.420	37.848	39.276						

Table B-2. Blade Element Performance (Continued)

PERCENT DESIGN SPEED = 50.11
 CORRECTED WEIGHT FLOW = 58.36
 CORRECTED ROTOR SPEED = 2689.00

INLET GUIDE VANE		STATION 0 - STATION 1			STATION 1 - STATION 2			SLOTTED ROTOR 2					
		90	70	50	30	10	PCT SPAN	90	70	50	30	10	
DIA	33.622	35.167	36.711	38.256	39.801	DIA	33.589	35.067	36.545	38.623	39.501		
BETA 0	0.000	0.000	0.000	0.000	0.000	BETA 1	16.240	16.905	17.761	17.965	19.070		
BETA 1	16.240	16.905	17.761	17.965	19.070	BETA 2	37.856	36.673	35.339	36.555	40.377		
V 0	242.36	242.36	242.36	242.36	242.36	BETA(PR) 1	48.967	50.005	51.675	53.422	55.601		
V 1	285.27	288.29	285.29	282.25	273.56	BETA(PR) 2	29.330	32.085	35.079	40.669	47.054		
V 2	242.36	242.36	242.36	242.36	242.36	V 1	285.27	288.29	285.29	282.25	273.56		
V 3	273.85	275.84	271.69	268.49	258.54	V 2	372.74	374.01	366.82	347.26	315.94		
V-THETA 0	-C.CC	-0.00	-0.00	-0.00	-0.00	VZ 1	273.89	275.84	271.69	268.49	258.54		
V-THETA 1	79.78	83.83	87.03	87.06	89.38	VZ 2	299.98	296.99	280.02	280.02	280.02		
M 0	0.2181	0.2181	0.2181	0.2181	0.2181	V-THETA 1	79.78	83.83	87.03	87.06	89.38		
M 1	0.2572	0.2600	0.2572	0.2545	0.2465	V-THETA 2	228.74	223.38	215.30	205.36	204.64		
TURN	-16.24	-16.90	-17.76	-17.97	-19.07	V(PR) 1	417.2	429.2	438.1	450.5	457.6		
UBAR	0.C466	-0.0054	0.0007	C.C113	0.0737	V(PR) 2	337.6	354.7	365.8	369.3	353.4		
DFAC	-0.012	-0.012	0.007	0.065	VTHETA PR1	-314.7	-328.8	-343.7	-361.8	-377.6			
EFFP	0.e8942	1.0128	0.9925	0.9700	0.7916	VTHETA PR2	-165.4	-188.1	-213.5	-240.8	-250.8		
INCID	0.C0CC	0.0000	0.0000	0.0000	0.0000	U 1	394.49	412.61	430.73	448.86	466.98		
DEV	7.800	7.065	7.079	8.635	9.810	U 2	394.10	411.44	428.78	446.12	463.46		
		STATOR 1			M 1	M 2	0.2572	0.2600	0.2572	0.2545	0.2465		
		STATION 2 - STATION 2A			M (PR) 1	M (PR) 2	0.3350	0.3350	0.3286	0.3109	0.2822		
		STATION 2 - STATION 2A			TURN(PR)	TURN(PR)	0.3017	0.3276	0.3307	0.3158	0.3158		
		STATION 2 - STATION 2A			UUBAR	UUBAR	0.0296	0.0035	-0.0158	0.0142	0.0905		
		STATION 2 - STATION 2A			DFAC	DFAC	0.3353	0.3133	0.2961	0.3039	0.3522		
		STATION 2 - STATION 2A			EFFP	EFFP	0.6734	0.8158	0.8551	0.8370	0.6951		
		STATION 2 - STATION 2A			EFF	EFF	0.6705	0.8141	0.8537	0.8356	0.6929		
		STATION 2 - STATION 2A			INCID	INCID	-3.19	-3.61	-3.36	-2.62	-1.19		
BETA 2	37.856	36.673	35.939	36.255	40.377	DEV	13.180	8.485	6.469	6.779	8.434		
BETA 2A	26.100	23.600	22.600	24.600	29.300	LOSS PARA	0.01042	0.00123	0.000538	0.000485	0.02875		
V 2	372.74	374.01	366.82	347.26	315.90								
V 2A	297.65	313.42	308.59	285.79	263.67								
VZ 2	294.30	299.98	296.99	280.02	240.65								
VZ 2A	267.30	287.21	284.89	259.85	229.68								
V-THETA 2	228.74	223.38	215.30	205.36	204.64								
V-THETA 2A	13C.95	125.48	118.59	118.97	128.89								
M 2	0.3331	0.3350	0.3286	C.3109	0.2822								
M 2A	0.2656	0.2806	0.2762	0.2555	0.2350								
TURN	11.756	13.073	13.339	11.655	11.077								
UBAR	0.1125	0.076	0.0812	0.1155	0.0839								
DFAC	0.3110	0.2763	0.2789	C.2952	0.2851								
EFFP	1.6336	8.3591	3.1172	1.2825	1.5201								
INCID	-5.059	-10.028	-11.001	-10.657	-6.557								
DEV	5.016	6.666	5.666	7.666	12.336								
DIA	33.564	36.992	36.720	37.868	39.776								

Table B-2. Blade Element Performance (Continued)

PERCENT DESIGN SPEED = 50.97
CORRECTED WEIGHT FLGHT = 60.66
CORRECTED ROTHR SPEED = 2735.00

INLET GUIDE VANE 2						STATION 0 - STATION 1						STATION 1 - STATION 2						SLOTTED ROTHR 2					
PCT SPAN	90	70	50	30	10	PCT SPAN	90	70	50	30	10	PCT SPAN	90	70	50	30	10	PCT SPAN	90	70	50	30	10
DIA	33.622	35.167	36.711	38.256	39.801	DIA	33.529	35.067	36.545	38.023	39.501	DIA	33.529	35.067	36.545	38.023	39.501	DIA	33.529	35.067	36.545	38.023	39.501
BETA 0	0.000	0.000	0.000	0.000	0.000	BETA 1	16.109	17.041	17.982	19.020	19.060	BETA 2	17.041	17.982	19.020	19.060	19.060	BETA 1	17.041	17.982	19.020	19.060	19.060
BETA 1	16.109	17.041	17.982	19.020	19.060	BETA 2	17.041	17.982	19.020	19.060	19.060	BETA (PR) 1	44.493	47.605	51.529	53.286	55.068	BETA (PR) 1	44.493	47.605	51.529	53.286	55.068
V 2	252.13	252.13	252.13	252.13	252.13	V 3	252.13	252.13	252.13	252.13	252.13	V 1	252.13	252.13	252.13	252.13	252.13	V 2	252.13	252.13	252.13	252.13	252.13
V 3	328.52	312.57	291.63	288.81	278.35	V 1	252.13	252.13	252.13	252.13	252.13	V 2	252.13	252.13	252.13	252.13	252.13	V 2	252.13	252.13	252.13	252.13	252.13
V 1	328.52	312.57	291.63	288.81	278.35	V 2	252.13	252.13	252.13	252.13	252.13	V 1	252.13	252.13	252.13	252.13	252.13	V 2	252.13	252.13	252.13	252.13	252.13
V 2	252.13	252.13	252.13	252.13	252.13	V 2	252.13	252.13	252.13	252.13	252.13	V 1	252.13	252.13	252.13	252.13	252.13	V 2	252.13	252.13	252.13	252.13	252.13
V 2	315.62	298.85	277.93	274.92	271.05	V 2	252.13	252.13	252.13	252.13	252.13	V 1	252.13	252.13	252.13	252.13	252.13	V 2	252.13	252.13	252.13	252.13	252.13
V 2	315.62	298.85	277.93	274.92	271.05	V 2	252.13	252.13	252.13	252.13	252.13	V 1	252.13	252.13	252.13	252.13	252.13	V 2	252.13	252.13	252.13	252.13	252.13
V-THETA 0	-0.000	-0.000	-0.000	-0.000	-0.000	V-THETA 1	91.15	88.33	88.49	90.99	90.99	V-THETA 2	91.15	91.60	91.60	91.60	91.60	V-THETA 1	91.15	91.60	91.60	91.60	91.60
M 3	0.2270	0.2270	0.2270	0.2270	0.2270	M 1	0.2630	0.2822	0.2822	0.2604	0.2604	M 2	0.2630	0.2822	0.2822	0.2822	0.2822	M 3	0.2630	0.2822	0.2822	0.2822	0.2822
M 1	0.2969	0.2969	0.2969	0.2969	0.2969	M 1	0.2630	0.2822	0.2822	0.2604	0.2604	M 2	0.2630	0.2822	0.2822	0.2822	0.2822	M 1	0.2630	0.2822	0.2822	0.2822	0.2822
TURN	-16.11	-17.04	-17.63	-17.84	-19.08	TURN	-17.63	-17.84	-19.08	-19.08	-19.08	TURN	-17.84	-19.08	-19.08	-19.08	-19.08	TURN	-17.84	-19.08	-19.08	-19.08	-19.08
UUBAR	0.0018	0.0018	0.0018	0.0018	0.0018	DFAC	-0.132	-0.054	0.023	0.037	0.086	VTHETA PR1	-310.1	-328.1	-349.8	-368.0	-384.9	VTHETA PR1	-310.1	-328.1	-349.8	-368.0	-384.9
DFAC	0.0467	0.0467	0.0467	0.0467	0.0467	EFFP	0.9967	0.9893	1.0003	0.7741	0.7741	VTHETA PR2	-185.8	-185.8	-185.8	-185.8	-185.8	VTHETA PR2	-185.8	-185.8	-185.8	-185.8	-185.8
EFFP	0.0000	0.0000	0.0000	0.0000	0.0000	INCID	0.0000	0.0000	0.0000	0.0000	0.0000	INCID	0.0000	0.0000	0.0000	0.0000	0.0000	INCID	0.0000	0.0000	0.0000	0.0000	0.0000
INCID	0.0000	0.0000	0.0000	0.0000	0.0000	DEV	7.931	6.929	7.209	8.758	9.800	U 1	401.23	419.67	438.10	456.54	474.97	U 1	401.23	419.67	438.10	456.54	474.97
DEV	7.931	6.929	7.209	8.758	9.800	U 2	401.23	419.67	438.10	456.54	474.97	U 2	401.23	419.67	438.10	456.54	474.97	U 2	401.23	419.67	438.10	456.54	474.97
U 2	401.23	419.67	438.10	456.54	474.97	STATGR 1	401.23	419.67	438.10	456.54	474.97	STATGR 2A	13.179	13.219	13.219	9.808	7.965	STATGR 1	401.23	419.67	438.10	456.54	474.97
STATGR 1	401.23	419.67	438.10	456.54	474.97	UUBAR	0.0065	0.0065	0.0065	0.0065	0.0065	UUBAR	0.0065	0.0065	0.0065	0.0065	0.0065	UUBAR	0.0065	0.0065	0.0065	0.0065	0.0065
UUBAR	0.0065	0.0065	0.0065	0.0065	0.0065	DFAC	0.3325	0.3325	0.3325	0.3325	0.3325	DFAC	0.3325	0.3325	0.3325	0.3325	0.3325	DFAC	0.3325	0.3325	0.3325	0.3325	0.3325
DFAC	0.3325	0.3325	0.3325	0.3325	0.3325	EFFP	0.718	0.718	0.718	0.718	0.718	EFF	0.7196	0.7196	0.7196	0.7196	0.7196	EFF	0.7196	0.7196	0.7196	0.7196	0.7196
EFFP	0.718	0.718	0.718	0.718	0.718	INCID	-7.67	-7.67	-7.67	-7.67	-7.67	INCID	-7.67	-7.67	-7.67	-7.67	-7.67	INCID	-7.67	-7.67	-7.67	-7.67	-7.67
INCID	-7.67	-7.67	-7.67	-7.67	-7.67	DEV	15.164	10.859	10.859	10.859	10.859	DEV	15.164	10.859	10.859	10.859	10.859	DEV	15.164	10.859	10.859	10.859	10.859
DEV	15.164	10.859	10.859	10.859	10.859	LOSS PARA	0.00228	0.00237	0.00237	0.00237	0.00237	LOSS PARA	0.00228	0.00237	0.00237	0.00237	0.00237	LOSS PARA	0.00228	0.00237	0.00237	0.00237	0.00237
LOSS PARA	0.00228	0.00237	0.00237	0.00237	0.00237	DFAC	0.2539	0.2539	0.2539	0.2539	0.2539	EFF	0.9792	0.9792	0.9792	0.9792	0.9792	EFF	0.9792	0.9792	0.9792	0.9792	0.9792
EFF	0.9792	0.9792	0.9792	0.9792	0.9792	INCID	-3.50	-3.50	-3.50	-3.50	-3.50	INCID	-3.50	-3.50	-3.50	-3.50	-3.50	INCID	-3.50	-3.50	-3.50	-3.50	-3.50
INCID	-3.50	-3.50	-3.50	-3.50	-3.50	BETA 2	34.140	33.326	33.749	33.286	35.068	BETA 2A	24.206	23.000	22.200	24.000	27.500	BETA 2A	24.206	23.000	22.200	24.000	27.500
BETA 2	34.140	33.326	33.749	33.286	35.068	BETA 2A	37.355	37.014	35.969	33.856	32.034	BETA 2A	37.355	37.014	35.969	33.856	32.034	BETA 2A	37.355	37.014	35.969	33.856	32.034
BETA 2A	37.355	37.014	35.969	33.856	32.034	V 2	305.47	305.67	299.08	283.02	262.19	V 2	305.47	305.67	299.08	283.02	262.19	V 2	305.47	305.67	299.08	283.02	262.19
V 2	305.47	305.67	299.08	283.02	262.19	V 2A	438.60	304.86	300.86	274.30	249.22	V 2A	438.60	304.86	300.86	274.30	249.22	V 2A	438.60	304.86	300.86	274.30	249.22
V 2A	438.60	304.86	300.86	274.30	249.22	V-THETA 2	215.01	208.72	199.83	185.81	184.05	V-THETA 2A	197.17	129.41	122.70	123.27	129.74	V-THETA 2	215.01	208.72	199.83	185.81	184.05
V-THETA 2	215.01	208.72	199.83	185.81	184.05	V-THETA 2A	197.17	129.41	122.70	123.27	129.74	V-THETA 2	197.17	129.41	122.70	123.27	129.74	V-THETA 2	197.17	129.41	122.70	123.27	129.74
V-THETA 2A	197.17	129.41	122.70	123.27	129.74	V 2	480.88	331.19	324.74	300.72	280.97	V 2	480.88	331.19	324.74	300.72	280.97	V 2	480.88	331.19	324.74	300.72	280.97
V 2	480.88	331.19	324.74	300.72	280.97	V 2	480.88	331.19	324.74	300.72	280.97	V 2	480.88	331.19	324.74	300.72	280.97	V 2	480.88	331.19	324.74	300.72	280.97
V 2	480.88	331.19	324.74	300.72	280.97	V 2	480.88	331.19	324.74	300.72	280.97	V 2	480.88	331.19	324.74	300.72	280.97	V 2	480.88	331.19	324.74	300.72	280.97
V 2	480.88	331.19	324.74	300.72	280.97	V 2	480.88	331.19	324.74	300.72	280.97	V 2	480.88	331.19	324.74	300.72	280.97	V 2	480.88	331.19	324.74	300.72	280.97
V 2	480.88	331.19	324.74	300.72	280.97	V 2	480.88	331.19	324.74	300.72	280.97	V 2	480.88	331.19	324.74	300.72	280.97	V 2	480.88	331.19	324.74	300.72	280.97
V 2	480.88	331.19	324.74	300.72	280.97	V 2	480.88	331.19	324.74	300.72	280.97	V 2	480.88	331.19	324.74	300.72	280.97	V 2	480.88	331.19	324.74	300.72	280.97
V 2	480.88	331.19	324.74	300.72	280.97	V 2	480.88	331.19	324.74	300.72	280.97	V 2	480.88	331.19	324.74	300.72	280.97	V 2	480.88	331.19	324.74	300.72	280.97
V 2	480.88	331.19	324.74	300.72	280.97	V 2	480.88	331.19	324.74	300.72	280.97	V 2	480.88	331.19	324.74	300.72	280.97	V 2	480.88	331.19	324.74	300.72	280

Table B-2. Blade Element Performance (Continued)

PERCENT DESIGN SPEED = 69.51
 CORRECTED WEIGHT FLOW = 85.62
 CORRECTED ROTOR SPEED = 3730.00

INLET GUIDE VANE 2							SLOTTED ROTOR 2						
STATION 0 - STATION 1							STATION 1 - STATION 2						
PCT SPAN	90	70	50	30	10	PCT SPAN	90	70	50	30	10		
DIA	33.622	35.167	36.711	38.256	39.801	DIA	33.589	35.067	36.545	38.023	39.501		
BETA 0	0.000	0.000	0.000	0.000	0.000	BETA 1	15.370	16.792	17.183	16.846	17.900		
BETA 1	15.370	16.792	17.183	16.846	17.900	BETA 2	32.855	32.882	32.707	31.822	32.201		
V 0	366.40	366.40	366.40	366.40	366.40	BETA(PR) 1	45.594	46.462	48.134	50.450	52.429		
V 1	437.92	441.49	435.24	429.76	419.46	BETA(PR) 2	27.504	32.133	35.342	40.600	45.324		
VZ 0	366.40	366.40	366.40	366.40	366.40	V 1	437.92	441.49	435.24	429.76	419.46		
VZ 1	422.26	422.66	415.82	411.31	399.15	V 2	557.88	533.20	523.09	492.87	462.94		
V-THETA 0	-0.00	-0.00	-0.00	-0.00	-0.00	VZ 1	422.26	422.66	415.82	411.31	399.15		
V-THETA 1	116.07	127.54	128.58	124.54	128.92	VZ 2	468.65	447.77	440.15	418.79	391.73		
M 0	0.3318	0.3318	0.3318	0.3318	0.3318	V-THETA 1	116.07	127.54	128.58	124.54	128.92		
M 1	0.3984	0.4018	0.3959	0.3908	0.3811	V-THETA 2	302.66	289.48	282.65	259.88	246.69		
TURN	-15.37	-16.79	-17.18	-16.85	-17.90	V(PRI) 1	603.5	613.6	626.7	646.0	654.6		
UUBAR	0.481	0.0027	0.0045	0.0110	0.0592	V(PRI) 2	528.4	528.8	539.6	551.6	557.2		
DFAC	-0.045	-0.027	-0.008	0.004	0.040	VTHETA PR1	-431.1	-444.8	-468.9	-498.1	-518.8		
EFFP	0.5037	0.9944	0.9897	0.9729	0.8465	VTHETA PR2	-244.0	-281.2	-312.1	-359.0	-396.2		
INCID	0.0000	0.0000	0.0000	0.0000	0.0000	U 1	547.20	572.35	597.48	622.62	647.77		
DEV	8.670	7.178	7.657	9.754	10.980	U 2	546.67	570.72	594.78	618.83	642.89		
						M 1	0.3984	0.4018	0.3959	0.3908	0.3811		
						M 2	0.5028	0.4813	0.4712	0.4446	0.4160		
						STATGR 1							
						M(PRI) 1	0.5491	0.5584	0.5701	0.5874	0.5948		
						M(PRI) 2	0.4762	0.4773	0.4861	0.4976	0.5007		
						TURN(PRI)	18.091	14.329	13.092	9.850	7.104		
						UUBAR	0.0144	0.0328	0.0416	0.0576	0.0619		
						DFAC	0.2496	0.2508	0.2494	0.2456	0.2394		
						EFFP	0.8483	0.9201	0.8430	0.9631	0.7640		
BETA 2	32.855	32.882	32.707	31.822	32.201	EFF	0.8459	0.9190	0.8409	0.9626	0.7515		
BETA 2A	24.000	22.300	22.200	23.600	27.000	INCID	-6.56	-7.15	-6.60	-5.59	-4.36		
V 2	557.88	533.20	523.09	492.87	462.94								
V 2A	475.38	465.95	458.04	432.29	402.16	DEV	11.354	8.533	6.102	6.690	6.674		
VZ 2	468.65	447.77	440.15	418.79	391.73	LOSS PARA	0.00510	0.01161	0.01477	0.01976	0.02032		
VZ 2A	434.28	431.10	424.09	396.14	358.33								
V-THETA 2	289.48	282.65	259.88	246.69									
V-THETA 2A	192.35	176.81	173.07	173.07									
M 2	0.5028	0.4813	0.4712	0.4446									
M 2A	0.4253	0.4185	0.4117	0.3882									
TURN	8.855	10.582	10.507	8.222									
UUBAR	0.1693	0.1347	0.1426	0.1536									
DFAC	0.2297	0.2184	0.2200	0.2069									
EFFP	0.4128	0.5278	0.9994	0.3802									
INCID	-14.07	-14.07	-14.24	-15.13									
DEV	7.06	5.36	5.26	6.66									
DIA	33.564	34.992	36.420	37.848									

Table B-2. Blade Element Performance (Continued)

PERCENT DESIGN SPEED = 69.42
 CORRECTED WEIGHT FLOW = 60.76
 CORRECTED ROTOR SPEED = 3725.00

INLET GUIDE VANE 2							SLOTTED ROTOR 2							SLOTTED ROTOR 2				
STATION 0 - STATION 1				STATION 1 - STATION 2			STATION 1 - STATION 2				STATION 1 - STATION 2				STATION 1 - STATION 2			
PCT SPAN	90	70	50	30	10	PCT SPAN	90	70	50	30	10	PCT SPAN	90	70	50	30	10	
DIA	33.622	35.167	36.711	38.256	39.801	DIA	33.589	35.067	36.545	38.023	39.501							
BETA 0	0.000	0.000	0.000	0.000	0.000	BETA 1	16.233	16.966	16.966	17.259	17.665							
BETA 1	16.233	16.966	17.259	17.665	18.214	BETA 2	59.698	51.000	47.599	48.490	57.874							
V 0	252.83	252.83	252.83	252.83	252.83	BETA(PR) 1	57.765	58.666	60.453	61.083	63.676							
V 1	302.23	306.84	301.14	306.56	289.77	BETA(PR) 2	39.787	38.791	38.263	42.139	49.675							
VZ 0	252.83	252.83	252.83	252.83	252.83	V 1	303.23	306.84	301.14	306.56	289.77							
VZ 1	291.14	293.48	287.58	292.10	275.25	V 2	425.33	444.25	467.60	458.29	435.75							
V-THETA 0	-0.00	-0.00	-0.00	-0.00	-0.00	VZ 1	291.14	293.48	287.58	292.10	275.25							
V-THETA 1	84.77	89.54	89.35	93.02	90.57	VZ 2	214.60	279.23	315.31	303.73	231.72							
M 0	0.2276	0.2276	0.2276	0.2276	0.2276	V-THETA 1	84.77	89.54	89.35	93.02	96.57							
M 1	0.2736	0.2769	0.2717	0.2767	0.2613	V-THETA 2	367.22	345.52	345.29	343.19	369.03							
TURN	-16.23	-16.97	-17.26	-17.66	-18.21	V(PR) 1	545.8	564.4	583.2	604.1	622.7							
UUBAR	0.037	-0.0519	-0.0366	-0.0289	c.0210	V(PR) 2	279.3	358.2	401.6	409.6	358.1							
DFAC	-0.041	-0.032	-0.010	-0.021	0.042	VTHETA PR1	-461.7	-482.0	-507.3	-528.8	-556.3							
EFFP	0.9918	1.1198	1.0931	1.0637	0.9387	VTHETA PR2	-178.7	-224.4	-248.7	-274.8	-273.0							
INCID	0.0000	0.0000	0.0000	0.0000	0.0000	U 1	546.47	571.58	596.68	621.79	646.90							
DEV	7.8C7	7.004	7.581	8.935	10.666	U 2	545.93	569.96	593.98	618.00	642.02							
STATOR 1																		
STATION 2 - STATION 2A																		
PCT SPAN	90	70	50	30	10	M 2	0.3736	0.2736	0.2173	0.2767	0.2513							
BETA 2	59.698	51.057	47.599	48.490	57.874	M(PR) 1	0.4926	0.5094	0.5262	0.5452	0.5598							
BETA 2A	29.100	27.300	26.700	30.700	35.800	M(PR) 2	0.2457	0.3155	0.3549	0.3615	0.3142							
V 2	425.33	444.25	467.60	458.29	435.75	TURN(PR)	17.978	19.875	22.190	18.944	14.000							
V 2A	254.61	267.78	357.26	340.58	323.12	UUBAR	0.2508	0.1139	0.0474	0.0593	0.2149							
VZ 2	214.60	279.23	315.31	303.73	231.72	DFAC	0.6915	0.5575	0.5062	0.4132	0.4045							
VZ 2A	222.47	237.95	319.17	292.84	262.04	EFFP	0.5810	0.6302	0.7507	0.7436	0.6326							
V-THETA 2	367.22	345.52	345.29	343.19	369.03	EFF	0.5732	0.6227	0.7450	0.7377	0.6244							
V-THETA 2A	123.82	122.82	160.52	173.88	189.01	INCID	5.61	5.06	5.42	5.04	6.89							
M 2	0.3742	0.3912	0.4132	0.4045	0.3823	DEV	23.637	15.191	9.023	8.229	11.325							
M 2A	0.2232	0.2351	0.3152	0.3000	0.2842	LOSS PARA	0.07709	0.03711	0.01619	0.01983	0.06501							
TURN	30.598	23.757	20.899	17.790	22.074													
UUBAR	0.0737	0.1636	0.0251	0.0835	0.0824													
DFAC	0.6401	0.6158	0.4158	0.4322	0.4624													
EFFP	2.3196	2.3448	3.9534	2.8507	-1.9801													
INCID	12.75	4.11	0.65	1.54	10.92													
DEV	12.16	10.36	9.76	13.76	18.86													
DIA	33.564	34.992	36.240	37.848	39.276													

Table B-2. Blade Element Performance (Continued)

PERCENT DESIGN SPEED = 68.77

CORRECTED WEIGHT FLOW = 65.06

CORRECTED ROTOR SPEED = 3690.00

INLET GUIDE VANE 2										SLOTTED ROTOR 2									
STATION 0 - STATION 1					STATION 1 - STATION 2					STATION 1 - STATION 2					STATION 1 - STATION 2				
PCT SPAN	90	70	50	30	10	PCT SPAN	90	70	50	30	PCT SPAN	90	70	50	30	10			
DIA	33.622	35.167	36.711	38.256	39.801	DIA	33.589	35.067	36.545	38.023	39.501								
BETA 0	0.000	0.000	0.000	0.000	0.000	BETA 1	16.595	17.255	17.651	18.074	18.375								
BETA 1	16.595	17.225	17.651	18.074	18.735	BETA 2	52.92	45.631	44.639	45.772	53.319								
V 0	271.73	271.73	271.73	271.73	271.73	BETA(PR) 1	55.111	56.497	57.909	59.793	61.746								
V 1	326.12	325.60	324.26	316.98	307.58	BETA(PR) 2	33.601	35.601	37.828	41.738	47.460								
V 2 0	271.73	271.73	271.73	271.73	271.73	V 1	326.12	325.60	324.26	316.98	307.58								
V 2 1	312.54	310.99	308.99	301.34	291.29	V 2	451.05	464.50	468.80	477.25	437.72								
V-THETA 0	-C.00	-C.00	-C.00	-C.00	-C.00	VZ 1	312.54	310.99	308.99	301.34	291.29								
V-THETA 1	92.14	96.42	98.32	98.34	98.79	VZ 2	271.94	324.82	333.57	318.94	261.48								
M 0	0.2449	0.2449	0.2449	0.2449	0.2449	V-THETA 1	93.14	96.42	98.32	98.34	98.79								
M 1	0.2946	0.2942	0.2942	0.2929	0.2776	V-THETA 2	359.86	332.05	327.65	351.04	351.04								
TURN	-16.60	-17.23	-17.65	-18.07	-18.73	V(PRI) 1	546.14	563.4	581.6	598.9	615.3								
UBAR	0.0836	0.0353	0.0387	0.0420	0.0486	V(PRI) 2	326.6	399.5	422.3	427.4	385.7								
DFAC	-0.038	-0.017	-0.017	-0.021	-0.059	V(THETA) PRI 1	-448.2	-469.8	-492.8	-517.6	-542.0								
EFFP	0.8441	0.9269	0.9186	0.8983	0.7653	V(THETA) PRI 2	-180.9	-232.6	-259.0	-284.5	-285.0								
INCID	0.0000	0.0000	0.0000	0.0000	0.0000	U 1	541.34	566.21	591.07	615.95	640.82								
DEV	7.445	6.745	7.189	8.526	10.145	M 1	0.2946	540.81	564.60	588.60	612.20	635.99							
						M 2	0.3980	0.4124	0.4292	0.2863	0.2776								
						M(PR) 1	0.4937	0.5090	0.5254	0.5409	0.5554								
						M(PR) 2	0.2882	0.3546	0.3752	0.3789	0.3408								
						TURN(PR)	21.471	20.891	20.082	18.055	14.287								
						UBAR	0.1718	0.0288	0.0058	0.0411	0.1717								
						DFAC	0.5995	0.4684	0.4586	0.4646	0.5702								
BETA 2	52.922	45.631	44.639	45.772	53.319	EFFP	0.6110	0.7901	0.8459	0.8009	0.6703								
BETA 2A	28.800	26.200	25.700	28.400	32.400	EFF	0.6037	0.7858	0.8426	0.7967	0.6635								
V 2	451.05	464.50	468.80	457.25	437.72	INCID	2.95	2.95	2.88	3.75	4.96								
V 2A	284.57	325.05	354.66	340.44	306.51	DEV	17.490	12.001	8.588	7.828	8.810								
V 2 2	271.94	324.82	333.57	318.94	261.48	LOSS PARA	0.05721	0.00979	0.00197	0.01383	0.05425								
V 2 3	245.37	291.66	319.58	299.46	258.80														
V-THETA 2	355.86	332.05	329.40	327.65	351.04														
V-THETA 2A	137.C9	143.51	153.80	161.92	164.24														
M 2	0.2580	0.4124	0.4165	C.4054	0.3858														
M 2A	0.2505	0.2872	0.3141	C.3007	0.2698														
TURN	24.122	19.431	18.939	17.372	20.919														
UBAR	0.103C	0.0840	0.0421	C.0787	0.1459														
DFAC	0.5751	0.4772	0.4140	0.4274	0.5102														
EFFP	3.2674	1.5148	2.2152	1.6318	4.5666														
INCID	5.97	-1.32	-2.31	-1.18	6.37														
DEV	11.86	9.26	8.76	11.46	15.46														
DIA	33.564	34.992	36.420	37.848	39.276														

Table B-2. Blade Element Performance (Continued)

PERCENT DESIGN SPEED = 68.21
 CORRECTED WEIGHT FLOW = 70.98
 CORRECTED ROTOR SPEED = 3660.00

INLET GUIDE VANE 2						STATION 1 - STATION 2					
STATION 0 - STATION 1						STATION 1 - STATION 2			SLOTTED ROTOR 2		
PCT SPAN	90	70	50	30	10	PCT SPAN	90	70	50	30	10
DIA	33.622	35.167	36.711	38.256	39.801	DIA	33.589	35.067	36.545	38.023	39.501
BETA 0	0.000	0.000	0.000	0.000	0.000	BETA 1	16.517	17.256	18.088	17.968	19.337
BETA 1	16.517	17.256	18.088	17.968	19.337	BETA 2	46.152	41.976	45.153	42.343	47.890
V 0	298.21	298.21	298.21	298.21	298.21	BETA(PR) 1	52.404	53.205	54.870	56.815	58.727
V 1	351.07	356.20	352.85	346.54	337.25	BETA(PR) 2	32.385	33.027	36.464	41.180	46.304
VZ 0	298.21	298.21	298.21	298.21	298.21	V 1	351.07	356.30	352.85	346.54	337.25
VZ 1	336.59	340.26	335.42	329.64	318.22	V 2	461.54	486.08	479.89	459.96	439.18
V-THETA 0	-0.00	-0.00	-0.00	-0.00	-0.00	VZ 1	336.59	340.26	335.42	329.64	318.22
V-THETA 1	95.81	105.69	109.55	106.90	111.67	VZ 2	317.34	361.36	359.34	339.97	294.50
M 0	0.2690	0.2690	0.2690	0.2690	0.2690	V-THETA 1	99.81	105.69	109.55	106.90	111.67
M 1	0.3176	0.3225	0.3193	0.3134	0.3049	V-THETA 2	335.14	325.10	318.06	309.81	325.81
TURN	-16.52	-17.26	-18.09	-17.97	-19.34	V(PR) 1	551.7	568.9	582.9	602.3	613.0
UUBAR	0.0512	-0.0098	0.0068	0.0138	0.0582	V(PR) 2	375.8	431.0	446.8	451.7	424.0
DFAC	-0.0119	-0.0113	0.006	0.024	0.066	V(THETA PR1)	-437.1	-455.9	-476.7	-504.0	-523.9
EFFP	0.8863	1.0226	0.9837	0.9634	0.8321	V(THETA PR2)	-201.3	-234.9	-265.6	-297.4	-305.0
INCID	0.0000	0.0000	0.0000	0.0000	0.0000	U 1	536.94	561.61	586.27	610.94	635.61
DEV	7.523	6.714	6.752	8.632	9.543	U 2	536.41	560.01	583.62	607.22	630.82
						M 1	0.3176	0.3225	0.3193	0.3134	0.3149
						M 2	0.4091	0.4337	0.4284	0.4101	0.3896
						M(PR) 1	0.4991	0.5149	0.5274	0.5447	0.5542
						M(PR) 2	0.3331	0.3845	0.3989	0.4027	0.3761
						TURN(PR)	20.019	26.238	18.406	15.635	12.723
						UUBAR	0.1200	0.0036	-0.0141	0.0292	0.1215
						DFAC	0.4913	0.4961	0.3928	0.4073	0.4786
BETA 2	46.562	41.976	41.513	42.343	47.890	EFFP	0.6364	0.8613	0.9213	0.8912	0.7386
BETA 2A	28.500	25.100	24.100	26.800	32.100	EFF	0.6302	0.8586	0.9197	0.8891	0.7338
V 2	461.54	486.08	479.89	459.96	439.18	INCID	0.024	-0.35	-0.16	0.78	1.94
V 2A	315.34	367.41	370.41	358.32	322.34	DEV	16.235	9.427	7.224	7.270	7.354
VZ 2	317.34	361.36	359.34	339.97	294.50	LOSS PARA	0.04052	0.00126	0.00494	0.00990	0.03940
V-THETA 2	277.15	332.72	338.08	319.83	273.06						
V-THETA 2A	335.14	325.10	318.06	309.81	325.10						
M 2	0.4091	0.4337	0.4284	0.4101	0.3896						
M 2A	0.2785	0.3266	0.3293	0.3182	0.2852						
TURN	18.062	16.876	17.413	15.543	15.790						
UUBAR	0.0922	0.0647	0.0622	0.0522	0.1204						
DFAC	0.4837	0.3960	0.3865	0.3740	0.4398						
EFFP	1.9171	1.8271	1.5214	1.4055	1.9930						
INCID	-0.39	-4.97	-5.44	-4.61	0.94						
DEV	11.56	8.16	7.16	9.86	15.16						
DIA	33.564	34.992	36.420	37.848	39.276						

**APPENDIX C
REFERENCES**

1. NASA CR-54544, PWA FR-1713, "Single Stage Experimental Evaluation of Slotted Rotor and Stator Blading, Part I Analysis and Design," July 1966.
2. NASA CR-54545, PWA FR-1669, "Single Stage Experimental Evaluation of Slotted Rotor and Stator Blading, Part II Annular Cascade Investigation of Slot Location and Geometry," September 1966.
3. NASA SP-36, "Aerodynamic Design of Axial-Flow Compressors," 1965.
4. NASA CR-54546, PWA FR-2110, "Single Stage Experimental Evaluation of Slotted Rotor Stator Blading, Part III Data and Performance for Slotted Rotor 1," 1966.